



Roland SIEGWART
Illah R. NOURBAKHSH
Davide SCARAMUZZA

SECOND EDITION

Introduction to

Autonomous Mobile Robots

Introduction to Autonomous Mobile Robots

Intelligent Robotics and Autonomous Agents

Edited by Ronald C. Arkin

A list of the books published in the Intelligent Robotics and Autonomous Agents series can be found at the back of the book.

Introduction to Autonomous Mobile Robots

second edition

Roland Siegwart, Illah R. Nourbakhsh, and Davide Scaramuzza

The MIT Press
Cambridge, Massachusetts
London, England

© 2011 Massachusetts Institute of Technology
Original edition © 2004

All rights reserved. No part of this book may be reproduced in any form by any electronic or mechanical means (including photocopying, recording, or information storage and retrieval) without permission in writing from the publisher.

For information about special quantity discount, please email special_sales@mitpress.mit.edu

This book was set in Times Roman by the authors using Adobe FrameMaker 9.0.
Printed and bound in the United States of America.

Library of Congress Cataloging-in-Publication Data

Siegwart, Roland.

Introduction to autonomous mobile robots. - 2nd ed. / Roland Siegwart, Illah R. Nourbakhsh, and Davide Scaramuzza.

p. cm. - (Intelligent robotics and autonomous agents series)

Includes bibliographical references and index.

ISBN 978-0-262-01535-6 (hardcover : alk. paper) 1. Mobile robots. 2. Autonomous robots. I. Nourbakhsh, Illah Reza, 1970-. II. Scaramuzza, Davide. III. Title.

TJ211.415.S54 2011

629.8'932-dc22

2010028053

10 9 8 7 6 5 4 3 2 1

To Luzia and my children, Janina, Malin, and Yanik, who give me their support and freedom to grow every day — RS

To my parents, Susi and Yvo, who opened my eyes — RS

To Marti, Mitra, and Nikou, who are my love and my inspiration — IRN

To my parents, Fatemeh and Mahmoud, who let me disassemble and investigate everything in our home — IRN

To my parents, Paola and Ermanno, who encouraged and supported my choices every day and introduced me to robotics at the age of three — DS

To my sisters, Lisa and Silvia, for their love — DS

Slides and exercises that go with this book are available at:

<http://www.mobilerobots.org>

Contents

Acknowledgments	xiii
Preface	xv
1 Introduction	1
1.1 Introduction	1
1.2 An Overview of the Book	11
2 Locomotion	13
2.1 Introduction	13
2.1.1 Key issues for locomotion	16
2.2 Legged Mobile Robots	17
2.2.1 Leg configurations and stability	18
2.2.2 Consideration of dynamics	21
2.2.3 Examples of legged robot locomotion	25
2.3 Wheeled Mobile Robots	35
2.3.1 Wheeled locomotion: The design space	35
2.3.2 Wheeled locomotion: Case studies	43
2.4 Aerial Mobile Robots	50
2.4.1 Introduction	50
2.4.2 Aircraft configurations	52
2.4.3 State of the art in autonomous VTOL	52
2.5 Problems	56
3 Mobile Robot Kinematics	57
3.1 Introduction	57
3.2 Kinematic Models and Constraints	58

3.2.1 Representing robot position	58
3.2.2 Forward kinematic models	61
3.2.3 Wheel kinematic constraints	63
3.2.4 Robot kinematic constraints	71
3.2.5 Examples: Robot kinematic models and constraints	73
3.3 Mobile Robot Maneuverability	77
3.3.1 Degree of mobility	77
3.3.2 Degree of steerability	81
3.3.3 Robot maneuverability	82
3.4 Mobile Robot Workspace	84
3.4.1 Degrees of freedom	84
3.4.2 Holonomic robots	85
3.4.3 Path and trajectory considerations	87
3.5 Beyond Basic Kinematics	90
3.6 Motion Control (Kinematic Control)	91
3.6.1 Open loop control (trajectory-following)	91
3.6.2 Feedback control	92
3.7 Problems	99
4 Perception	101
4.1 Sensors for Mobile Robots	101
4.1.1 Sensor classification	101
4.1.2 Characterizing sensor performance	103
4.1.3 Representing uncertainty	109
4.1.4 Wheel/motor sensors	115
4.1.5 Heading sensors	116
4.1.6 Accelerometers	119
4.1.7 Inertial measurement unit (IMU)	121
4.1.8 Ground beacons	122
4.1.9 Active ranging	125
4.1.10 Motion/speed sensors	140
4.1.11 Vision sensors	142
4.2 Fundamentals of Computer Vision	142
4.2.1 Introduction	142
4.2.2 The digital camera	142
4.2.3 Image formation	148
4.2.4 Omnidirectional cameras	159
4.2.5 Structure from stereo	169
4.2.6 Structure from motion	180

4.2.7 Motion and optical flow	189
4.2.8 Color tracking	192
4.3 Fundamentals of Image Processing	195
4.3.1 Image filtering	196
4.3.2 Edge detection	199
4.3.3 Computing image similarity	207
4.4 Feature Extraction	208
4.5 Image Feature Extraction: Interest Point Detectors	212
4.5.1 Introduction	212
4.5.2 Properties of the ideal feature detector	213
4.5.3 Corner detectors	215
4.5.4 Invariance to photometric and geometric changes	220
4.5.5 Blob detectors	227
4.6 Place Recognition	234
4.6.1 Introduction	234
4.6.2 From bag of features to visual words	235
4.6.3 Efficient location recognition by using an inverted file	236
4.6.4 Geometric verification for robust place recognition	237
4.6.5 Applications	237
4.6.6 Other image representations for place recognition	238
4.7 Feature Extraction Based on Range Data (Laser, Ultrasonic)	242
4.7.1 Line fitting	243
4.7.2 Six line-extraction algorithms	248
4.7.3 Range histogram features	259
4.7.4 Extracting other geometric features	260
4.8 Problems	262
5 Mobile Robot Localization	265
5.1 Introduction	265
5.2 The Challenge of Localization: Noise and Aliasing	266
5.2.1 Sensor noise	267
5.2.2 Sensor aliasing	268
5.2.3 Effector noise	269
5.2.4 An error model for odometric position estimation	270
5.3 To Localize or Not to Localize: Localization-Based Navigation Versus Programmed Solutions	275
5.4 Belief Representation	278
5.4.1 Single-hypothesis belief	278
5.4.2 Multiple-hypothesis belief	280

5.5	Map Representation	284
5.5.1	Continuous representations	284
5.5.2	Decomposition strategies	287
5.5.3	State of the art: Current challenges in map representation	294
5.6	Probabilistic Map-Based Localization	296
5.6.1	Introduction	296
5.6.2	The robot localization problem	297
5.6.3	Basic concepts of probability theory	299
5.6.4	Terminology	302
5.6.5	The ingredients of probabilistic map-based localization	304
5.6.6	Classification of localization problems	306
5.6.7	Markov localization	307
5.6.8	Kalman filter localization	322
5.7	Other Examples of Localization Systems	342
5.7.1	Landmark-based navigation	344
5.7.2	Globally unique localization	345
5.7.3	Positioning beacon systems	346
5.7.4	Route-based localization	347
5.8	Autonomous Map Building	348
5.8.1	Introduction	348
5.8.2	SLAM: The simultaneous localization and mapping problem	349
5.8.3	Mathematical definition of SLAM	351
5.8.4	Extended Kalman Filter (EKF) SLAM	353
5.8.5	Visual SLAM with a single camera	356
5.8.6	Discussion on EKF SLAM	359
5.8.7	Graph-based SLAM	361
5.8.8	Particle filter SLAM	363
5.8.9	Open challenges in SLAM	364
5.8.10	Open source SLAM software and other resources	365
5.9	Problems	366
6	Planning and Navigation	369
6.1	Introduction	369
6.2	Competences for Navigation: Planning and Reacting	370
6.3	Path Planning	371
6.3.1	Graph search	373
6.3.2	Potential field path planning	386
6.4	Obstacle avoidance	393
6.4.1	Bug algorithm	393

6.4.2 Vector field histogram	397
6.4.3 The bubble band technique	399
6.4.4 Curvature velocity techniques	401
6.4.5 Dynamic window approaches	402
6.4.6 The Schlegel approach to obstacle avoidance	404
6.4.7 Nearness diagram	405
6.4.8 Gradient method	405
6.4.9 Adding dynamic constraints	406
6.4.10 Other approaches	406
6.4.11 Overview	406
6.5 Navigation Architectures	409
6.5.1 Modularity for code reuse and sharing	410
6.5.2 Control localization	410
6.5.3 Techniques for decomposition	411
6.5.4 Case studies: tiered robot architectures	416
6.6 Problems	423
 Bibliography	 425
Books	425
Papers	427
Referenced Webpages	444
 Index	 447

Acknowledgments

This book is the result of inspirations and contributions from many researchers and students at the Swiss Federal Institutes of Technology Zurich (ETH) and Lausanne (EPFL), Carnegie Mellon University's Robotics Institute, Pittsburgh (CMU), and many others around the globe.

We would like to thank all the researchers in mobile robotics who make this field so rich and stimulating by sharing their goals and visions with the community. It is their work that enabled us to collect the material for this book.

The most valuable and direct support and contribution for this second edition came from our current collaborators at ETH. We would like to thank Friedrich Fraundorfer for his contribution to the section on location recognition; Samir Bouabdallah for his contribution to the section on flying robots; Christian David Remy for his contribution to the section on considerations of dynamics; Martin Rufli for his contribution to path planning; Agostino Martinelli for his careful checking of some of the equations; Deon Sabatta and Jonathan Claassens for their careful review of some sections and their fruitful discussions; and Sarah Bulliard for her useful suggestions. Furthermore, we would like to renew our acknowledgments to the people who contributed to the first edition. In particular Kai Arras for his contribution to uncertainty representation and Kalman filter localization; Matt Mason for his contribution to kinematics; Al Rizzi for his guidance on feedback control; Roland Philippson and Jan Persson for their contribution to obstacle avoidance; Gilles Caprari and Yves Piguet for their input and suggestions on motion control; Marco Lauria for offering his talent for some of the figures; Marti Louw for her efforts on the cover design; and Nicola Tomatis, Remy Blank, and Marie-Jo Pellaud.

This book was also inspired by other courses, especially by the lecture notes on mobile robotics at the Swiss Federal Institutes of Technology, both in Lausanne (EPFL) and Zurich (ETH). The material for this book has been used for lectures at EPFL, ETH, and CMU since 1997. We thank the hundreds of students who followed the lecture and contributed through their corrections and comments.

It has been a pleasure to work with MIT Press, the publisher of this book. Thanks to Gregory McNamee for his careful and valuable copy-editing, and to Ada Brunstein, Katherine Almeida, Abby Streeter Roake, Marc Lowenthal, and Susan Clark from MIT Press for their help in editing and finalizing the book.

Preface

Mobile robotics is a young field. Its roots include many engineering and science disciplines, from mechanical, electrical, and electronics engineering to computer, cognitive, and social sciences. Each of these parent fields has its share of introductory textbooks that excite and inform prospective students, preparing them for future advanced coursework and research. Our objective in writing this textbook is to provide mobile robotics with such a preparatory guide.

This book presents an introduction to the fundamentals of mobile robotics, spanning the mechanical, motor, sensory, perceptual, and cognitive layers that comprise our field of study. A collection of workshop proceedings and journal publications could present the new student with a snapshot of the state of the art in all aspects of mobile robotics. But here we aim to present a foundation—a formal introduction to the field. The formalism and analysis herein will prove useful even as the frontier of the state-of-the-art advances due to the rapid progress in all of the subdisciplines of mobile robotics.

This second edition largely extends the content of the first edition. In particular, chapters 2, 4, 5, and 6 have been notably expanded and updated to the most recent, state-of-the-art acquisitions in both computer vision and robotics. In particular, we have added in chapter 2 the most recent and popular examples of mobile, legged, and micro aerial robots. In chapter 4, we have added the description of new sensors—such as 3D laser rangefinders, time-of-flight cameras, IMUs, and omnidirectional cameras—and tools—such as image filtering, camera calibration, structure-from-stereo, structure-from-motion, visual odometry, the most popular feature detectors for camera (Harris, FAST, SURF, SIFT) and laser images, and finally bag-of-feature approaches for place recognition and image retrieval. In chapter 5, we have added an introduction to probability theory, and improved and expanded the description of Markov and Kalman filter localization using a better formalism and more examples. Furthermore, we have also added the description of the Simultaneous Localization and Mapping (SLAM) problem along with a description of the most popular approaches to solve it such as extended-Kalman-filter SLAM, graph-based SLAM, particle filter SLAM, and the most recent monocular visual SLAM. Finally, in chapter 6 we have added the description of graph-search algorithms for path planning such as breadth-first, depth first, Dijkstra, A*, D*, and rapidly exploring random trees. Besides these many new additions, we have also provided state-of-the-art references and links to online resources

and downloadable software.

We hope that this book will empower both undergraduate and graduate robotics students with the background knowledge and analytical tools they will need to evaluate and even criticize mobile robot proposals and artifacts throughout their careers. This textbook is suitable as a whole for introductory mobile robotics coursework at both the undergraduate and graduate level. Individual chapters such as those on perception or kinematics can be useful as overviews in more focused courses on specific subfields of robotics.

The origins of this book bridge the Atlantic Ocean. The authors have taught courses on mobile robotics at the undergraduate and graduate level at Stanford University, ETH Zurich, Carnegie Mellon University and EPFL. Their combined set of curriculum details and lecture notes formed the earliest versions of this text. We have combined our individual notes, provided overall structure and then test-taught using this textbook for two additional years before settling on the first edition in 2004, and another six years for the current, published text.

For an overview of the organization of the book and summaries of individual chapters, refer to section 1.2.

Finally, for the teacher and the student: we hope that this textbook will prove to be a fruitful launching point for many careers in mobile robotics. That would be the ultimate reward.

1 Introduction

1.1 Introduction

Robotics has achieved its greatest success to date in the world of industrial manufacturing. Robot arms, or *manipulators*, comprise a \$ 2 billion industry. Bolted at its shoulder to a specific position in the assembly line, the robot arm can move with great speed and accuracy to perform repetitive tasks such as spot welding and painting (figure 1.1). In the electronics industry, manipulators place surface-mounted components with superhuman precision, making the portable telephone and laptop computer possible.

Yet, for all of their successes, these commercial robots suffer from a fundamental disadvantage: lack of mobility. A fixed manipulator has a limited range of motion that depends

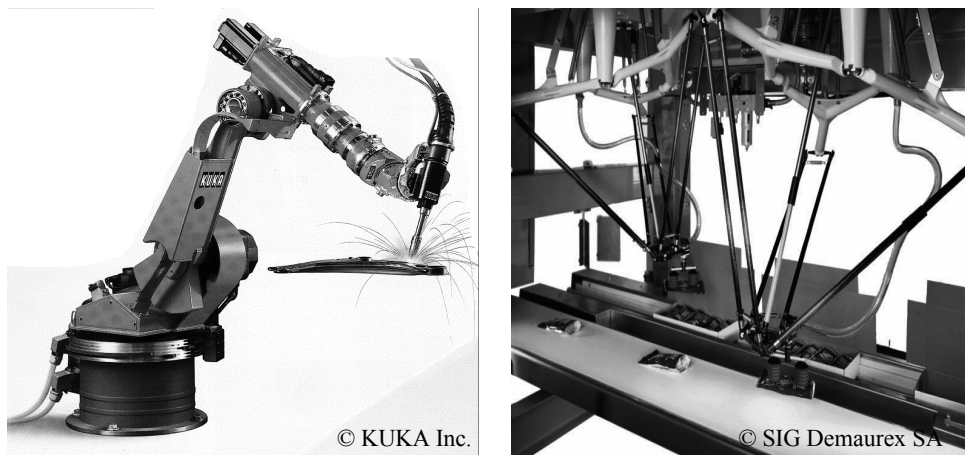


Figure 1.1

Picture of auto assembly plant-spot welding robot of KUKA and a parallel robot Delta of SIG Demaurex SA (invented at EPFL [305]) during packaging of chocolates.

on where it is bolted down. In contrast, a mobile robot would be able to travel throughout the manufacturing plant, flexibly applying its talents wherever it is most effective.

This book focuses on the technology of mobility: how can a mobile robot move unsupervised through real-world environments to fulfill its tasks? The first challenge is locomotion itself. How should a mobile robot move, and what is it about a particular locomotion mechanism that makes it superior to alternative locomotion mechanisms?

Hostile environments such as Mars trigger even more unusual locomotion mechanisms (figure 1.2). In dangerous and inhospitable environments, even on Earth, such *teleoperated* systems have gained popularity (figures 1.3-1.6). In these cases, the low-level complexities of the robot often make it impossible for a human operator to control its motions directly. The human performs localization and cognition activities but relies on the robot's control scheme to provide motion control.

For example, Plustech's walking robot provides automatic leg coordination while the human operator chooses an overall direction of travel (figure 1.3). Figure 1.6 depicts an underwater vehicle that controls three propellers to stabilize the robot submarine autonomously in spite of underwater turbulence and water currents while the operator chooses position goals for the submarine to achieve.

Other commercial robots operate not where humans *cannot* go, but rather share space with humans in human environments (figure 1.7). These robots are compelling not for reasons of mobility but because of their *autonomy*, and so their ability to maintain a sense of position and to navigate without human intervention is paramount.

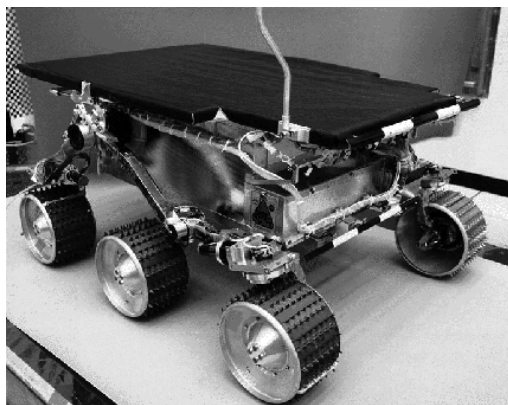


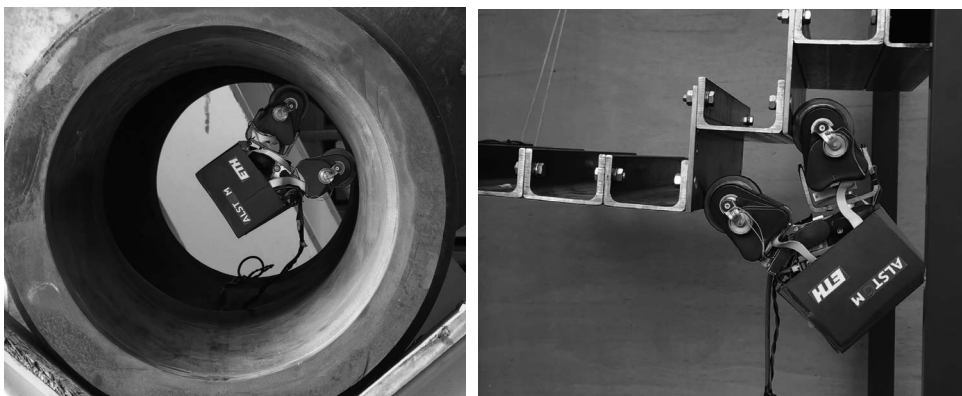
Figure 1.2

The mobile robot Sojourner was used during the Pathfinder mission to explore Mars in summer 1997. It was almost completely teleoperated from Earth. However, some on-board sensors allowed for obstacle detection (http://ranier.oact.hq.nasa.gov/telerobotics_page/telerobotics.shtml).

© NASA/JPL.

**Figure 1.3**

Plustech developed the first application-driven walking robot. It is designed to move wood out of the forest. The leg coordination is automated, but navigation is still done by the human operator on the robot. (<http://www.plustech.fi>). © Plustech.

**Figure 1.4**

The MagneBike robot developed by ASL (ETH Zurich) and ALSTOM. MagneBike is a magnetic wheeled robot with high mobility for inspecting complex shaped structures such as ferromagnetic pipes and turbines (<http://www.asl.ethz.ch/>). © ALSTOM / ETH Zurich.



Figure 1.5

Picture of Pioneer, a robot designed to explore the Sarcophagus at Chernobyl. © Wide World Photos.



Figure 1.6

The autonomous underwater vehicle (AUV) Sirius being retrieved after a mission aboard the RV Southern Surveyor © Robin Beaman—James Cook University.

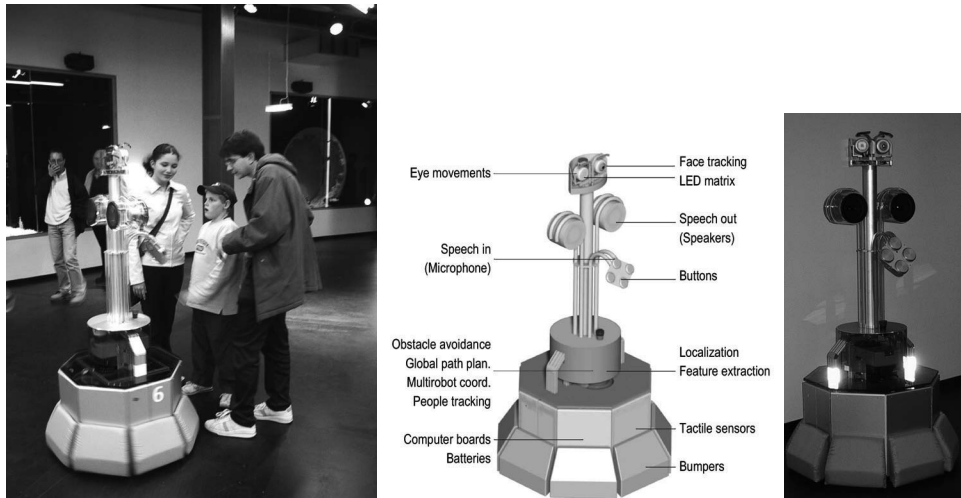
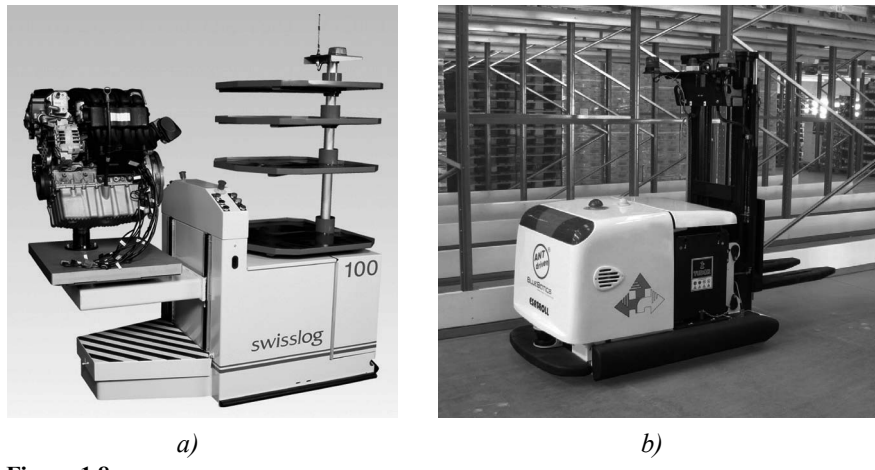


Figure 1.7

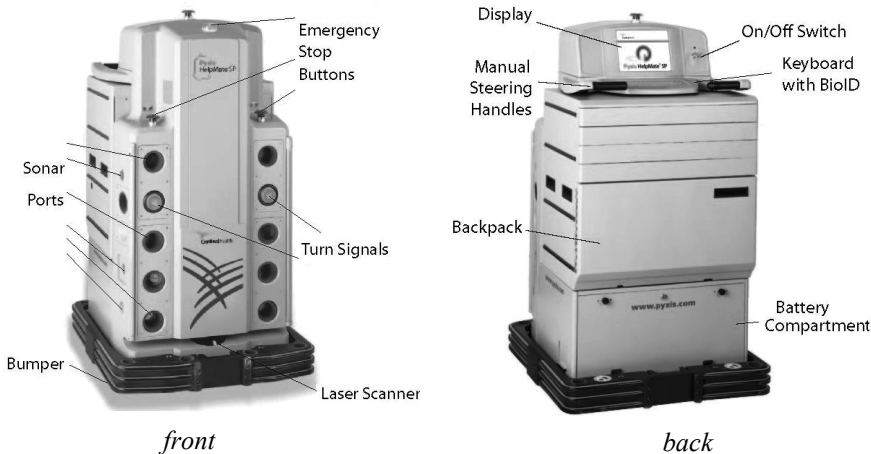
Tour-guide robots are able to interact and present exhibitions in an educational way [85, 251, 288, 310,]. Ten Roboboxes have operated during five months at the Swiss exhibition EXPO.02, meeting hundreds of thousands of visitors. They were developed by EPFL [288] (<http://robotics.epfl.ch>) and commercialized by BlueBotics (<http://www.bluebotics.com>).

For example, AGV (autonomous guided vehicle) robots (figure 1.8) autonomously deliver parts between various assembly stations by following special electrical guidewires installed in the floor (figure 1.8a) or, differently, by using onboard lasers to localize within a user-specified map (figure 1.8b). The Helpmate service robot transports food and medication throughout hospitals by tracking the position of ceiling lights, which are manually specified to the robot beforehand (figure 1.9). Several companies have developed autonomous cleaning robots, mainly for large buildings (figure 1.10). One such cleaning robot is in use at the Paris Metro. Other specialized cleaning robots take advantage of the regular geometric pattern of aisles in supermarkets to facilitate the localization and navigation tasks.

Research into high-level questions of cognition, localization, and navigation can be performed using standard research robot platforms that are tuned to the laboratory environment. This is one of the largest current markets for mobile robots. Various mobile robot platforms are available for programming, ranging in terms of size and terrain capability. Very popular research robots are the Pioneer, BIBA, and the *e-puck* (figures 1.11-1.13) and also very small robots like the Alice from EPFL (Swiss Federal Institute of Technology at Lausanne) (figure 1.14).

**Figure 1.8**

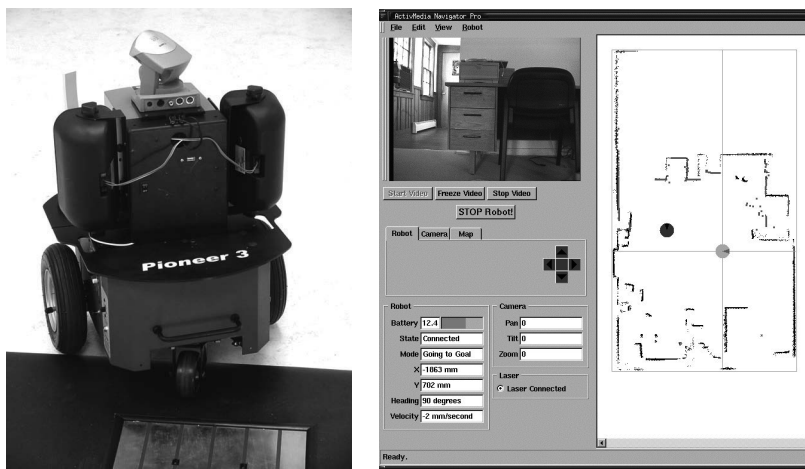
(a) Autonomous guided vehicle (AGV) by SWISSLOG used to transport motor blocks from one assembly station to another. It is guided by an electrical wire installed in the floor. © Swisslog.
 (b) Equipped with the Autonomous Navigation Technology (ANT) from BlueBotics, Paquito, the autonomous forklift by Esatroll, does not rely on electrical wires, magnetic plots, or reflectors, but rather uses the onboard safety lasers to localize itself with respect to the shape of the environment. Image courtesy of BlueBotics (<http://www.bluebotics.com>).

**Figure 1.9**

HELMATE is a mobile robot used in hospitals for transportation tasks. It has various on-board sensors for autonomous navigation in the corridors. The main sensor for localization is a camera looking to the ceiling. It can detect the lamps on the ceiling as references, or landmarks (<http://www.pyxis.com>). © Pyxis Corp.

**Figure 1.10**

(a) The Robot40 is a consumer robot developed and sold by Cleanfix for cleaning large gymnasiums. The navigation system of Robo40 is based on a sophisticated sonar and infrared system (<http://www.cleanfix.com>). © Cleanfix. (b) The RoboCleaner RC 3000 covers badly soiled areas with a special driving strategy until it is really clean. Optical sensors measure the degree of pollution of the aspirated air (<http://www.karcher.de>). © Alfred Kärcher GmbH & Co.

**Figure 1.11**

PIONEER is a modular mobile robot offering various options like a gripper or an on-board camera. It is equipped with a sophisticated navigation library developed at SRI, Stanford, CA. Reprinted with permission from ActivMedia Robotics, <http://www.MobileRobots.com>.

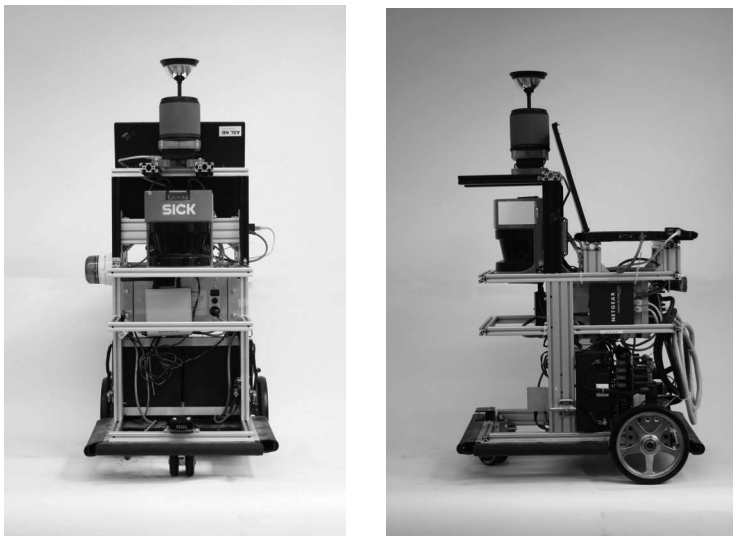


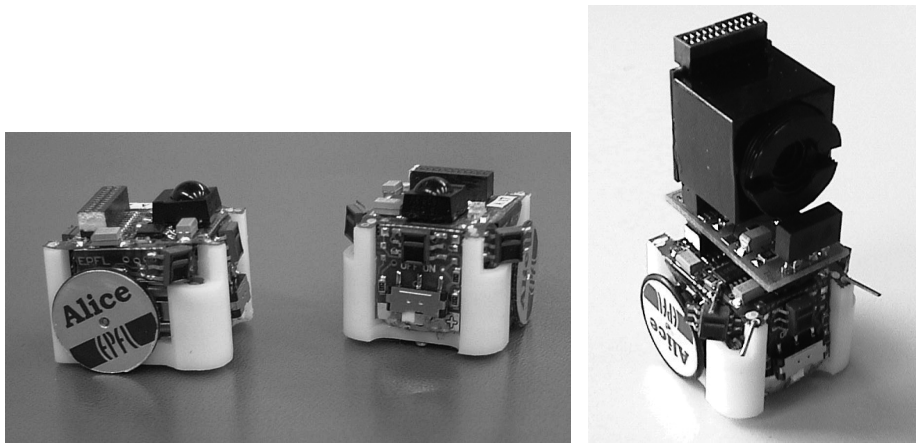
Figure 1.12

BIBA is a very sophisticated mobile robot developed for research purposes and built by BlueBotics (<http://www.bluebotics.com/>). It has a large variety of sensors for high-performance navigation tasks.



Figure 1.13

The *e-puck* is an educational desktop mobile robot developed at the EPFL [226]. It is only about 70 mm in diameter. As extensions to the basic capabilities, various modules such as additional sensors, actuators, or computational power have been developed. In this picture, two example extensions are shown: (center) an omnidirectional camera and (right) an infrared distance scanner (<http://www.e-puck.org/>). © Ecole Polytechnique Fédérale de Lausanne (EPFL).

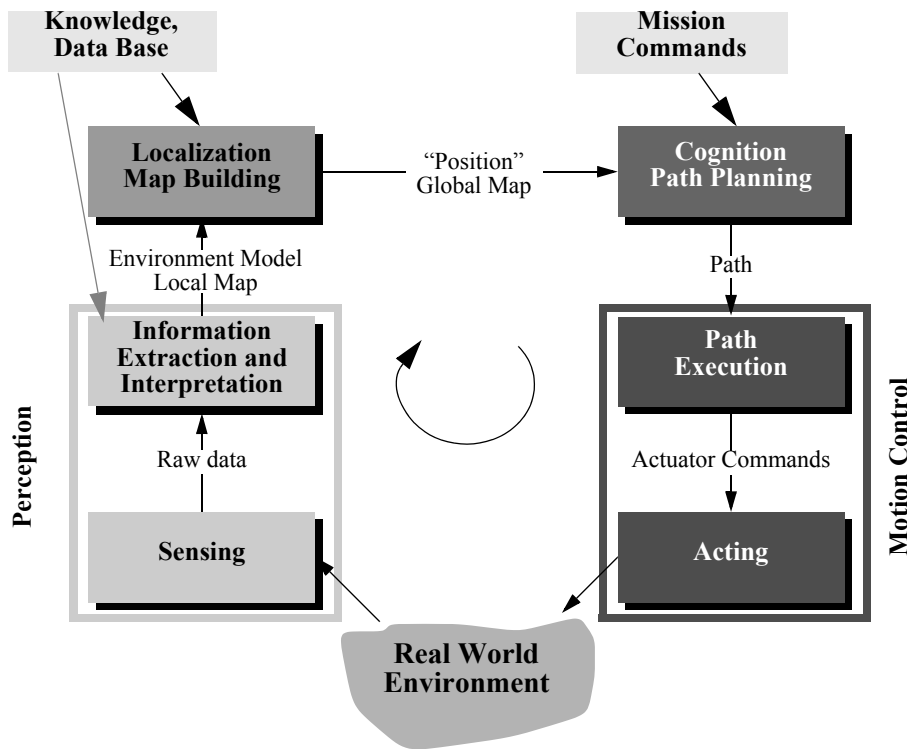
**Figure 1.14**

Alice is one of the smallest fully autonomous robots. It is approximately $2 \times 2 \times 2$ cm, it has an autonomy of about 8 hours and uses infrared distance sensors, tactile whiskers, or even a small camera for navigation [93].

Although mobile robots have a broad set of applications and markets as summarized above, there is one fact that is true of virtually every successful mobile robot: its design involves the integration of many different bodies of knowledge. No mean feat, this makes mobile robotics as interdisciplinary a field as there can be. To solve locomotion problems, the mobile roboticist must understand mechanism and kinematics, dynamics and control theory. To create robust perceptual systems, the mobile roboticist must leverage the fields of signal analysis and specialized bodies of knowledge such as computer vision to properly employ a multitude of sensor technologies. Localization and navigation demand knowledge of computer algorithms, information theory, artificial intelligence, and probability theory.

Figure 1.15 depicts an abstract control scheme for mobile robot systems that we will use throughout this text. This figure identifies many of the main bodies of knowledge associated with mobile robotics.

This book provides an introduction to all aspects of mobile robotics, including software and hardware design considerations, related technologies, and algorithmic techniques. The intended audience is broad, including both undergraduate and graduate students in introductory mobile robotics courses, as well as individuals fascinated by the field. Although it is not absolutely required, a familiarity with matrix algebra, calculus, probability theory, and computer programming will significantly enhance the reader's experience.

**Figure 1.15**

Reference control scheme for mobile robot systems used throughout this book.

Mobile robotics is a large field, and this book focuses not on robotics in general, or on mobile robot applications, but rather on mobility itself. From mechanism and perception to localization and navigation, this book focuses on the techniques and technologies that enable robust *mobility*.

Clearly, a useful, commercially viable mobile robot does more than just move. It polishes the supermarket floor, keeps guard in a factory, mows the golf course, provides tours in a museum, or provides guidance in a supermarket. The aspiring mobile roboticist will start with this book but will quickly graduate to coursework and research specific to the desired application, integrating techniques from fields as disparate as human-robot interaction, computer vision, and speech understanding.

1.2 An Overview of the Book

This book introduces the different aspects of a robot in modules, much like the modules shown in figure 1.15. Chapters 2 and 3 focus on the robot’s low-level *locomotive ability*. Chapter 4 presents an in-depth view of *perception*. Chapters 5 and 6 take us to the higher-level challenges of *localization* and *mapping* and even higher-level *cognition*, specifically the *ability to navigate robustly*. Each chapter builds upon previous chapters, and so the reader is encouraged to start at the beginning, even if his or her interest is primarily at the high level. Robotics is peculiar in that solutions to high-level challenges are most meaningful only in the context of a solid understanding of the low-level details of the system.

Chapter 2, “Locomotion,” begins with a survey of the most important mechanisms that enable locomotion: wheels, legs, and flight. Numerous robotic examples demonstrate the particular talents of each form of locomotion. But designing a robot’s locomotive system properly requires the ability to evaluate its overall motion capabilities quantitatively. Chapter 3, “Mobile Robot Kinematics,” applies principles of kinematics to the whole robot, beginning with the kinematic contribution of each wheel and graduating to an analysis of robot maneuverability enabled by each mobility mechanism configuration.

The greatest single shortcoming in conventional mobile robotics is, without doubt, perception: mobile robots can travel across much of earth’s man-made surfaces, but they cannot perceive the world nearly as well as humans and other animals. Chapter 4, “Perception,” begins a discussion of this challenge by presenting a clear language for describing the performance envelope of mobile robot sensors. With this language in hand, chapter 4 goes on to present many of the off-the-shelf sensors available to the mobile roboticist, describing their basic principles of operation as well as their performance limitations. The most promising sensor for the future of mobile robotics is vision, and chapter 4 includes an overview of the theory of camera image formation, omnidirectional vision, camera calibration, structure from stereovision, structure from motion, and visual odometry. But perception is more than sensing. Perception is also the *interpretation* of sensed data in meaningful ways. The second half of chapter 4 describes strategies for feature extraction that have been most useful in both computer vision and mobile robotics applications, including extraction of geometric shapes from range sensing data, as well as point features (such as Harris, SIFT, SURF, FAST, and so on) from camera images. Furthermore, a section is dedicated to the description of the most recent bag-of-feature approach that became popular for place recognition and image retrieval.

Armed with locomotion mechanisms and outfitted with hardware and software for perception, the mobile robot can move and perceive the world. The first point at which mobility and sensing must meet is localization: mobile robots often need to maintain a sense of position. Chapter 5, “Mobile Robot Localization,” describes approaches that obviate the need for direct localization, then delves into fundamental ingredients of successful local-

ization strategies: belief representation and map representation. Case studies demonstrate various localization schemes, including both Markov localization and Kalman filter localization. The final part of chapter 5 is devoted to a description of the Simultaneous Localization and Mapping (SLAM) problem along with a description of the most popular approaches to solve it such as extended-Kalman-filter SLAM, graph-based SLAM, particle filter SLAM, and the most recent monocular visual SLAM.

Mobile robotics is so young a discipline that it lacks a standardized architecture. There is as yet no established robot operating system. But the question of architecture is of paramount importance when one chooses to address the higher-level competences of a mobile robot: how does a mobile robot navigate robustly from place to place, interpreting data, and localizing and controlling its motion all the while? For this highest level of robot competence, which we term *navigation competence*, there are numerous mobile robots that showcase particular architectural strategies. Chapter 6, “Planning and Navigation,” surveys the state of the art of robot navigation, showing that today’s various techniques are quite similar, differing primarily in the manner in which they *decompose* the problem of robot control. But first, chapter 6 addresses two skills that a competent, navigating robot usually must demonstrate: obstacle avoidance and path planning.

There is far more to know about the cross-disciplinary field of mobile robotics than can be contained in a single book. We hope, though, that this broad introduction will place the reader in the context of the collective wisdom of mobile robotics. This is only the beginning. With luck, the first robot you program or build will have only good things to say about you.

2 Locomotion

2.1 Introduction

A mobile robot needs locomotion mechanisms that enable it to move unbounded throughout its environment. But there are a large variety of possible ways to move, and so the selection of a robot's approach to locomotion is an important aspect of mobile robot design. In the laboratory, there are research robots that can walk, jump, run, slide, skate, swim, fly, and, of course, roll. Most of these locomotion mechanisms have been inspired by their biological counterparts (see figure 2.1).

There is, however, one exception: the actively powered wheel is a human invention that achieves extremely high efficiency on flat ground. This mechanism is not completely foreign to biological systems. Our bipedal walking system can be approximated by a rolling polygon, with sides equal in length d to the span of the step (figure 2.2). As the step size decreases, the polygon approaches a circle or wheel. But nature did not develop a fully rotating, actively powered joint, which is the technology necessary for wheeled locomotion.

Biological systems succeed in moving through a wide variety of harsh environments. Therefore, it can be desirable to copy their selection of locomotion mechanisms. However, replicating nature in this regard is extremely difficult for several reasons. To begin with, mechanical complexity is easily achieved in biological systems through structural replication. Cell division, in combination with specialization, can readily produce a millipede with several hundred legs and several tens of thousands of individually sensed cilia. In man-made structures, each part must be fabricated individually, and so no such economies of scale exist. Additionally, the cell is a microscopic building block that enables extreme miniaturization. With very small size and weight, insects achieve a level of robustness that we have not been able to match with human fabrication techniques. Finally, the biological energy storage system and the muscular and hydraulic activation systems used by large animals and insects achieve torque, response time, and conversion efficiencies that far exceed similarly scaled man-made systems.

Type of motion	Resistance to motion	Basic kinematics of motion
Flow in a Channel	Hydrodynamic forces	Eddies
Crawl	Friction forces	Longitudinal vibration
Sliding	Friction forces	Transverse vibration
Running	Loss of kinetic energy	Periodic bouncing on a spring
Walking	Loss of kinetic energy	Rolling of a polygon (see figure 2.2)

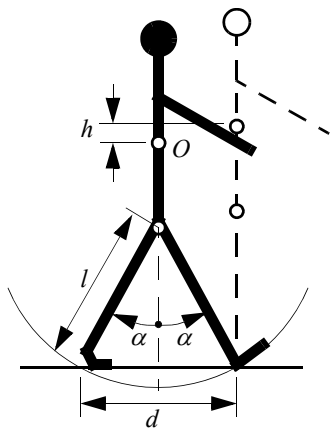
Figure 2.1

Locomotion mechanisms used in biological systems.

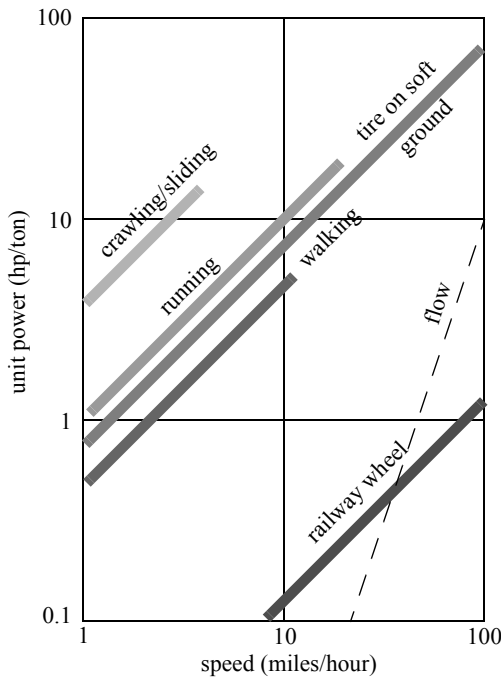
Owing to these limitations, mobile robots generally locomote either using wheeled mechanisms, a well-known human technology for vehicles, or using a small number of articulated legs, the simplest of the biological approaches to locomotion (see figure 2.2).

In general, legged locomotion requires higher degrees of freedom and therefore greater mechanical complexity than wheeled locomotion. Wheels, in addition to being simple, are extremely well suited to flat ground. As figure 2.3 depicts, on flat surfaces wheeled locomotion is one to two orders of magnitude more efficient than legged locomotion. The railway is ideally engineered for wheeled locomotion because rolling friction is minimized on a hard and flat steel surface. But as the surface becomes soft, wheeled locomotion accumulates inefficiencies due to rolling friction, whereas legged locomotion suffers much less because it consists only of point contacts with the ground. This is demonstrated in figure 2.3 by the dramatic loss of efficiency in the case of a tire on soft ground.

In effect, the efficiency of wheeled locomotion depends greatly on environmental qualities, particularly the flatness and hardness of the ground, while the efficiency of legged

**Figure 2.2**

A biped walking system can be approximated by a rolling polygon, with sides equal in length d to the span of the step. As the step size decreases, the polygon approaches a circle or wheel with the radius l .

**Figure 2.3**

Specific power versus attainable speed of various locomotion mechanisms [52].

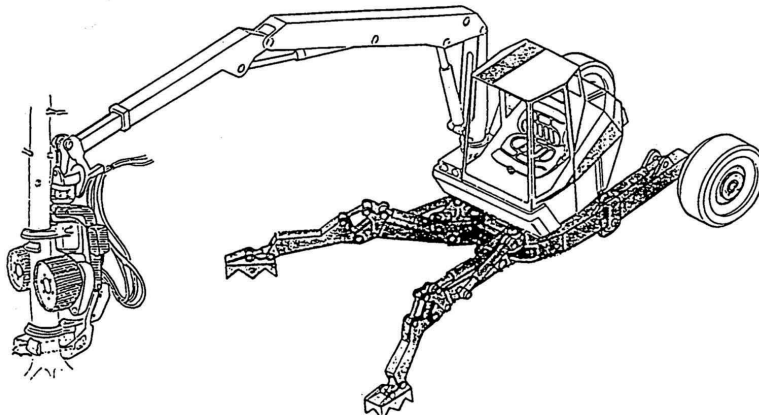


Figure 2.4

RoboTrac, a hybrid wheel-leg vehicle for rough terrain [282].

locomotion depends on the leg mass and body mass, both of which the robot must support at various points in a legged gait.

It is understandable, therefore, that nature favors legged locomotion, since locomotion systems in nature must operate on rough and unstructured terrain. For example, in the case of insects in a forest, the vertical variation in ground height is often an order of magnitude greater than the total height of the insect. By the same token, the human environment frequently consists of engineered, smooth surfaces, both indoors and outdoors. Therefore, it is also understandable that virtually all industrial applications of mobile robotics utilize some form of wheeled locomotion. Recently, for more natural outdoor environments, there has been some progress toward hybrid and legged industrial robots such as the forestry robot shown in figure 2.4.

In section 2.1.1, we present general considerations that concern all forms of mobile robot locomotion. Following this, in sections 2.2, 2.3, and 2.4 we present overviews of legged locomotion, wheeled locomotion, and aerial locomotion techniques for mobile robots.

2.1.1 Key issues for locomotion

Locomotion is the complement of manipulation. In manipulation, the robot arm is fixed but moves objects in the workspace by imparting force to them. In locomotion, the environment is fixed and the robot moves by imparting force to the environment. In both cases, the scientific basis is the study of actuators that generate interaction forces and mechanisms

that implement desired kinematic and dynamic properties. Locomotion and manipulation thus share the same core issues of stability, contact characteristics, and environmental type:

- stability
 - number and geometry of contact points
 - center of gravity
 - static/dynamic stability
 - inclination of terrain
- characteristics of contact
 - contact point/path size and shape
 - angle of contact
 - friction
- type of environment
 - structure
 - medium (e.g., water, air, soft or hard ground)

A theoretical analysis of locomotion begins with mechanics and physics. From this starting point, we can formally define and analyze all manner of mobile robot locomotion systems. However, this book focuses on the mobile robot *navigation* problem, particularly stressing perception, localization, and cognition. Thus, we will not delve deeply into the physical basis of locomotion. Nevertheless, the three remaining sections in this chapter present overviews of issues in legged locomotion [52], wheeled locomotion, and aerial locomotion. Chapter 3 presents a more detailed analysis of the kinematics and control of wheeled mobile robots.

2.2 Legged Mobile Robots

Legged locomotion is characterized by a series of point contacts between the robot and the ground. The key advantages include adaptability and maneuverability in rough terrain (figure 2.5). Because only a set of point contacts is required, the quality of the ground between those points does not matter as long as the robot can maintain adequate ground clearance. In addition, a walking robot is capable of crossing a hole or chasm so long as its reach exceeds the width of the hole. A final advantage of legged locomotion is the potential to manipulate objects in the environment with great skill. An excellent insect example, the dung beetle, is capable of rolling a ball while locomoting by way of its dexterous front legs.

The main disadvantages of legged locomotion include power and mechanical complexity. The leg, which may include several degrees of freedom, must be capable of sustaining part of the robot's total weight, and in many robots it must be capable of lifting and lowering the robot. Additionally, high maneuverability will only be achieved if the legs have a

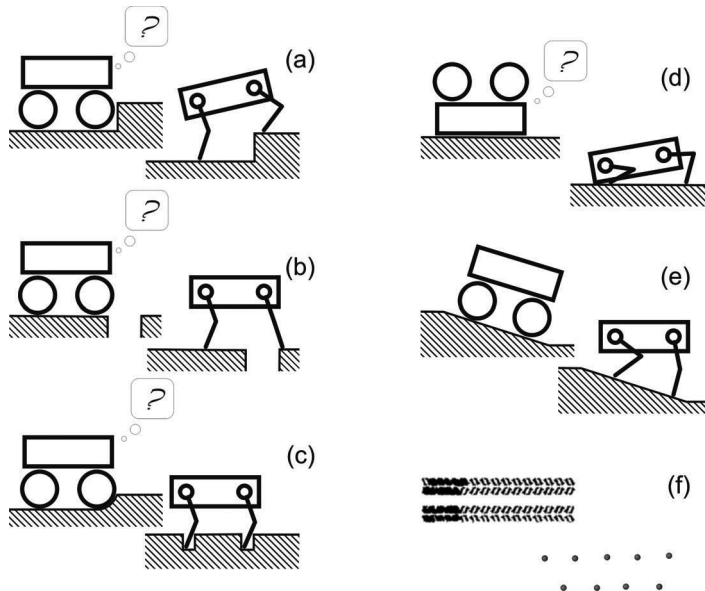


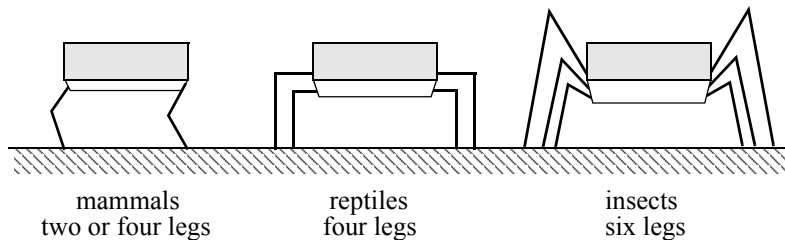
Figure 2.5 Legged robots are particularly suited for rough terrain, where they are able to traverse obstacles such as steps (a), gaps (b), or sandy patches (c) that are impassable for wheeled systems. Additionally, the high number of degrees of freedom allows the robot to stand up when fallen (d) and keep its payload leveled (e). Because legged systems do not require a continuous path for support, they can rely on a few selected footholds, which also reduces the environmental impact (f). Image courtesy of D. Remy.

sufficient number of degrees of freedom to impart forces in a number of different directions.

2.2.1 Leg configurations and stability

Because legged robots are biologically inspired, it is instructive to examine biologically successful legged systems. A number of different leg configurations have been successful in a variety of organisms (figure 2.6). Large animals, such as mammals and reptiles, have four legs, whereas insects have six or more legs. In some mammals, the ability to walk on only two legs has been perfected. Especially in the case of humans, balance has progressed to the point that we can even jump with one leg.¹ This exceptional maneuverability comes at a price: much more complex active control to maintain balance.

1. In child development, one of the tests used to determine if the child is acquiring advanced locomotion skills is the ability to jump on one leg.

**Figure 2.6**

Arrangement of the legs of various animals.

In contrast, a creature with three legs can exhibit a static, stable pose provided that it can ensure that its center of gravity is within the tripod of ground contact. Static stability, demonstrated by a three-legged stool, means that balance is maintained with no need for motion. A small deviation from stability (e.g., gently pushing the stool) is passively corrected toward the stable pose when the upsetting force stops.

But a robot must be able to lift its legs in order to walk. In order to achieve static walking, a robot must have at least four legs, moving one of it at a time. For six legs, it is possible to design a gait in which a statically stable tripod of legs is in contact with the ground at all times (figure 2.9).

Insects and spiders are immediately able to walk when born. For them, the problem of balance during walking is relatively simple. Mammals, with four legs, can achieve static walking, which, however, is less stable due to the high center of gravity than, for example, reptile walking. Fawns, for example, spend several minutes attempting to stand before they are able to do so, then spend several more minutes learning to walk without falling. Humans, with two legs, can also stand statically stable due to their large feet. Infants require months to stand and walk, and even longer to learn to jump, run, and stand on one leg.

There is also the potential for great variety in the complexity of each individual leg. Once again, the biological world provides ample examples at both extremes. For instance, in the case of the caterpillar, each leg is extended using hydraulic pressure by constricting the body cavity and forcing an increase in pressure, and each leg is retracted longitudinally by relaxing the hydraulic pressure, then activating a single tensile muscle that pulls the leg in toward the body. Each leg has only a single degree of freedom, which is oriented longitudinally along the leg. Forward locomotion depends on the hydraulic pressure in the body, which extends the distance between pairs of legs. The caterpillar leg is therefore mechanically very simple, using a minimal number of extrinsic muscles to achieve complex overall locomotion.

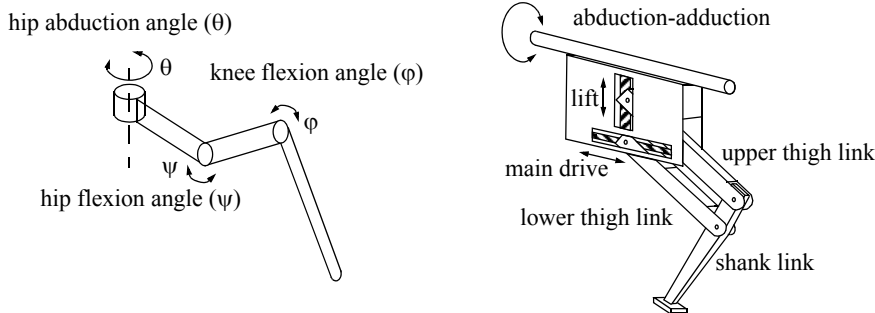


Figure 2.7
Two examples of legs with three degrees of freedom.

At the other extreme, the human leg has more than seven major degrees of freedom, combined with further actuation at the toes. More than fifteen muscle groups actuate eight complex joints.

In the case of legged mobile robots, a minimum of two degrees of freedom is generally required to move a leg forward by lifting the leg and swinging it forward. More common is the addition of a third degree of freedom for more complex maneuvers, resulting in legs such as those shown in figure 2.7. Recent successes in the creation of bipedal walking robots have added a fourth degree of freedom at the ankle joint. The ankle enables the robot to shift the resulting force vector of the ground contact by actuating the pose of the sole of the foot.

In general, adding degrees of freedom to a robot leg increases the maneuverability of the robot, both augmenting the range of terrains on which it can travel and the ability of the robot to travel with a variety of gaits. The primary disadvantages of additional joints and actuators are, of course, energy, control, and mass. Additional actuators require energy and control, and they also add to leg mass, further increasing power and load requirements on existing actuators.

In the case of a multilegged mobile robot, there is the issue of leg coordination for locomotion, or gait control. The number of possible gaits depends on the number of legs [52]. The gait is a sequence of lift and release events for the individual legs. For a mobile robot with k legs, the total number of distinct event sequences N for a walking machine is:

$$N = (2k - 1)! \quad (2.1)$$

For a biped walker $k = 2$ legs, the number of distinct event sequences N is:

$$N = (2k - 1)! = 3! = 3 \cdot 2 \cdot 1 = 6 \quad (2.2)$$

The six distinct event sequences that can be combined for more complex sequences are:

1. both legs down – right down / left up – both legs down;
2. both legs down – right leg up / left leg down – both legs down;
3. both legs down – both legs up – both legs down;
4. right leg down / left leg up – right leg up / left leg down – right leg down / left leg up;
5. right leg down / left leg up – both legs up – right leg down / left leg up;
6. right leg up / left leg down – both legs up – right leg up / left leg down.

Of course, this quickly grows quite large. For example, a robot with six legs has far more events:

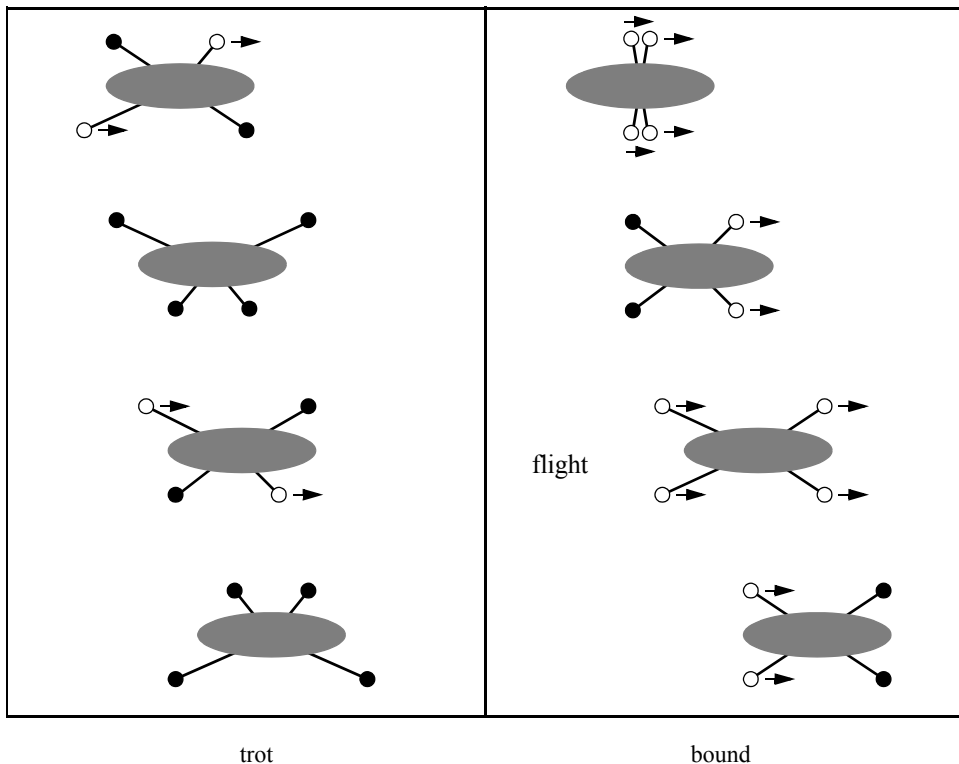
$$N = 11! = 39916800, \quad (2.3)$$

with an even higher number of theoretically possible gaits.

Figures 2.8 and 2.9 depict several four-legged gaits and the static six-legged tripod gait.

2.2.2 Consideration of dynamics

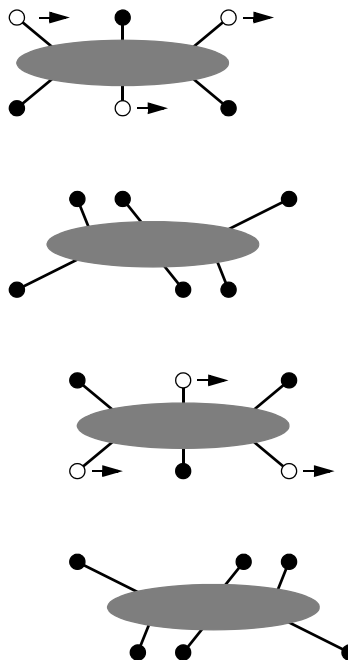
The *cost of transportation* expresses how much energy a robot uses to travel a certain distance. To better compare differently sized systems, this value is usually normalized by the robot's weight and expressed in $J/(N \cdot m)$ —a dimensionless quantity—where J stands for joule, N for newton, and m for meter. When a robot moves with constant speed on a level surface, its potential and kinetic energy remain constant. In theory, no physical work is necessary to keep it moving, which makes it possible to get from one place to another with zero cost of transportation. In reality, however, some energy is always dissipated, and robots have to be equipped with actuators and batteries to compensate for the losses. For a wheeled robot, the main causes for such losses are the friction in the drive train and the rolling resistance of the wheels on the ground. Similarly, friction is present in the joints of legged systems and energy is dissipated by the foot-ground interaction. However, these effects cannot explain why legged systems usually consume considerably more energy than their wheeled counterparts. The bulk part of energy loss actually originates in the fact that legs—in contrast to wheels or tracks—are not performing a continuous motion, but are periodically moving back and forth. Joints have to undergo alternating phases of acceleration and deceleration, and, as we have only a very limited ability to recuperate the negative work of deceleration, energy is irrecoverably lost in the process. Because of the segmented structure of

**Figure 2.8**

Two gaits with four legs.

the legs, it can even happen that energy that is fed into one joint (e.g., the knee) is simultaneously dissipated in another joint (e.g., the hip) without creating any net work at the feet. Therefore, actuators are working against each other [180].

A solution to this problem is a better exploitation of the dynamics of the mechanical structure. The natural oscillations of pendula and springs, can—if they are well designed—automatically create the required periodic motions. For example, the motion of a swinging leg can be grasped by the dynamics of a simple double pendulum. If the lengths and the inertial properties of the leg segments are correctly selected, such a pendulum will automatically swing forward, clear the ground, and extend the leg to touch the ground in front of the main body. If, on the other side, a foot is on the ground and the leg is kept stiff, an inverted pendulum motion will efficiently propel the main body forward. During running, these inverted pendulum dynamics are additionally enhanced by springs, which store

**Figure 2.9**

Static walking with six legs. A tripod formed by three legs always exists.

energy during the ground phase and allow the main body to take off for the subsequent flight phase (figure 2.10).

With this approach it is, in fact, possible to build legged robots that do not have actuation of any kind. Such passive dynamic walkers [211,344] walk down a shallow incline (which compensates for frictional losses), but, because no actuators are present, no negative work is performed and energetic losses due to braking are eliminated. In addition to creating a periodic motion, the dynamics of such walkers must be designed to ensure dynamic stability. The mechanical structure must passively reject small disturbances which would otherwise accumulate over time and eventually cause the robot to fall. Actuated robots built according to these principles can walk with a remarkable efficiency [104] and one of them, the Cornell Ranger, currently holds the distance record for autonomous legged robots [345] (figure 2.11).

Passive dynamic walkers also have a striking similarity to the physique and motion patterns of human gait. During the evolution, humans and animals have become quite efficient walkers, and a look at electromyography recordings shows that during walking our muscles

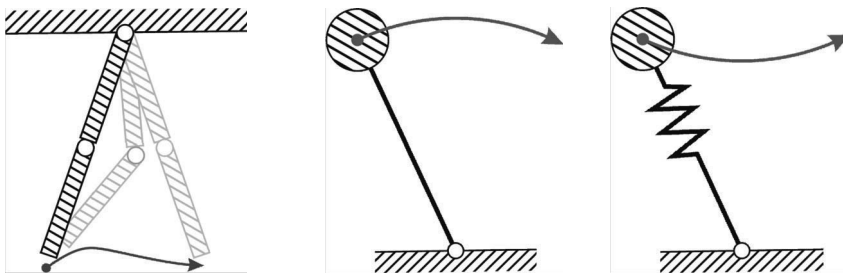


Figure 2.10 Dynamic elements that are exploited in energy efficient walking include the double-pendulum for leg swing, the inverted pendulum for the stance phase of walking, and springy legs for running gaits. Image courtesy of D. Remy.

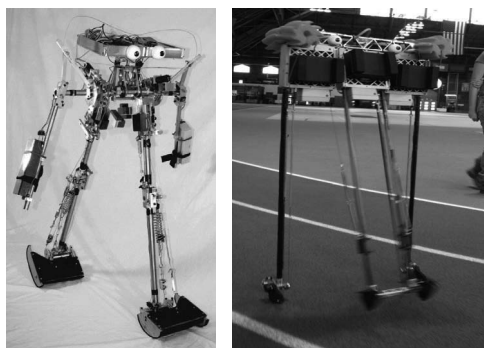


Figure 2.11 The Cornell powered two-legged and four-legged biped robots. In April 2008, the four-legged bipedal robot Ranger walked a distance of 9.07 km without being touched by a person. Image courtesy of the Biorobotics and Locomotion Lab—Cornell University.

are far less active than one would expect for a task in which most of our limbs are in constant motion. To some degree, humans are passive dynamic walkers.

It is obvious that such an exploitation of the mechanical dynamics can only work at specific velocities. When the locomotion speed changes, characteristic properties such as stride length or stride frequency change as well, and—because these have to be matched with the spring and pendulum oscillations of the mechanical structure—more and more actuator effort is needed to force the joints to follow their required trajectories. For human walking, the optimal walking speed is approximately 1 m/s, which is also the range that subjectively feels most comfortable. For both higher and lower speeds, the cost of transportation will increase, and more energy is needed to travel the same distance. For this reason, humans change their gait from walking to running when they want to travel at higher speeds, which is more efficient than just performing the same motion faster and faster.

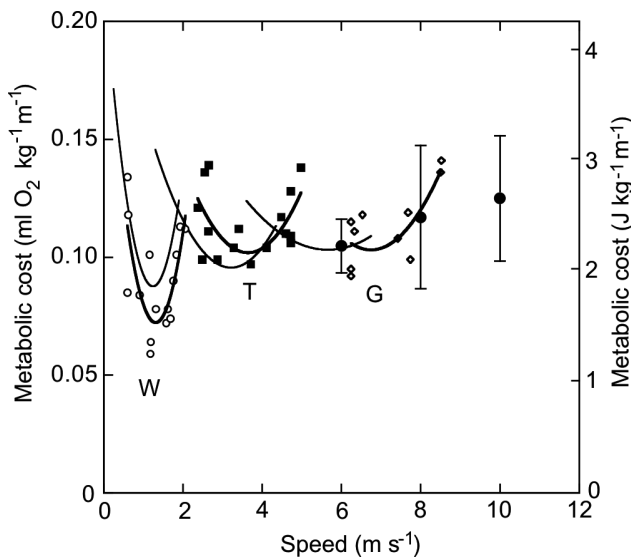


Figure 2.12 Metabolic cost of transportation (here normalized by body mass) for different gaits of horses: walking (W), running (R), and galloping (G). Each gait has a specific velocity that minimizes energy expenditure. This explains why animals and humans change their gait when traveling at different speeds. Image courtesy of A. E. Minetti [221].

Changing the gait allows us to use a different set of natural dynamics, which better matches the stride frequency and step length that are needed for higher velocities. Likewise, the wide variety of gaits found in animals can be explained by the use of different sets of dynamic elements, which minimize the energy necessary for transportation (figure 2.12).

2.2.3 Examples of legged robot locomotion

Although there are no high-volume industrial applications to date, legged locomotion is an important area of long-term research. Several interesting designs are presented here, beginning with the one-legged robot and finishing with six-legged robots.

2.2.3.1 One leg

The minimum number of legs a legged robot can have is, of course, one. Minimizing the number of legs is beneficial for several reasons. Body mass is particularly important to walking machines, and the single leg minimizes cumulative leg mass. Leg coordination is required when a robot has several legs, but with one leg no such coordination is needed. Perhaps most important, the one-legged robot maximizes the basic advantage of legged locomotion: legs have single points of contact with the ground in lieu of an entire track, as

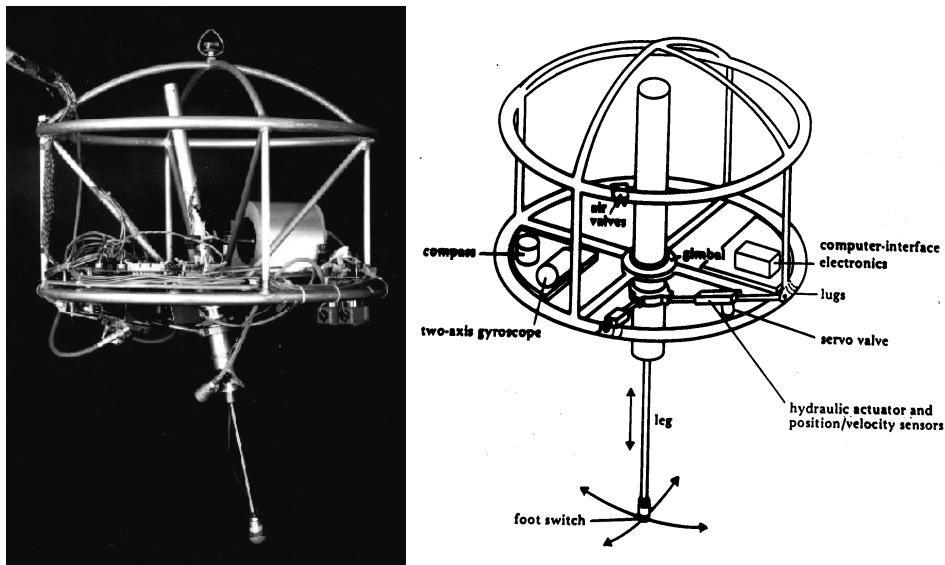


Figure 2.13

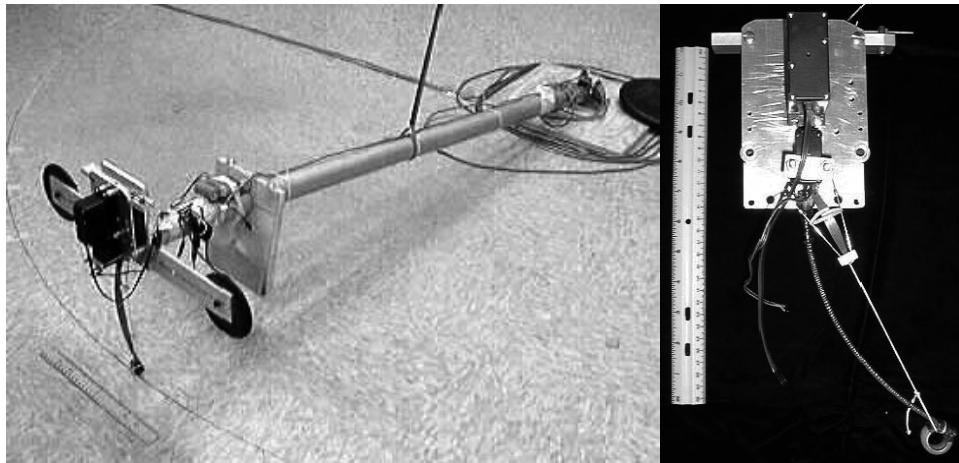
The Raibert hopper [42, 264]. Image courtesy of the LegLab and Marc Raibert. © 1983.

with wheels. A single-legged robot requires only a sequence of single contacts, making it amenable to the roughest terrain. Furthermore, a hopping robot can dynamically cross a gap that is larger than its stride by taking a running start, whereas a multilegged walking robot that cannot run is limited to crossing gaps that are as large as its reach.

The major challenge in creating a single-legged robot is balance. For a robot with one leg, static walking is not only impossible, but static stability when stationary is also impossible. The robot must actively balance itself by either changing its center of gravity or by imparting corrective forces. Thus, the successful single-legged robot must be dynamically stable.

Figure 2.13 shows the Raibert hopper [42, 264], one of the best-known single-legged hopping robots created. This robot makes continuous corrections to body attitude and to robot velocity by adjusting the leg angle with respect to the body. The actuation is hydraulic, including high-power longitudinal extension of the leg during stance to hop back into the air. Although powerful, these actuators require a large, off-board hydraulic pump to be connected to the robot at all times.

Figure 2.14 shows a more energy-efficient design that takes advantage of well-designed mechanical dynamics [83]. Instead of supplying power by means of an off-board hydraulic pump, the bow leg hopper is designed to capture the kinetic energy of the robot as it lands,

**Figure 2.14**

The 2D single bow leg hopper [83]. Image courtesy of H. Benjamin Brown and Garth Zeglin, CMU.

using an efficient bow spring leg. This spring returns approximately 85% of the energy, meaning that stable hopping requires only the addition of 15% of the required energy on each hop. This robot, which is constrained along one axis by a boom, has demonstrated continuous hopping for 20 minutes using a single set of batteries carried on board the robot. As with the Raibert hopper, the bow leg hopper controls velocity by changing the angle of the leg to the body at the hip joint.

Ringrose [266] demonstrates the very important duality of mechanics and controls as applied to a single-legged hopping machine. Often clever mechanical design can perform the same operations as complex active control circuitry. In this robot, the physical shape of the foot is exactly the right curve so that when the robot lands without being perfectly vertical, the proper corrective force is provided from the impact, making the robot vertical by the next landing. This robot is dynamically stable, and is furthermore passive. The correction is provided by physical interactions between the robot and its environment, with no computer or any active control in the loop.

2.2.3.2 Two legs (biped)

A variety of successful bipedal robots have been demonstrated over the past ten years. Two legged robots have been shown to run, jump, travel up and down stairways, and even do aerial tricks such as somersaults. In the commercial sector, both Honda and Sony have made significant advances over the past decade that have enabled highly capable bipedal robots. Both companies designed small, powered joints that achieve power-to-weight per-

**Specifications:**

Weight:	7 kg
Height:	58 cm
Neck DOF:	4
Body DOF:	2
Arm DOF:	2×5
Legs DOF:	2×6
Five-finger Hands	

Figure 2.15

The Sony SDR-4X II. © 2003 Sony Corporation.

formance unheard of in commercially available servomotors. These new “intelligent” servos provide not only strong actuation but also compliant actuation by means of torque sensing and closed-loop control.

The Sony Dream Robot, model SDR-4X II, is shown in figure 2.15. This current model is the result of research begun in 1997 with the basic objective of motion entertainment and communication entertainment (i.e., dancing and singing). This robot with thirty-eight degrees of freedom has seven microphones for fine localization of sound, image person recognition, on-board miniature stereo depth-map reconstruction, and limited speech recognition. Given the goal of fluid and entertaining motion, Sony spent considerable effort designing a motion prototyping application system to enable their engineers to script dances in a straightforward manner. Note that the SDR-4X II is relatively small, standing at 58 cm and weighing only 7 kg.

The Honda humanoid project has a significant history, but, again, it has tackled the very important engineering challenge of actuation. Figure 2.16 shows model P2, which is an immediate predecessor to the most recent Asimo (advanced step in innovative mobility) model. Note that the latest Honda Asimo model is still much larger than the SDR-4X at 120 cm tall and 52 kg. This enables practical mobility in the human world of stairs and ledges while maintaining a nonthreatening size and posture. Perhaps the first robot to demonstrate



Specifications:

Maximum speed:	2 km/h
Autonomy:	15 min
Weight:	210 kg
Height:	1.82 m
Leg DOF:	2 × 6
Arm DOF:	2 × 7

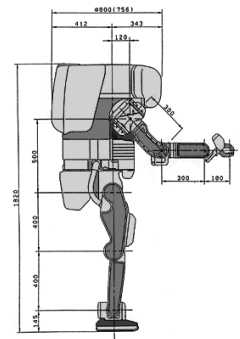


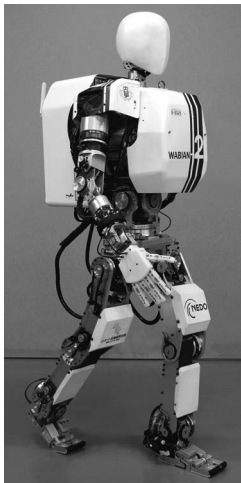
Figure 2.16

The humanoid robot P2 from Honda, Japan. © Honda Motor Cooperation.

biomimetic bipedal stair climbing and descending, these Honda humanoid series robots are being designed not for entertainment purposes but as human aids throughout society. Honda refers, for instance, to the height of Asimo as the minimum height that enables it to manage nonetheless operation of the human world, for instance, control of light switches.

An important feature of bipedal robots is their anthropomorphic shape. They can be built to have the same approximate dimensions as humans, and this makes them excellent vehicles for research in human-robot interaction. WABIAN-2R is a robot built at Waseda University, Japan (figure 2.17) for just such research [255]. WABIAN-2R is designed to emulate human motion, and it is even designed to dance like a human.

Bipedal robots can only be statically stable within some limits, and so robots such as P2 and WABIAN-2R generally must perform continuous balance-correcting servoing even when standing still. Furthermore, each leg must have sufficient capacity to support the full weight of the robot. In the case of four-legged robots, the balance problem is facilitated along with the load requirements of each leg. An elegant design of a biped robot is the Spring Flamingo of MIT (figure 2.18). This robot inserts springs in series with the leg actuators to achieve a more elastic gait. Combined with “kneecaps” that limit knee joint angles, the Flamingo achieves surprisingly biomimetic motion.

**Specifications:**

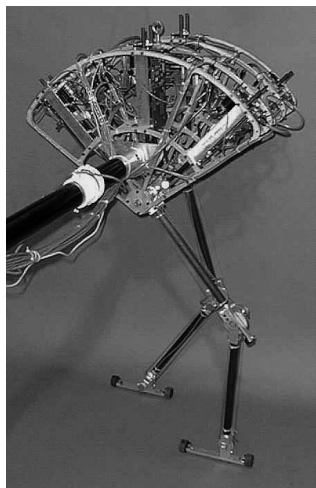
Weight: 64 [kg] (with batteries)
Height: 1.55 [m]

DOF:

Leg:	6×2
Foot:	1×2 (passive)
Waist:	2
Trunk:	2
Arm:	7×2
Hand:	3×2
Neck:	3

Figure 2.17

The humanoid robot WABIAN-2R developed at Waseda University in Japan [255] (<http://www.takanishi.mech.waseda.ac.jp/>). © Atsuo Takanishi Lab, Waseda University.

**Figure 2.18**

The Spring Flamingo developed at MIT [262]. Image courtesy of Jerry Pratt, MIT Leg Laboratory.

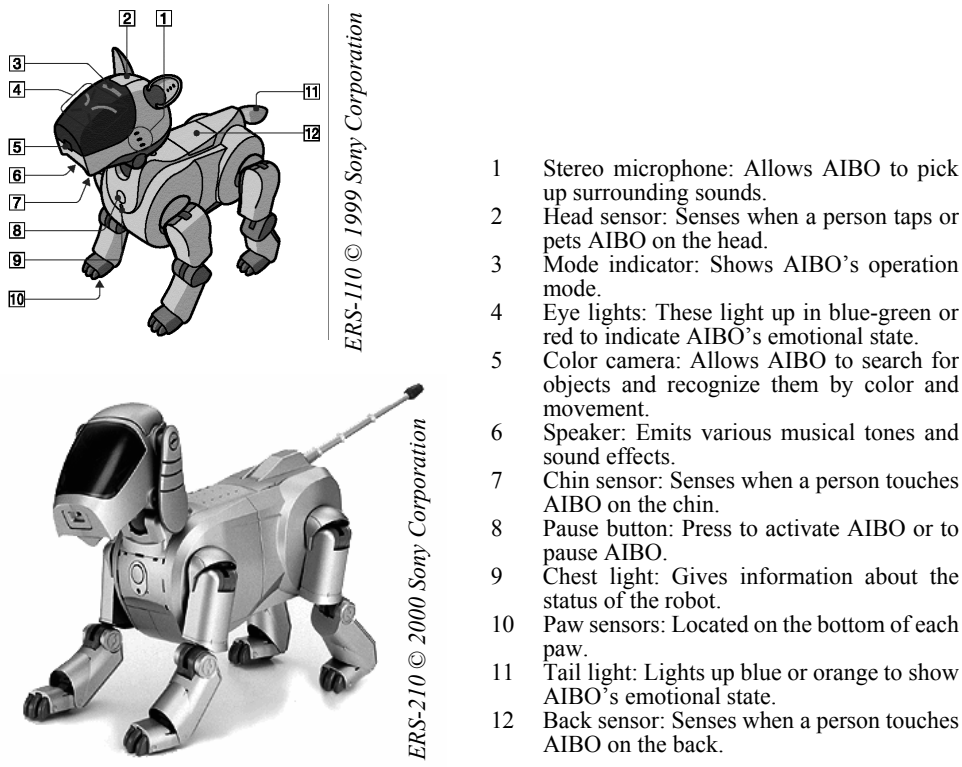


Figure 2.19
AIBO, the artificial dog from Sony, Japan.

2.2.3.3 Four legs (quadruped)

Although standing still on four legs is passively stable, walking remains challenging because to remain stable, the robot's center of gravity must be actively shifted during the gait. Sony invested several million dollars to develop a four-legged robot called AIBO (figure 2.19). To create this robot, Sony produced both a new robot operating system that is near real-time and new geared servomotors that are of sufficiently high torque to support the robot, yet are back-drivable for safety. In addition to developing custom motors and software, Sony incorporated a color vision system that enables AIBO to chase a brightly colored ball. The robot is able to function for at most one hour before requiring recharging. Early sales of the robot have been very strong, with more than 60,000 units sold in the first year. Nevertheless, the number of motors and the technology investment behind this robot dog resulted in a very high price of approximately \$1,500.

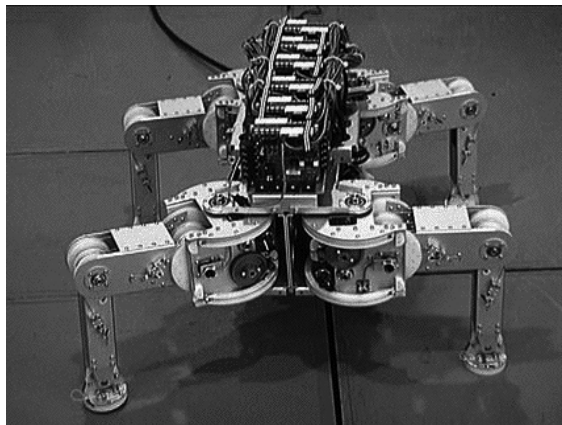


Figure 2.20

Titan VIII, a quadruped robot developed at Tokyo Institute of Technology (<http://www-robot.mes.titech.ac.jp>). © Tokyo Institute of Technology.

Specifications:

Weight:	19 kg
Height:	0.25 m
DOF:	4×3

Four-legged robots have the potential to serve as effective artifacts for research in human-robot interaction (figure 2.20). Humans can treat the Sony robot, for example, as a pet and might develop an emotional relationship similar to that between man and dog. Furthermore, Sony has designed AIBO's walking style and general behavior to emulate learning and maturation, resulting in dynamic behavior over time that is more interesting for the owner who can track the changing behavior. As the challenges of high energy storage and motor technology are solved, it is likely that quadruped robots much more capable than AIBO will become common throughout the human environment.

BigDog and LittleDog (figure 2.21) are two recent examples of quadruped robots developed by Boston Dynamics and commissioned by the American Defense Advanced Research Projects Agency (DARPA). BigDog is a rough-terrain robot that walks, runs, climbs, and carries heavy loads. It is powered by an engine that drives a hydraulic actuation system. Its legs are articulated like an animal's, with compliant elements to absorb shock and recycle energy between two steps. The goal of this project is to make it able to go anywhere people and animals can go. The program is funded by the Tactical Technology Office at DARPA. Conversely, LittleDog is a small-size robot designed for research on learning locomotion. Each leg has a large range of motion and is powered by three electric motors. Therefore, the robot is strong enough for climbing and dynamic locomotion gaits.

Another example four-legged robot is ALoF, the quadruped developed at the ASL (ETH Zurich) (figure 2.22). This robot serves as a platform to study energy-efficient locomotion. This is done by exploiting passive dynamic in ways that have shown to be effective in bipedal robots, as has been explained in section 2.2.2.



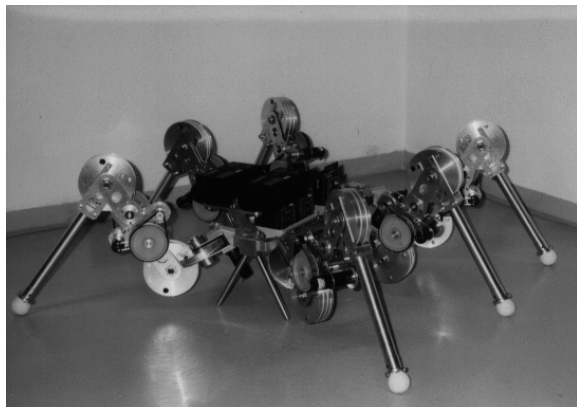
Figure 2.21 LittleDog and BigDog quadruped robots developed by Boston Dynamics. Image courtesy of Boston Dynamics (<http://www.bostondynamics.com>).



Figure 2.22 ALoF, the quadruped robot developed at the ASL (ETH Zurich), has been built to investigate energy efficient locomotion. This is done by exploiting passive dynamics (<http://www.asl.ethz.ch/>). © ASL-ETH Zurich.

2.2.3.4 Six legs (hexapod)

Six-legged configurations have been extremely popular in mobile robotics because of their static stability during walking, thus reducing the control complexity (figures 2.23 and 1.3). In most cases, each leg has three degrees of freedom, including hip flexion, knee flexion,



Specifications:

Maximum speed:	0.5 m/s
Weight:	16 kg
Height:	0.3 m
Length:	0.7 m
No. of legs:	6
DOF in total:	6×3
Power consumption:	10 W

Figure 2.23

Laron II, a hexapod platform developed at the University of Karlsruhe, Germany.
© University of Karlsruhe.

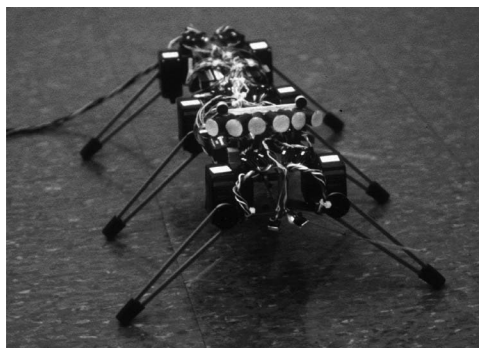


Figure 2.24

Genghis, one of the most famous walking robots from MIT, uses hobby servomotors as its actuators (<http://www.ai.mit.edu/projects/genghis>). © MIT AI Lab.

and hip abduction (see figure 2.7). Genghis is a commercially available hobby robot that has six legs, each of which has two degrees of freedom provided by hobby servos (figure 2.24). Such a robot, which consists only of hip flexion and hip abduction, has less maneuverability in rough terrain but performs quite well on flat ground. Because it consists of a straightforward arrangement of servomotors and straight legs, such robots can be readily built by a robot hobbyist.

Insects, which are arguably the most successful locomoting creatures on earth, excel at traversing all forms of terrain with six legs, even upside down. Currently, the gap between

the capabilities of six-legged insects and artificial six-legged robots is still quite large. Interestingly, this is not due to a lack of sufficient numbers of degrees of freedom on the robots. Rather, insects combine a small number of active degrees of freedom with passive structures, such as microscopic barbs and textured pads, that increase the gripping strength of each leg significantly. Robotic research into such passive tip structures has only recently begun. For example, a research group is attempting to re-create the complete mechanical function of the cockroach leg [124].

It is clear from these examples that legged robots have much progress to make before they are competitive with their biological equivalents. Nevertheless, significant gains have been realized recently, primarily due to advances in motor design. Creating actuation systems that approach the efficiency of animal muscles remains far from the reach of robotics, as does energy storage with the energy densities found in organic life forms.

2.3 Wheeled Mobile Robots

The wheel has been by far the most popular locomotion mechanism in mobile robotics and in man-made vehicles in general. It can achieve very good efficiencies, as demonstrated in figure 2.3, and it does so with a relatively simple mechanical implementation.

In addition, balance is not usually a research problem in wheeled robot designs, because wheeled robots are almost always designed so that all wheels are in ground contact at all times. Thus, three wheels are sufficient to guarantee stable balance, although, as we shall see below, two-wheeled robots can also be stable. When more than three wheels are used, a suspension system is required to allow all wheels to maintain ground contact when the robot encounters uneven terrain.

Instead of worrying about balance, wheeled robot research tends to focus on the problems of traction and stability, maneuverability, and control: can the robot wheels provide sufficient traction and stability for the robot to cover all of the desired terrain, and does the robot's wheeled configuration enable sufficient control over the velocity of the robot?

2.3.1 Wheeled locomotion: The design space

As we shall see, there is a very large space of possible wheel configurations when one considers possible techniques for mobile robot locomotion. We begin by discussing the wheel in detail, since there are a number of different wheel types with specific strengths and weaknesses. We then examine complete wheel configurations that deliver particular forms of locomotion for a mobile robot.

2.3.1.1 Wheel design

There are four major wheel classes, as shown in figure 2.25. They differ widely in their kinematics, and therefore the choice of wheel type has a large effect on the overall kinemat-

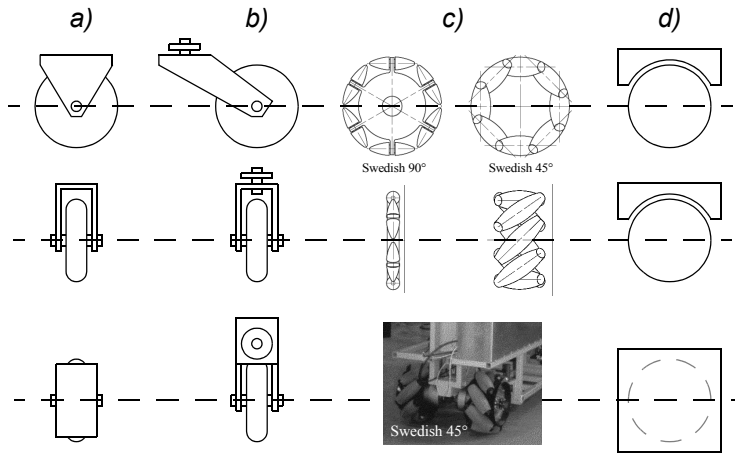


Figure 2.25

The four basic wheel types. (a) Standard wheel: two degrees of freedom; rotation around the (motorized) wheel axle and the contact point.(b) castor wheel: two degrees of freedom; rotation around an offset steering joint. (c) Swedish wheel: three degrees of freedom; rotation around the (motorized) wheel axle, around the rollers, and around the contact point. (d) Ball or spherical wheel: realization technically difficult.

ics of the mobile robot. The standard wheel and the castor wheel have a primary axis of rotation and are thus highly directional. To move in a different direction, the wheel must be steered first along a vertical axis. The key difference between these two wheels is that the standard wheel can accomplish this steering motion with no side effects, since the center of rotation passes through the contact patch with the ground, whereas the castor wheel rotates around an offset axis, causing a force to be imparted to the robot chassis during steering.

The Swedish wheel and the spherical wheel are both designs that are less constrained by directionality than the conventional standard wheel. The Swedish wheel functions as a normal wheel but provides low resistance in another direction as well, sometimes perpendicular to the conventional direction, as in the Swedish 90, and sometimes at an intermediate angle, as in the Swedish 45. The small rollers attached around the circumference of the wheel are passive and the wheel's primary axis serves as the only actively powered joint. The key advantage of this design is that, although the wheel rotation is powered only along the one principal axis (through the axle), the wheel can kinematically move with very little friction along many possible trajectories, not just forward and backward.

The spherical wheel is a truly omnidirectional wheel, often designed so that it may be actively powered to spin along any direction. One mechanism for implementing this spherical design imitates the computer mouse, providing actively powered rollers that rest against the top surface of the sphere and impart rotational force.



Figure 2.26

The Tartan Racing self-driving vehicle developed at CMU, which won the 2007 DARPA Urban Challenge. Image courtesy of the Tartan Racing Team—<http://www.tartanracing.org>.

Regardless of what wheel is used, in robots designed for all-terrain environments and in robots with more than three wheels, a suspension system is normally required to maintain wheel contact with the ground. One of the simplest approaches to suspension is to design flexibility into the wheel itself. For instance, in the case of some four-wheeled indoor robots that use castor wheels, manufacturers have applied a deformable tire of soft rubber to the wheel to create a primitive suspension. Of course, this limited solution cannot compete with a sophisticated suspension system in applications where the robot needs a more dynamic suspension for significantly nonflat terrain.

2.3.1.2 Wheel geometry

The choice of wheel types for a mobile robot is strongly linked to the choice of wheel arrangement, or wheel geometry. The mobile robot designer must consider these two issues simultaneously when designing the locomoting mechanism of a wheeled robot. Why do wheel type and wheel geometry matter? Three fundamental characteristics of a robot are governed by these choices: maneuverability, controllability, and stability.

Unlike automobiles, which are largely designed for a highly standardized environment (the road network), mobile robots are designed for applications in a wide variety of situations. Automobiles all share similar wheel configurations because there is one region in the design space that maximizes maneuverability, controllability, and stability for their standard environment: the paved roadway. However, there is no single wheel configuration that maximizes these qualities for the variety of environments faced by different mobile robots. So you will see great variety in the wheel configurations of mobile robots. In fact, few robots use the Ackerman wheel configuration of the automobile because of its poor maneuverability, with the exception of mobile robots designed for the road system (figure 2.26).

Table 2.1 gives an overview of wheel configurations ordered by the number of wheels. This table shows both the selection of particular wheel types and their geometric configuration on the robot chassis. Note that some of the configurations shown are of little use in mobile robot applications. For instance, the two-wheeled bicycle arrangement has moderate maneuverability and poor controllability. Like a single-legged hopping machine, it can never stand still. Nevertheless, this table provides an indication of the large variety of wheel configurations that are possible in mobile robot design.

The number of variations in table 2.1 is quite large. However, there are important trends and groupings that can aid in comprehending the advantages and disadvantages of each configuration. We next identify some of the key trade-offs in terms of the three issues we identified earlier: stability, maneuverability, and controllability.

2.3.1.3 Stability

Surprisingly, the minimum number of wheels required for static stability is two. As shown above, a two-wheel differential-drive robot can achieve static stability if the center of mass is below the wheel axle. Cye is a commercial mobile robot that uses this wheel configuration (figure 2.27).

However, under ordinary circumstances such a solution requires wheel diameters that are impractically large. Dynamics can also cause a two-wheeled robot to strike the floor with a third point of contact, for instance, with sufficiently high motor torques from standstill. Conventionally, static stability requires a minimum of three wheels, with the additional caveat that the center of gravity must be contained within the triangle formed by the ground contact points of the wheels. Stability can be further improved by adding more wheels, although once the number of contact points exceeds three, the hyperstatic nature of the geometry will require some form of flexible suspension on uneven terrain.

2.3.1.4 Maneuverability

Some robots are omnidirectional, meaning that they can move at any time in any direction along the ground plane (x, y) regardless of the orientation of the robot around its vertical axis. This level of maneuverability requires wheels that can move in more than just one direction, and so omnidirectional robots usually employ Swedish or spherical wheels that are powered. A good example is Uranus (figure 2.30), a robot that uses four Swedish wheels to rotate and translate independently and without constraints.

In general, the ground clearance of robots with Swedish and spherical wheels is somewhat limited due to the mechanical constraints of constructing omnidirectional wheels. An interesting recent solution to the problem of omnidirectional navigation while solving this ground-clearance problem is the four-castor wheel configuration in which each castor wheel is actively steered and actively translated. In this configuration, the robot is truly omnidirectional because, even if the castor wheels are facing a direction perpendicular to

Table 2.1

Wheel configurations for rolling vehicles

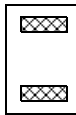
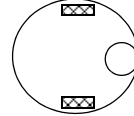
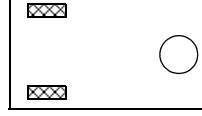
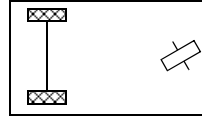
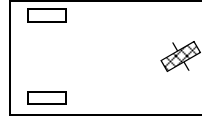
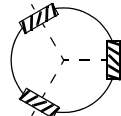
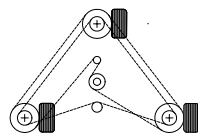
# of wheels	Arrangement	Description	Typical examples
2		One steering wheel in the front, one traction wheel in the rear	Bicycle, motorcycle
		Two-wheel differential drive with the center of mass (COM) below the axle	Cye personal robot
3		Two-wheel centered differential drive with a third point of contact	Nomad Scout, smartRob EPFL
		Two independently driven wheels in the rear/front, one unpowered omnidirectional wheel in the front/rear	Many indoor robots, including the EPFL robots Pygmalion and Alice
		Two connected traction wheels (differential) in rear, one steered free wheel in front	Piaggio minitrucks
		Two free wheels in rear, one steered traction wheel in front	Neptune (Carnegie Mellon University), Hero-1
		Three motorized Swedish or spherical wheels arranged in a triangle; omnidirectional movement is possible	Stanford wheel Tribolo EPFL, Palm Pilot Robot Kit (CMU)
		Three synchronously motorized and steered wheels; the orientation is not controllable	“Synchro drive” Denning MRV-2, Georgia Institute of Technology, I-Robot B24, Nomad 200

Table 2.1

Wheel configurations for rolling vehicles

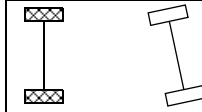
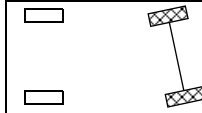
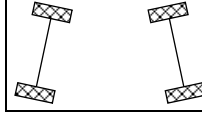
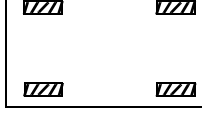
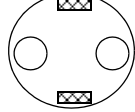
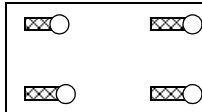
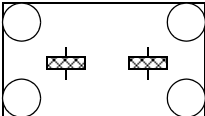
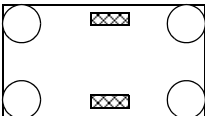
# of wheels	Arrangement	Description	Typical examples
4		Two motorized wheels in the rear, two steered wheels in the front; steering has to be different for the two wheels to avoid slipping/skidding.	Car with rear-wheel drive
		Two motorized and steered wheels in the front, two free wheels in the rear; steering has to be different for the two wheels to avoid slipping/skidding.	Car with front-wheel drive
		Four steered and motorized wheels	Four-wheel drive, four-wheel steering Hyperion (CMU)
		Two traction wheels (differential) in rear/front, two omnidirectional wheels in the front/rear	Charlie (DMT-EPFL)
		Four omnidirectional wheels	Carnegie Mellon Uranus
		Two-wheel differential drive with two additional points of contact	EPFL Khepera, Hyperbot Chip
		Four motorized and steered castor wheels	Nomad XR4000

Table 2.1

Wheel configurations for rolling vehicles

# of wheels	Arrangement	Description	Typical examples
6		Two motorized and steered wheels aligned in center, one omnidirectional wheel at each corner	First
		Two traction wheels (differential) in center, one omnidirectional wheel at each corner	Terregator (Carnegie Mellon University)
Icons for the each wheel type are as follows:			
	unpowered omnidirectional wheel (spherical, castor, Swedish)		
	motorized Swedish wheel (Stanford wheel)		
	unpowered standard wheel		
	motorized standard wheel		
	motorized and steered castor wheel		
	steered standard wheel		
	connected wheels		

the desired direction of travel, the robot can still move in the desired direction by steering these wheels. Because the vertical axis is offset from the ground-contact path, the result of this steering motion is robot motion.

In the research community, other classes of mobile robots are popular that achieve high maneuverability, only slightly inferior to that of the omnidirectional configurations. In such robots, motion in a particular direction may initially require a rotational motion. With a circular chassis and an axis of rotation at the center of the robot, such a robot can spin without

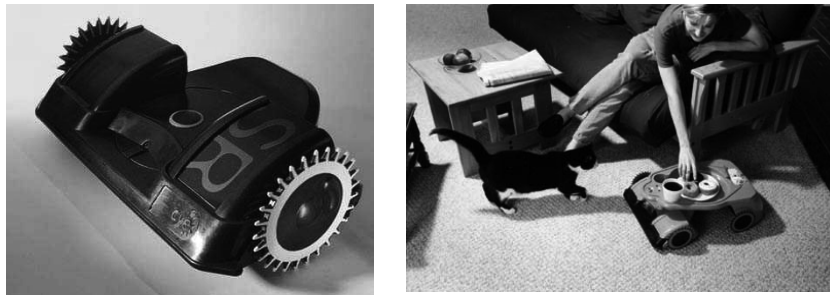


Figure 2.27

Cye, a domestic robot, was designed to vacuum floors and make domestic deliveries.

changing its ground footprint. The most popular such robot is the two-wheel differential-drive robot where the two wheels rotate around the center point of the robot. One or two additional ground contact points may be used for stability, based on the application specifics.

In contrast to these configurations, consider the Ackerman steering configuration common in automobiles. Such a vehicle typically has a turning diameter that is larger than the car. Furthermore, for such a vehicle to move sideways requires a parking maneuver consisting of repeated changes in direction forward and backward. Nevertheless, Ackerman steering geometries have been especially popular in the hobby robotics market, where a robot can be built by starting with a remote control racecar kit and adding sensing and autonomy to the existing mechanism. In addition, the limited maneuverability of Ackerman steering has an important advantage: its directionality and steering geometry provide it with very good lateral stability in high-speed turns.

2.3.1.5 Controllability

There is generally an inverse correlation between controllability and maneuverability. For example, the omnidirectional designs such as the four-caster wheel configuration require significant processing to convert desired rotational and translational velocities to individual wheel commands. Furthermore, such omnidirectional designs often have greater degrees of freedom at the wheel. For instance, the Swedish wheel has a set of free rollers along the wheel perimeter. These degrees of freedom cause an accumulation of slippage, tend to reduce dead-reckoning accuracy, and increase the design complexity.

Controlling an omnidirectional robot for a specific direction of travel is also more difficult and often less accurate when compared to less maneuverable designs. For example, an Ackerman steering vehicle can go straight simply by locking the steerable wheels and driving the drive wheels. In a differential-drive vehicle, the two motors attached to the two

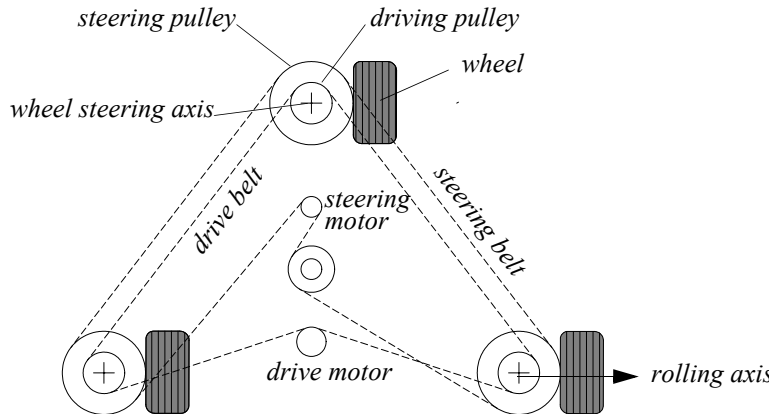


Figure 2.28

Synchro drive: The robot can move in any direction; however, the orientation of the chassis is not controllable.

wheels must be driven along exactly the same velocity profile, which can be challenging considering variations between wheels, motors, and environmental differences. With four-wheel omnidrive, such as the Uranus robot, which has four Swedish wheels, the problem is even harder because all four wheels must be driven at exactly the same speed for the robot to travel in a perfectly straight line.

In summary, there is no “ideal” drive configuration that simultaneously maximizes stability, maneuverability, and controllability. Each mobile robot application places unique constraints on the robot design problem, and the designer’s task is to choose the most appropriate drive configuration possible from among this space of compromises.

2.3.2 Wheeled locomotion: Case studies

We next describe four specific wheel configurations, in order to demonstrate concrete applications of the concepts discussed above to mobile robots built for real-world activities.

2.3.2.1 Synchro drive

The synchro drive configuration (figure 2.28) is a popular arrangement of wheels in indoor mobile robot applications. It is an interesting configuration because, although there are three driven and steered wheels, only two motors are used in total. The one translation motor sets the speed of all three wheels together, and the one steering motor spins all the wheels together about each of their individual vertical steering axes. But note that the wheels are being steered with respect to the robot chassis, and therefore there is no direct

way of reorienting the robot chassis. In fact, the chassis orientation does drift over time due to uneven tire slippage, causing rotational dead-reckoning error.

Synchro drive is particularly advantageous in cases where omnidirectionality is sought. So long as each vertical steering axis is aligned with the contact path of each tire, the robot can always reorient its wheels and move along a new trajectory without changing its footprint. Of course, if the robot chassis has directionality and the designers intend to reorient the chassis purposefully, then synchro drive is appropriate only when combined with an independently rotating turret that attaches to the wheel chassis. Commercial research robots such as the Nomadics 150 or the RWI B21r have been sold with this configuration (figure 1.12).

In terms of dead reckoning, synchro drive systems are generally superior to true omnidirectional configurations but inferior to differential-drive and Ackerman steering systems. There are two main reasons for this. First and foremost, the translation motor generally drives the three wheels using a single belt. Because of slop and backlash in the drive train, whenever the drive motor engages, the closest wheel begins spinning before the furthest wheel, causing a small change in the orientation of the chassis. With additional changes in motor speed, these small angular shifts accumulate to create a large error in orientation during dead reckoning. Second, the mobile robot has no direct control over the orientation of the chassis. Depending on the orientation of the chassis, the wheel thrust can be highly asymmetric, with two wheels on one side and the third wheel alone, or symmetric, with one wheel on each side and one wheel straight ahead or behind, as shown in figure 2.22. The asymmetric cases result in a variety of errors when tire-ground slippage can occur, again causing errors in dead reckoning of robot orientation.

2.3.2.2 Omnidirectional drive

As we will see later in section 3.4.2, omnidirectional movement is of great interest for complete maneuverability. Omnidirectional robots that are able to move in any direction (x, y, θ) at any time are also holonomic (see section 3.4.2). They can be realized by using spherical, castor, or Swedish wheels. Three examples of such holonomic robots are presented here.

Omnidirectional locomotion with three spherical wheels. The omnidirectional robot depicted in figure 2.29 is based on three spherical wheels, each actuated by one motor. In this design, the spherical wheels are suspended by three contact points, two given by spherical bearings and one by a wheel connected to the motor axle. This concept provides excellent maneuverability and is simple in design. However, it is limited to flat surfaces and small loads, and it is quite difficult to find round wheels with high friction coefficients.

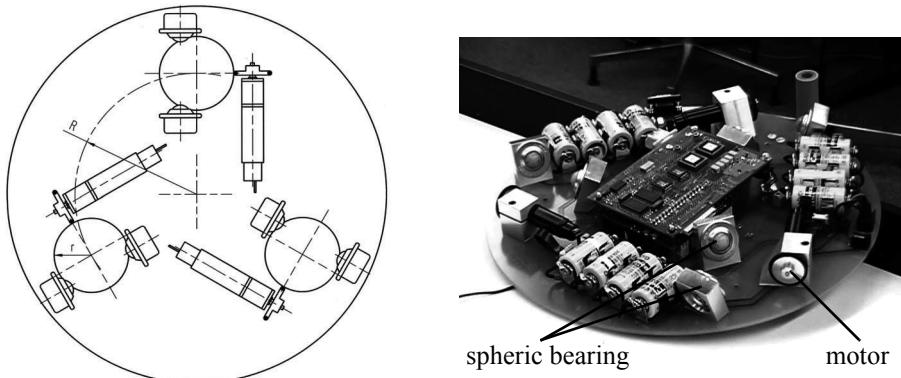


Figure 2.29

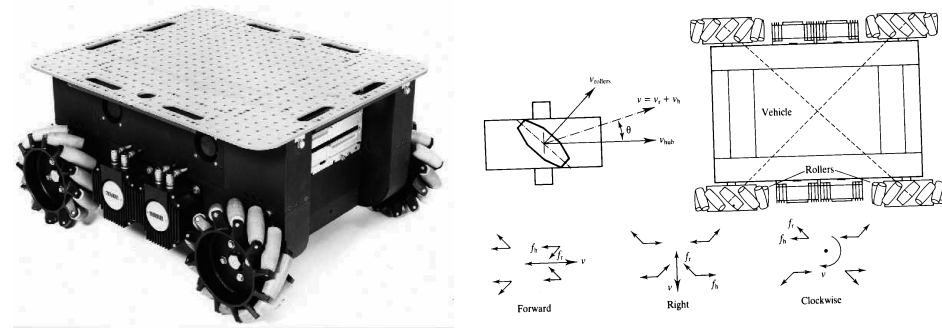
The Tribolo designed at EPFL (Swiss Federal Institute of Technology, Lausanne, Switzerland). Left: arrangement of spheric bearings and motors (bottom view). Right: Picture of the robot without the spherical wheels (bottom view).

Omnidirectional locomotion with four Swedish wheels. The omnidirectional arrangement depicted in figure 2.30 has been used successfully on several research robots, including the Carnegie Mellon Uranus. This configuration consists of four Swedish 45-degree wheels, each driven by a separate motor. By varying the direction of rotation and relative speeds of the four wheels, the robot can be moved along any trajectory in the plane and, even more impressively, can simultaneously spin around its vertical axis.

For example, when all four wheels spin “forward” or “backward,” the robot as a whole moves in a straight line forward or backward, respectively. However, when one diagonal pair of wheels is spun in the same direction and the other diagonal pair is spun in the opposite direction, the robot moves laterally.

This four-wheel arrangement of Swedish wheels is not minimal in terms of control motors. Because there are only three degrees of freedom in the plane, one can build a three-wheel omnidirectional robot chassis using three Swedish 90-degree wheels as shown in table 2.1. However, existing examples such as Uranus have been designed with four wheels owing to capacity and stability considerations.

One application for which such omnidirectional designs are particularly amenable is mobile manipulation. In this case, it is desirable to reduce the degrees of freedom of the manipulator arm to save arm mass by using the mobile robot chassis motion for gross motion. As with humans, it would be ideal if the base could move omnidirectionally with-

**Figure 2.30**

The Carnegie Mellon Uranus robot, an omnidirectional robot with four powered Swedish 45-wheels.

**Figure 2.31**

The Nomad XR4000 from Nomadic Technologies had an arrangement of four castor wheels for holonomic motion. All the castor wheels are driven and steered, thus requiring a precise synchronization and coordination to obtain a precise movement in x , y , and θ .

out greatly impacting the position of the manipulator tip, and a base such as Uranus can afford precisely such capabilities.

Omnidirectional locomotion with four castor wheels and eight motors. Another solution for omnidirectionality is to use castor wheels. This is done for the Nomad XR4000 from Nomadic Technologies (figure 2.31), giving it excellent maneuverability. Unfortunately, Nomadic has ceased production of mobile robots.

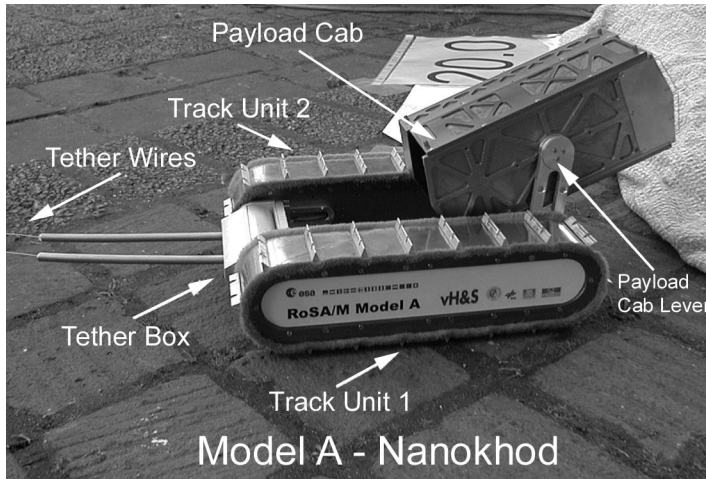


Figure 2.32

The microrover Nanokhod, developed by von Hoerner & Sulger GmbH and the Max Planck Institute, Mainz, for the European Space Agency (ESA), will probably go to Mars [302, 327].

The preceding three examples are drawn from table 2.1, but this is not an exhaustive list of all wheeled locomotion techniques. Hybrid approaches that combine legged and wheeled locomotion, or tracked and wheeled locomotion, can also offer particular advantages. Following are two unique designs created for specialized applications.

2.3.2.3 Tracked slip/skid locomotion

In the wheel configurations discussed earlier, we have made the assumption that wheels are not allowed to skid against the surface. An alternative form of steering, termed slip/skid, may be used to reorient the robot by spinning wheels that are facing the same direction at different speeds or in opposite directions. The army tank operates this way, and the Nanokhod (figure 2.32) is an example of a mobile robot based on the same concept.

Robots that make use of tread have much larger ground contact patches, and this can significantly improve their maneuverability in loose terrain compared to conventional wheeled designs. However, due to this large ground contact patch, changing the orientation of the robot usually requires a skidding turn, wherein a large portion of the track must slide against the terrain.

The disadvantage of such configurations is coupled to the slip/skid steering. Because of the large amount of skidding during a turn, the exact center of rotation of the robot is hard to predict and the exact change in position and orientation is also subject to variations depending on the ground friction. Therefore, dead reckoning on such robots is highly inac-

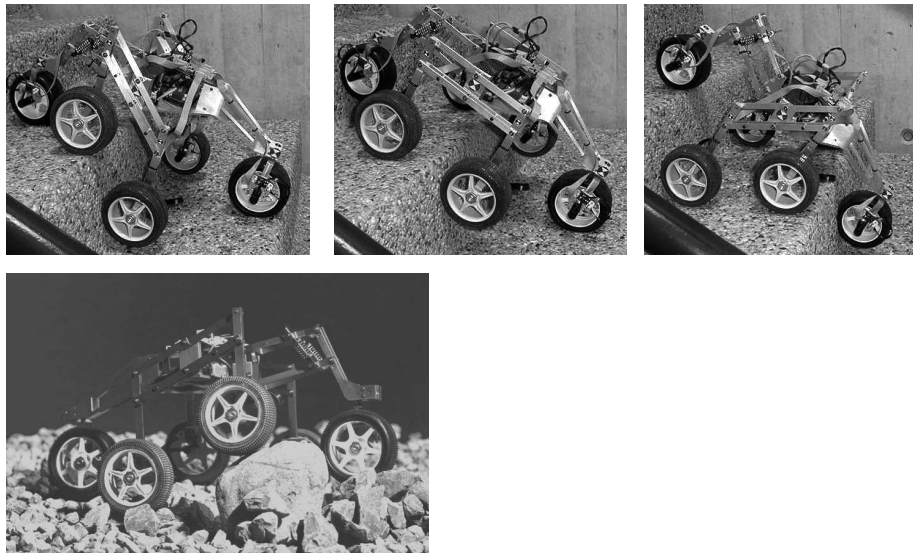


Figure 2.33

Shrimp, an all-terrain robot with outstanding passive climbing abilities (EPFL [184, 289]).

curate. This is the trade-off that is made in return for extremely good maneuverability and traction over rough and loose terrain. Furthermore, a slip/skid approach on a high-friction surface can quickly overcome the torque capabilities of the motors being used. In terms of power efficiency, this approach is reasonably efficient on loose terrain but extremely inefficient otherwise.

2.3.2.4 Walking wheels

Walking robots might offer the best maneuverability in rough terrain. However, they are inefficient on flat ground and need sophisticated control. Hybrid solutions, combining the adaptability of legs with the efficiency of wheels, offer an interesting compromise. Solutions that passively adapt to the terrain are of particular interest for field and space robotics. The Sojourner robot of NASA/JPL (see figure 1.2) represents such a hybrid solution, able to overcome objects up to the size of the wheels. A more recent mobile robot design for similar applications has been produced by EPFL (figure 2.33). This robot, called Shrimp, has six motorized wheels and is capable of climbing objects up to two times its wheel diameter [184, 289]. This enables it to climb regular stairs even though the robot is even smaller than the Sojourner. Using a rhombus configuration, the Shrimp has a steering wheel in the front and the rear and two wheels arranged on a bogie on each side. The front wheel has a spring suspension to guarantee optimal ground contact of all wheels at any time. The steer-

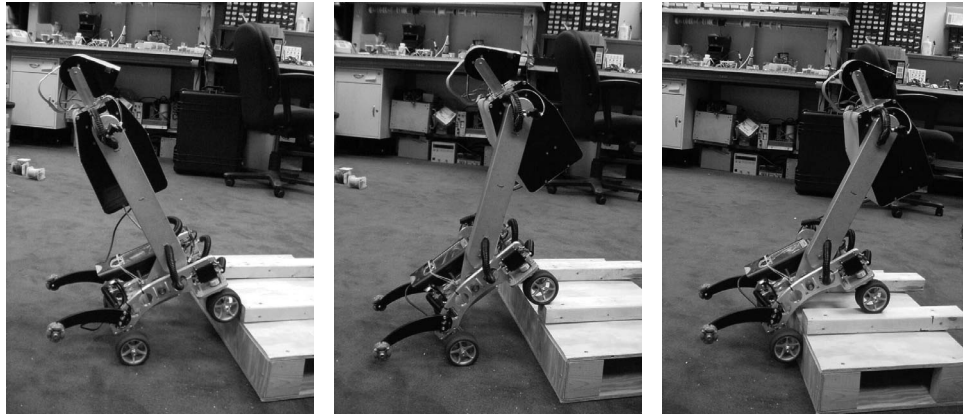


Figure 2.34

The Personal Rover, demonstrating ledge climbing using active center-of-mass shifting.

ing of the rover is realized by synchronizing the steering of the front and rear wheels and the speed difference of the bogie wheels. This allows for high-precision maneuvers and turning on the spot with minimum slip/skid of the four center wheels. The use of parallel articulations for the front wheel and the bogies creates a virtual center of rotation at the level of the wheel axis. This ensures maximum stability and climbing abilities even for very low friction coefficients between the wheel and the ground.

The climbing ability of the Shrimp is extraordinary in comparison to most robots of similar mechanical complexity, owing much to the specific geometry and thereby the manner in which the center of mass (COM) of the robot shifts with respect to the wheels over time. In contrast, the Personal Rover demonstrates active COM shifting to climb ledges that are also several times the diameter of its wheels, as demonstrated in figure 2.34. A majority of the weight of the Personal Rover is borne at the upper end of its swinging boom. A dedicated motor drives the boom to change the front/rear weight distribution in order to facilitate step-climbing. Because this COM-shifting scheme is active, a control loop must explicitly decide how to move the boom during a climbing scenario. In this case, the Personal Rover accomplished this closed-loop control by inferring terrain based on measurements of current flowing to each independently driven wheel [125].

As mobile robotics research matures, we find ourselves able to design more intricate mechanical systems. At the same time, the control problems of inverse kinematics and dynamics are now so readily conquered that these complex mechanics can in general be controlled. So, in the near future, we can expect to see a great number of unique, hybrid mobile robots that draw together advantages from several of the underlying locomotion

mechanisms that we have discussed in this chapter. They will be technologically impressive, and each will be designed as the expert robot for its particular environmental niche.

2.4 Aerial Mobile Robots

2.4.1 Introduction

Flying objects have always exerted a great fascination on humans, encouraging all kinds of research and development. This introduction is written in a time at which the robotics community is showing a growing interest in micro aerial vehicle (MAV) development. The scientific challenge in MAV design, control, and navigation in cluttered environments and the lack of existing solutions is the main leitmotiv. On the other hand, the broad field of applications in both military and civilian markets is encouraging the funding of MAV-related projects. However, the task is not trivial due to several open challenges.

In the field of sensing technologies, industry can currently provide a new generation of integrated micro inertial measurement units (IMU, section 4.1.7) composed generally of micro electro-mechanical systems (MEMS) technology, inertial and magneto-resistive sensors. The latest technology in high density power storage offers about 230Wh/kg (Li-Ion technology in 2009), which is a real jump ahead, especially for micro aerial robotics. This technology was originally developed for handheld applications and is now widely used in aerial robotics. The cost and size reduction of such systems makes it very interesting for the civilian market. Simultaneously, this reduction of cost and size implies performance limitations and thus a more challenging control problem. Moreover, the miniaturization of inertial sensors imposes the use of MEMS technology, which is still much less accurate than the conventional sensors because of noise and drift. The use of low-cost IMUs demands less effective data processing and thus a bad orientation data prediction in addition to a weak drift rejection. On the other hand, and in spite of the latest progress in miniature actuators, the scaling laws are still unfavorable and one has to face the problem of actuator saturation. That is to say, even though the design of micro aerial robots is possible, the control is still a challenging goal.

Investigating relations between size and weight of flying objects yields some interesting findings. Tennekes's Great Flight Diagram [50] (figure 2.35) plots weight versus wing loading for all sizes comprising insects, birds, and sailplanes all the way up to the Boeing 747. It illustrates the fundamental simplified assumption that the weight W scales with the wingspan b to the power of three (b^3), while the wing surface S may be seen as scaling with b^2 . Figure 2.35 shows Tennekes's Great Flight Diagram augmented with some unmanned solar airplanes and radio controlled airplanes [248] that are comparable to small robotic unmanned aerial systems. The curve W/S represents an average of the shown data points. Notice that different constructions still yield different results: the extremely lightweight solar airplane *Helios* by NASA, for example, with its 75 meters of wingspan and a surface

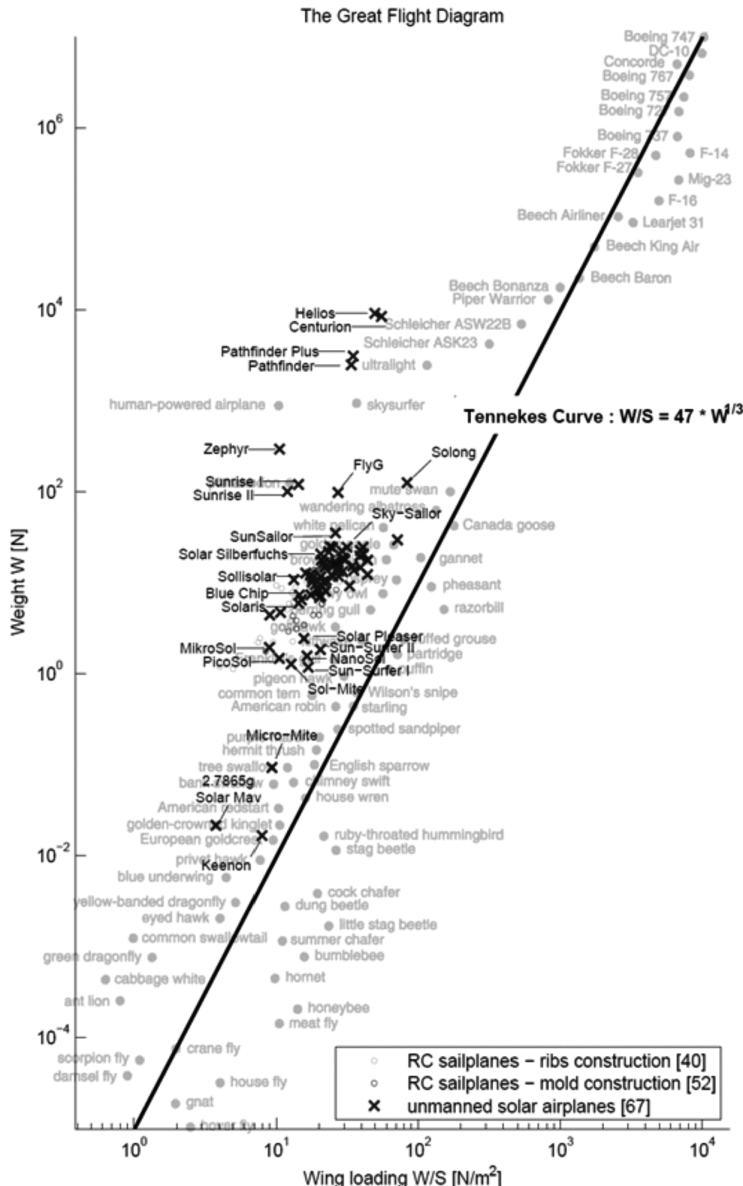


Figure 2.35 Tennekes's Great Flight Diagram [50] augmented with RC sailplanes and unmanned solar airplanes. Image courtesy of A. Noth [248].

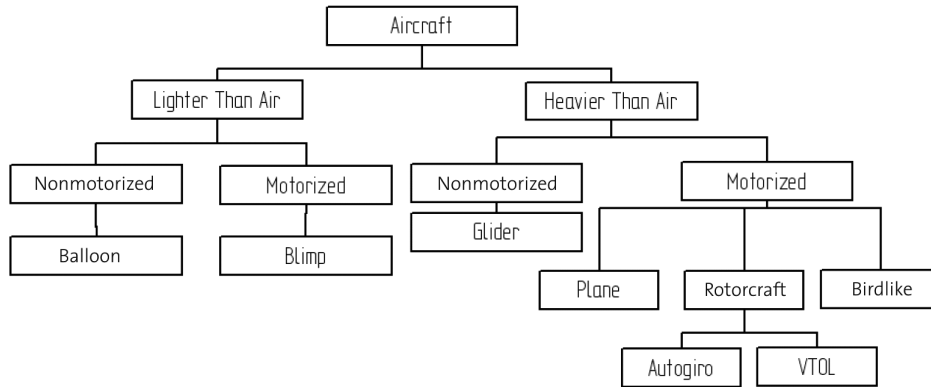


Figure 2.36 General classification of aircrafts.

area of 184 m^2 , has approximately the same wing loading as a pelican but it is heavier by a factor of 1,000 and of course is much larger.

2.4.2 Aircraft configurations

In general, aerial vehicles can be divided into two categories: Lighter Than Air (LTA) and Heavier Than Air (HTA). Figure 2.36 presents a general classification of aircraft depending on the flying principle and the propulsion mode. Table 2.2 gives a nonexhaustive comparison between different flying principles from the miniaturization point of view. From this table, one can easily conclude that Vertical Take-Off and Landing (VTOL) systems such as helicopters or blimps have an unquestionable advantage compared with the other concepts. This superiority is owed to their unique ability for vertical, stationary, and low-speed flight. The key advantage of blimps is the *autolift* and simplicity of control, which can be essential for critical applications, such as aerial surveillance and space exploration. However, VTOL vehicles in different configurations represent today one of the most promising flying concepts seen in terms of miniaturization. Figure 2.37 lists different configurations commonly used in MAV research and industry.

2.4.3 State of the art in autonomous VTOL

The state of the art in MAV research has dramatically changed in the last few years. The number of projects tackling this problem has considerably and suddenly increased. Until 2006, the main research problem was MAV stabilization, especially for mini quadrotors. Since 2007, the research community shifted its interest toward autonomous navigation, first outdoor and more recently even indoor.

Table 2.2 Flying principle comparison (1 = Bad, 3 = Good)

	Airplane	Helicopter	Bird	Autogiro	Blimp
Power cost	2	1	2	2	3
Control cost	2	1	1	2	3
Payload/volume	3	2	2	2	1
Maneuverability	2	3	3	2	1
Stationary flight	1	3	2	1	3
Low speed fly	1	3	2	2	3
Vulnerability	2	2	3	2	2
VTOL	1	3	2	1	3
Endurance	2	1	2	1	3
Miniaturization	2	3	3	2	1
Indoor usage	1	3	2	1	2
Total	19	25	24	18	25

The CSAIL laboratory at MIT is presently one of the leaders in terms of MAV navigation in GPS-denied environments. The quadrotor that it used in the 2009 edition of the AUVSI competition uses laser scanners to localize and navigate autonomously inside buildings. The quadrotor from ALU Freiburg [142] is also equipped with a laser scanner; it achieves global localization using a particle filter and a graph-based SLAM algorithm (both these algorithms will be treated in section 5.8.2). It is thus able to navigate autonomously indoors while avoiding obstacles. STARMAC, from Stanford University, targets the demonstration of multiagent control of quadrotors of about 1 kg, outdoors, using GPS. ETH Zurich is also participating in this endeavor with different projects. The European project sFly (www.sfly.org) targets outdoor autonomous navigation of a swarm of small quadrotors using monocular vision as the main sensor (no laser, no GPS). To the best of our knowledge, the smallest existing autonomous helicopter is the muFly helicopter, developed at ETH Zurich within the European project muFly (www.mufly.org): it weighs 80 g and has an overall span of 17.5 cm. In addition to an IMU, muFly is equipped with a 360-degree laser scanner, a down-looking micro camera, and a miniature omnidirectional camera that weighs less than 5 g. These projects are listed in figure 2.38.

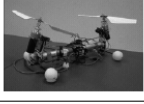
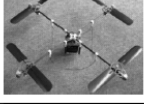
Configuration e.g.	Advantages	Drawbacks	Picture
Fixed-wing (AeroVironment)	Simple mechanics, silent operation	No hovering	
Single rotor (A. V de Rostyne)	Good controllability, good maneuverability	Complex mechanics, large rotor, long tail boom	
Axial rotor (Univ. of Maryland)	Simple mechanics, compactness	Complex aerodynamics	
Coaxial rotors (EPSON)	Simple mechanics, compactness	Complex aerodynamics	
Tandem rotors (Heudiasyc)	Good controllability, simple aerodynamics	Complex mechanics, large size	
Quadrotor (EPFL-ETHZ)	Good maneuverability, simple mechanics, increased payload	High energy consumption, large size	
Blimp (EPFL)	Low power, long flight operation, auto-lift	Large size, weak maneuverability	
Hybrid quadrotor-blimp (MIT)	Good maneuverability, good survivability	Large size, weak maneuverability	
Birdlike (Caltech)	Good maneuverability, compactness	Complex mechanics, complex control	
Insectlike (UC Berkeley)	Good maneuverability, compactness	Complex mechanics, complex control	
Fishlike (US Naval Lab)	Multimode mobility, efficient aerodynamics	Complex control, weak maneuverability	

Figure 2.37 Common MAV configurations.

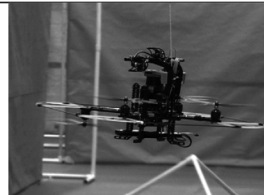
Projects	University	Status	Picture
MIT-MAV	MIT	Ended	
Freiburg MAV	ALU Freiburg	In progress	
Starmac	Stanford	In progress	
sFly	ETH Zürich	In progress	
muFly	ETH Zürich	Ended	

Figure 2.38 Progress in autonomous VTOL systems.

2.5 Problems

1. Consider an eight-legged walking robot. Consider gaits in terms of lift/release events as in this chapter. (a) How many possible events exist for this eight-legged machine? (b) Specify two different statically stable walking gaits using the notation of figure 2.8.
2. Describe two wheel configurations that enable omnidirectional motion that are not identified in section 2.3.2.2. Note that you may use any type of wheel in these two designs. Draw the configurations using the notation of table 2.1.
3. You wish to build a dynamically stable robot with a single wheel only. For each of the four basic wheel types, explain whether or not it may be used for such a robot.
4. **Challenge Question.**

Four-legged machines are normally not statically stable. Design a four-legged locomotion machine that is statically stable. Draw it and describe the gait used.

3 Mobile Robot Kinematics

3.1 Introduction

Kinematics is the most basic study of how mechanical systems behave. In mobile robotics, we need to understand the mechanical behavior of the robot both to design appropriate mobile robots for tasks and to understand how to create control software for an instance of mobile robot hardware.

Of course, mobile robots are not the first complex mechanical systems to require such analysis. Robot manipulators have been the subject of intensive study for more than thirty years. In some ways, manipulator robots are much more complex than early mobile robots: a standard welding robot may have five or more joints, whereas early mobile robots were simple differential-drive machines. In recent years, the robotics community has achieved a fairly complete understanding of the kinematics and even the dynamics (that is, relating to force and mass) of robot manipulators [13, 46].

The mobile robotics community poses many of the same kinematic questions as the robot manipulator community. A manipulator robot's workspace is crucial because it defines the range of possible positions that can be achieved by its end effector relative to its fixture to the environment. A mobile robot's workspace is equally important because it defines the range of possible poses that the mobile robot can achieve in its environment. The robot arm's controllability defines the manner in which active engagement of motors can be used to move from pose to pose in the workspace. Similarly, a mobile robot's controllability defines possible paths and trajectories in its workspace. Robot dynamics places additional constraints on workspace and trajectory due to mass and force considerations. The mobile robot is also limited by dynamics; for instance, a high center of gravity limits the practical turning radius of a fast, carlike robot because of the danger of rolling.

But the chief difference between a mobile robot and a manipulator arm also introduces a significant challenge for *position estimation*. A manipulator has one end fixed to the environment. Measuring the position of an arm's end effector is simply a matter of understanding the kinematics of the robot and measuring the position of all intermediate joints. The manipulator's position is thus always computable by looking at current sensor data. But a

mobile robot is a self-contained automaton that can wholly move with respect to its environment. There is no direct way to measure a mobile robot's position instantaneously. Instead, one must integrate the motion of the robot over time. Add to this the inaccuracies of *motion estimation* due to slippage and it is clear that measuring a mobile robot's position precisely is an extremely challenging task.

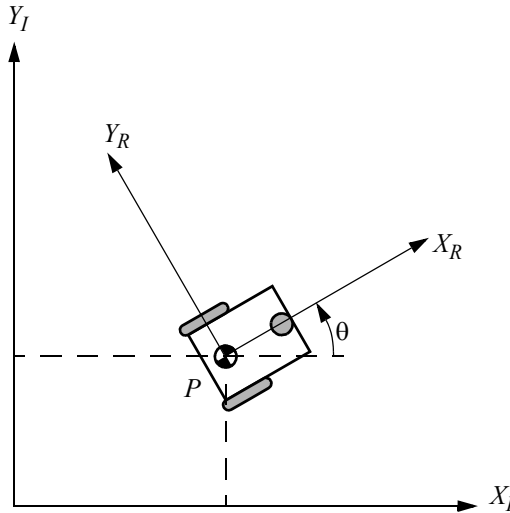
The process of understanding the motions of a robot begins with the process of describing the contribution each wheel provides for motion. Each wheel has a role in enabling the whole robot to move. By the same token, each wheel also imposes constraints on the robot's motion; for example, refusing to skid laterally. In the following section, we introduce notation that allows expression of robot motion in a global reference frame as well as the robot's local reference frame. Then, using this notation, we demonstrate the construction of simple forward kinematic models of motion, describing how the robot as a whole moves as a function of its geometry and individual wheel behavior. Next, we formally describe the kinematic constraints of individual wheels, and then combine these kinematic constraints to express the whole robot's kinematic constraints. With these tools, one can evaluate the paths and trajectories that define the robot's maneuverability.

3.2 Kinematic Models and Constraints

Deriving a model for the whole robot's motion is a bottom-up process. Each individual wheel contributes to the robot's motion and, at the same time, imposes constraints on robot motion. Wheels are tied together based on robot chassis geometry, and therefore their constraints combine to form constraints on the overall motion of the robot chassis. But the forces and constraints of each wheel must be expressed with respect to a clear and consistent reference frame. This is particularly important in mobile robotics because of its self-contained and mobile nature; a clear mapping between global and local frames of reference is required. We begin by defining these reference frames formally, then using the resulting formalism to annotate the kinematics of individual wheels and whole robots. Throughout this process we draw extensively on the notation and terminology presented in [90].

3.2.1 Representing robot position

Throughout this analysis we model the robot as a rigid body on wheels, operating on a horizontal plane. The total dimensionality of this robot chassis on the plane is three, two for position in the plane and one for orientation along the vertical axis, which is orthogonal to the plane. Of course, there are additional degrees of freedom and flexibility due to the wheel axles, wheel steering joints, and wheel castor joints. However, by robot *chassis* we refer only to the rigid body of the robot, ignoring the joints and degrees of freedom internal to the robot and its wheels.

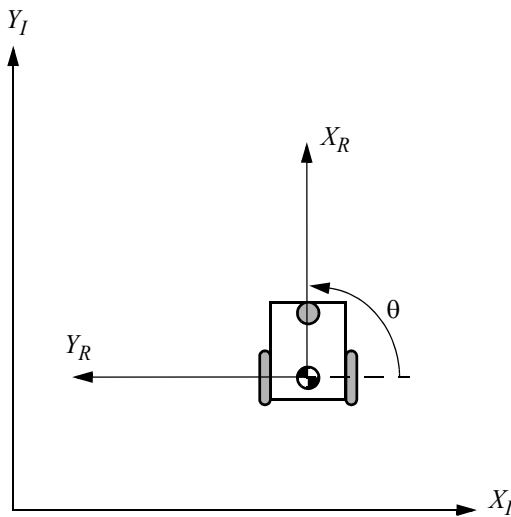
**Figure 3.1**

The global reference frame and the robot local reference frame.

In order to specify the position of the robot on the plane, we establish a relationship between the global reference frame of the plane and the local reference frame of the robot, as in figure 3.1. The axes X_I and Y_I define an arbitrary inertial basis on the plane as the global reference frame from some origin O : $\{X_I, Y_I\}$. To specify the position of the robot, choose a point P on the robot chassis as its position reference point. The basis $\{X_R, Y_R\}$ defines two axes relative to P on the robot chassis and is thus the robot's local reference frame. The position of P in the global reference frame is specified by coordinates x and y , and the angular difference between the global and local reference frames is given by θ . We can describe the pose of the robot as a vector with these three elements. Note the use of the subscript I to clarify the basis of this pose as the global reference frame:

$$\xi_I = \begin{bmatrix} x \\ y \\ \theta \end{bmatrix} \quad (3.1)$$

To describe robot motion in terms of component motions, it will be necessary to map motion along the axes of the global reference frame to motion along the axes of the robot's local reference frame. Of course, the mapping is a function of the current pose of the robot. This mapping is accomplished using the *orthogonal rotation matrix*:

**Figure 3.2**

The mobile robot aligned with a global axis.

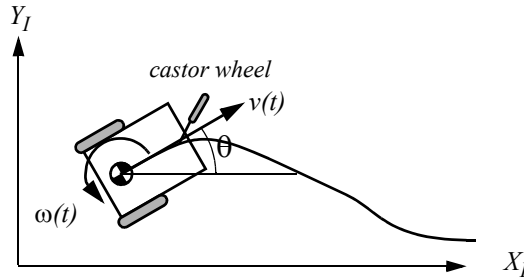
$$R(\theta) = \begin{bmatrix} \cos\theta & \sin\theta & 0 \\ -\sin\theta & \cos\theta & 0 \\ 0 & 0 & 1 \end{bmatrix}. \quad (3.2)$$

This matrix can be used to map motion in the global reference frame $\{X_I, Y_I\}$ to motion in terms of the local reference frame $\{X_R, Y_R\}$. This operation is denoted by $R(\theta)\dot{\xi}_I$ because the computation of this operation depends on the value of θ :

$$\dot{\xi}_R = R\left(\frac{\pi}{2}\right)\dot{\xi}_I. \quad (3.3)$$

For example, consider the robot in figure 3.2. For this robot, because $\theta = \frac{\pi}{2}$ we can easily compute the instantaneous rotation matrix R :

$$R\left(\frac{\pi}{2}\right) = \begin{bmatrix} 0 & 1 & 0 \\ -1 & 0 & 0 \\ 0 & 0 & 1 \end{bmatrix}. \quad (3.4)$$

**Figure 3.3**

A differential-drive robot in its global reference frame.

Given some velocity $(\dot{x}, \dot{y}, \dot{\theta})$ in the global reference frame we can compute the components of motion along this robot's local axes X_R and Y_R . In this case, due to the specific angle of the robot, motion along X_R is equal to \dot{y} , and motion along Y_R is $-\dot{x}$:

$$\dot{\xi}_R = R\left(\frac{\pi}{2}\right)\dot{\xi}_I = \begin{bmatrix} 0 & 1 & 0 \\ -1 & 0 & 0 \\ 0 & 0 & 1 \end{bmatrix} \begin{bmatrix} \dot{x} \\ \dot{y} \\ \dot{\theta} \end{bmatrix} = \begin{bmatrix} \dot{y} \\ -\dot{x} \\ \dot{\theta} \end{bmatrix}. \quad (3.5)$$

3.2.2 Forward kinematic models

In the simplest cases, the mapping described by equation (3.3) is sufficient to generate a formula that captures the forward kinematics of the mobile robot: how does the robot move, given its geometry and the speeds of its wheels? More formally, consider the example shown in figure 3.3.

This differential drive robot has two wheels, each with diameter r . Given a point P centered between the two drive wheels, each wheel is a distance l from P . Given r , l , θ , and the spinning speed of each wheel, $\dot{\phi}_1$ and $\dot{\phi}_2$, a forward kinematic model would predict the robot's overall speed in the global reference frame:

$$\dot{\xi}_I = \begin{bmatrix} \dot{x} \\ \dot{y} \\ \dot{\theta} \end{bmatrix} = f(l, r, \theta, \dot{\phi}_1, \dot{\phi}_2). \quad (3.6)$$

From equation (3.3) we know that we can compute the robot's motion in the global reference frame from motion in its local reference frame: $\dot{\xi}_I = R(\theta)^{-1}\dot{\xi}_R$. Therefore, the strat-

egy will be to first compute the contribution of each of the two wheels in the local reference frame, $\dot{\xi}_R$. For this example of a differential-drive chassis, this problem is particularly straightforward.

Suppose that the robot's local reference frame is aligned such that the robot moves forward along $+X_R$, as shown in figure 3.1. First, consider the contribution of each wheel's spinning speed to the translation speed at P in the direction of $+X_R$. If one wheel spins while the other wheel contributes nothing and is stationary, since P is halfway between the two wheels, it will move instantaneously with half the speed: $\dot{x}_{r1} = (1/2)r\dot{\varphi}_1$ and $\dot{x}_{r2} = (1/2)r\dot{\varphi}_2$. In a differential-drive robot, these two contributions can simply be added to calculate the \dot{x}_R component of $\dot{\xi}_R$. Consider, for example, a differential robot in which each wheel spins with equal speed but in opposite directions. The result is a stationary, spinning robot. As expected, \dot{x}_R will be zero in this case. The value of \dot{y}_R is even simpler to calculate. Neither wheel can contribute to sideways motion in the robot's reference frame, and so \dot{y}_R is always zero. Finally, we must compute the rotational component $\dot{\theta}_R$ of $\dot{\xi}_R$. Once again, the contributions of each wheel can be computed independently and just added. Consider the right wheel (we will call this wheel 1). Forward spin of this wheel results in *c*ounterclockwise rotation at point P . Recall that if wheel 1 spins alone, the robot pivots around wheel 2. The rotation velocity ω_1 at P can be computed because the wheel is instantaneously moving along the arc of a circle of radius $2l$:

$$\omega_1 = \frac{r\dot{\varphi}_1}{2l}. \quad (3.7)$$

The same calculation applies to the left wheel, with the exception that forward spin results in *c*lockwise rotation at point P :

$$\omega_2 = \frac{-r\dot{\varphi}_2}{2l}. \quad (3.8)$$

Combining these individual formulas yields a kinematic model for the differential-drive example robot:

$$\dot{\xi}_I = R(\theta)^{-1} \begin{bmatrix} \frac{r\dot{\varphi}_1}{2} + \frac{r\dot{\varphi}_2}{2} \\ 0 \\ \frac{r\dot{\varphi}_1}{2l} + \frac{-r\dot{\varphi}_2}{2l} \end{bmatrix}. \quad (3.9)$$

We can now use this kinematic model in an example. However, we must first compute $R(\theta)^{-1}$. In general, calculating the inverse of a matrix may be challenging. In this case, however, it is easy because it is simply a transform from $\dot{\xi}_R$ to $\dot{\xi}_I$ rather than vice versa:

$$R(\theta)^{-1} = \begin{bmatrix} \cos\theta & -\sin\theta & 0 \\ \sin\theta & \cos\theta & 0 \\ 0 & 0 & 1 \end{bmatrix}. \quad (3.10)$$

Suppose that the robot is positioned such that $\theta = \pi/2$, $r = 1$, and $l = 1$. If the robot engages its wheels unevenly, with speeds $\dot{\phi}_1 = 4$ and $\dot{\phi}_2 = 2$, we can compute its velocity in the global reference frame:

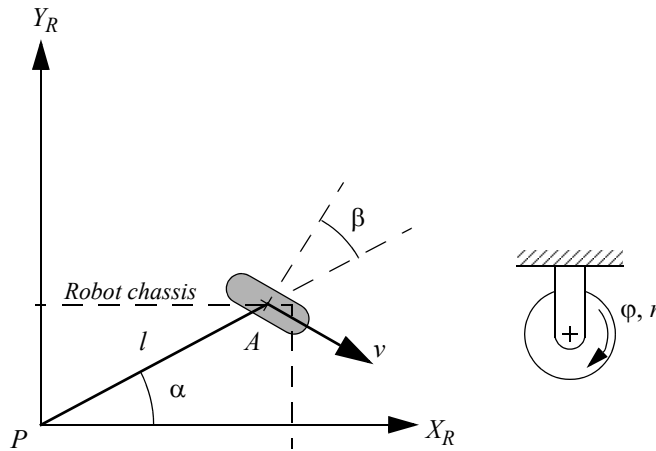
$$\dot{\xi}_I = \begin{bmatrix} \dot{x} \\ \dot{y} \\ \dot{\theta} \end{bmatrix} = \begin{bmatrix} 0 & -1 & 0 \\ 1 & 0 & 0 \\ 0 & 0 & 1 \end{bmatrix} \begin{bmatrix} 3 \\ 0 \\ 1 \end{bmatrix} = \begin{bmatrix} 0 \\ 3 \\ 1 \end{bmatrix}. \quad (3.11)$$

So this robot will move instantaneously along the y -axis of the global reference frame with speed 3 while rotating with speed 1. This approach to kinematic modeling can provide information about the motion of a robot given its component wheel speeds in straightforward cases. However, we wish to determine the space of possible motions for each robot chassis design. To do this, we must go further, describing formally the constraints on robot motion imposed by each wheel. Section 3.2.3 begins this process by describing constraints for various wheel types; the rest of this chapter provides tools for analyzing the characteristics and workspace of a robot given these constraints.

3.2.3 Wheel kinematic constraints

The first step to a kinematic model of the robot is to express constraints on the motions of individual wheels. Just as shown in section 3.2.2, the motions of individual wheels can later be combined to compute the motion of the robot as a whole. As discussed in chapter 2, there are four basic wheel types with widely varying kinematic properties. Therefore, we begin by presenting sets of constraints specific to each wheel type.

However, several important assumptions will simplify this presentation. We assume that the plane of the wheel always remains vertical and that there is in all cases one single point of contact between the wheel and the ground plane. Furthermore, we assume that there is no sliding at this single point of contact. That is, the wheel undergoes motion only under conditions of pure rolling and rotation about the vertical axis through the contact point. For a more thorough treatment of kinematics, including sliding contact, refer to [38].

**Figure 3.4**

A fixed standard wheel and its parameters.

Under these assumptions, we present two constraints for every wheel type. The first constraint enforces the concept of rolling contact—that the wheel must roll when motion takes place in the appropriate direction. The second constraint enforces the concept of no lateral slippage—that the wheel must not slide orthogonal to the wheel plane.

3.2.3.1 Fixed standard wheel

The fixed standard wheel has no vertical axis of rotation for steering. Its angle to the chassis is thus fixed, and it is limited to motion back and forth along the wheel plane and rotation around its contact point with the ground plane. Figure 3.4 depicts a fixed standard wheel A and indicates its position pose relative to the robot's local reference frame $\{X_R, Y_R\}$. The position of A is expressed in polar coordinates by distance l and angle α . The angle of the wheel plane relative to the chassis is denoted by β , which is fixed since the fixed standard wheel is not steerable. The wheel, which has radius r , can spin over time, and so its rotational position around its horizontal axle is a function of time t : $\varphi(t)$.

The rolling constraint for this wheel enforces that all motion along the direction of the wheel plane must be accompanied by the appropriate amount of wheel spin so that there is pure rolling at the contact point:

$$[\sin(\alpha + \beta) - \cos(\alpha + \beta) (-l) \cos \beta] R(\theta) \dot{\xi}_I - r \dot{\varphi} = 0. \quad (3.12)$$

The first term of the sum denotes the total motion along the wheel plane. The three elements of the vector on the left represent mappings from each of \dot{x} , \dot{y} , $\dot{\theta}$ to their contributions for motion along the wheel plane. Note that the $R(\theta)\dot{\xi}_I$ term is used to transform the motion parameters $\dot{\xi}_I$ that are in the global reference frame $\{X_I, Y_I\}$ into motion parameters in the local reference frame $\{X_R, Y_R\}$ as shown in example equation (3.5). This is necessary because all other parameters in the equation, α , β , l , are in terms of the robot's local reference frame. This motion along the wheel plane must be equal, according to this constraint, to the motion accomplished by spinning the wheel, $r\dot{\varphi}$.

The sliding constraint for this wheel enforces that the component of the wheel's motion orthogonal to the wheel plane must be zero:

$$[\cos(\alpha + \beta) \ \sin(\alpha + \beta) \ l \sin \beta] R(\theta) \dot{\xi}_I = 0. \quad (3.13)$$

For example, suppose that wheel A is in a position such that $\{(\alpha = 0), (\beta = 0)\}$. This would place the contact point of the wheel on X_I with the plane of the wheel oriented parallel to Y_I . If $\theta = 0$, then the sliding constraint [equation (3.13)] reduces to

$$\begin{bmatrix} 1 & 0 & 0 \\ 0 & 1 & 0 \\ 0 & 0 & 1 \end{bmatrix} \begin{bmatrix} \dot{x} \\ \dot{y} \\ \dot{\theta} \end{bmatrix} = \begin{bmatrix} 1 & 0 & 0 \end{bmatrix} \begin{bmatrix} \dot{x} \\ \dot{y} \\ \dot{\theta} \end{bmatrix} = 0. \quad (3.14)$$

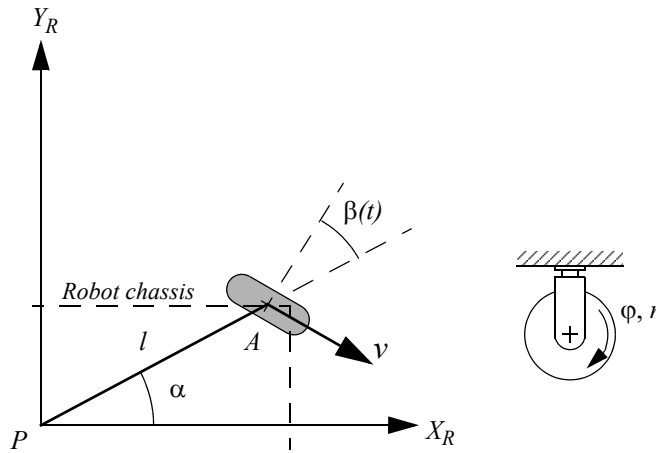
This constrains the component of motion along X_I to be zero, and since X_I and X_R are parallel in this example, the wheel is constrained from sliding sideways, as expected.

3.2.3.2 Steered standard wheel

The steered standard wheel differs from the fixed standard wheel only in that there is an additional degree of freedom: the wheel may rotate around a vertical axis passing through the center of the wheel and the ground contact point. The equations of position for the steered standard wheel (figure 3.5) are identical to that of the fixed standard wheel shown in figure 3.4 with one exception. The orientation of the wheel to the robot chassis is no longer a single fixed value, β , but instead varies as a function of time: $\beta(t)$. The rolling and sliding constraints are

$$[\sin(\alpha + \beta) \ -\cos(\alpha + \beta) \ (-l) \cos \beta] R(\theta) \dot{\xi}_I - r\dot{\varphi} = 0. \quad (3.15)$$

$$[\cos(\alpha + \beta) \ \sin(\alpha + \beta) \ l \sin \beta] R(\theta) \dot{\xi}_I = 0. \quad (3.16)$$

**Figure 3.5**

A steered standard wheel and its parameters.

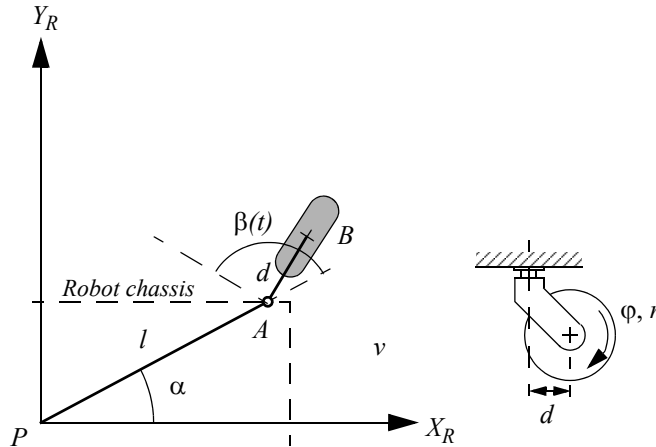
These constraints are identical to those of the fixed standard wheel because, unlike $\dot{\phi}$, $\dot{\beta}$ does not have a direct impact on the instantaneous motion constraints of a robot. It is only by integrating over time that changes in steering angle can affect the mobility of a vehicle. This may seem subtle, but is a very important distinction between change in steering position, $\dot{\beta}$, and change in wheel spin, $\dot{\phi}$.

3.2.3.3 Castor wheel

Castor wheels are able to steer around a vertical axis. However, unlike the steered standard wheel, the vertical axis of rotation in a castor wheel does not pass through the ground contact point. Figure 3.6 depicts a castor wheel, demonstrating that formal specification of the castor wheel's position requires an additional parameter.

The wheel contact point is now at position B , which is connected by a rigid rod AB of fixed length d to point A , fixes the location of the vertical axis about which B steers, and this point A has a position specified in the robot's reference frame, as in figure 3.6. We assume that the plane of the wheel is aligned with AB at all times. Similar to the steered standard wheel, the castor wheel has two parameters that vary as a function of time. $\phi(t)$ represents the wheel spin over time as before. $\beta(t)$ denotes the steering angle and orientation of AB over time.

For the castor wheel, the rolling constraint is identical to equation (3.15) because the offset axis plays no role during motion that is aligned with the wheel plane:

**Figure 3.6**

A castor wheel and its parameters.

$$[\sin(\alpha + \beta) - \cos(\alpha + \beta) (-l) \cos \beta] R(\theta) \dot{\xi}_I - r \dot{\varphi} = 0. \quad (3.17)$$

The castor geometry does, however, have significant impact on the sliding constraint. The critical issue is that the lateral force on the wheel occurs at point A because this is the attachment point of the wheel to the chassis. Because of the offset ground contact point relative to A , the constraint that there be zero lateral movement would be wrong. Instead, the constraint is much like a rolling constraint, in that appropriate rotation of the vertical axis must take place:

$$[\cos(\alpha + \beta) \sin(\alpha + \beta) d + l \sin \beta] R(\theta) \dot{\xi}_I + d \dot{\beta} = 0. \quad (3.18)$$

In equation (3.18), any motion orthogonal to the wheel plane must be balanced by an equivalent and opposite amount of castor steering motion. This result is critical to the success of castor wheels because by setting the value of β any arbitrary lateral motion can be acceptable. In a steered standard wheel, the steering action does not by itself cause a movement of the robot chassis. But in a castor wheel, the steering action itself moves the robot chassis because of the offset between the ground contact point and the vertical axis of rotation.

**Figure 3.7**

Office chair with five castor wheels.

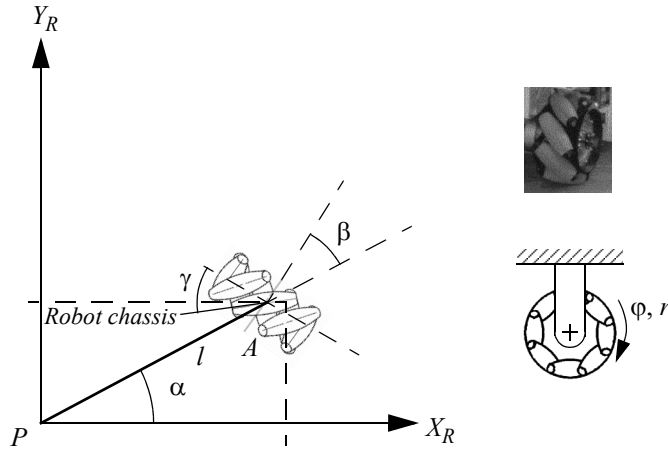
More concisely, it can be surmised from equations (3.17) and (3.18) that, given *any* robot chassis motion $\dot{\xi}_I$, there exists some value for spin speed $\dot{\phi}$ and steering speed $\dot{\beta}$ such that the constraints are met. Therefore, a robot with only castor wheels can move with any velocity in the space of possible robot motions. We term such systems *omnidirectional*.

A real-world example of such a system is the five-castor wheel office chair shown in figure 3.7. Assuming that all joints are able to move freely, you may select any motion vector on the plane for the chair and push it by hand. Its castor wheels will spin and steer as needed to achieve that motion without contact point sliding. By the same token, if each of the chair's castor wheels housed two motors, one for spinning and one for steering, then a control system would be able to move the chair along any trajectory in the plane. Thus, although the kinematics of castor wheels is somewhat complex, such wheels do not impose any real constraints on the kinematics of a robot chassis.

3.2.3.4 Swedish wheel

Swedish wheels have no vertical axis of rotation, yet are able to move *omnidirectionally* like the castor wheel. This is possible by adding a degree of freedom to the fixed standard wheel. Swedish wheels consist of a fixed standard wheel with rollers attached to the wheel perimeter with axes that are antiparallel to the main axis of the fixed wheel component. The exact angle γ between the roller axes and the wheel plane can vary, as shown in figure 3.8.

For example, given a Swedish 45-degree wheel, the motion vectors of the principal axis and the roller axes can be drawn as in figure 3.8. Since each axis can spin clockwise or counterclockwise, one can combine any vector along one axis with any vector along the other axis. These two axes are not necessarily independent (except in the case of the Swedish 90-degree wheel); however, it is visually clear that any desired direction of motion is achievable by choosing the appropriate two vectors.

**Figure 3.8**

A Swedish wheel and its parameters.

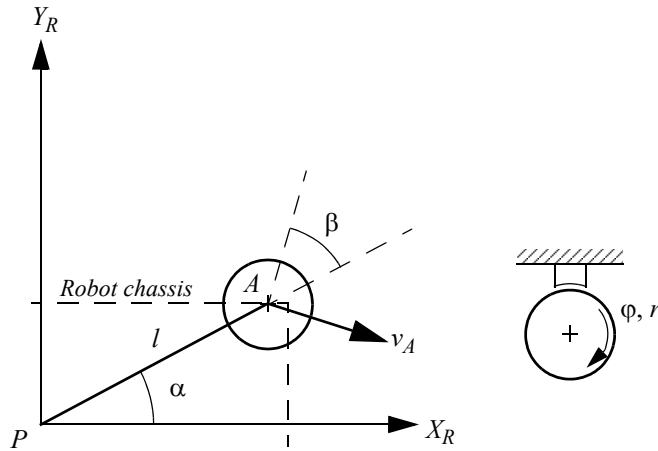
The pose of a Swedish wheel is expressed exactly as in a fixed standard wheel, with the addition of a term, γ , representing the angle between the main wheel plane and the axis of rotation of the small circumferential rollers. This is depicted in figure 3.8 within the robot's reference frame.

Formulating the constraint for a Swedish wheel requires some subtlety. The instantaneous constraint is due to the specific orientation of the small rollers. The axis around which these rollers spin is a zero component of velocity at the contact point. That is, moving in that direction without spinning the main axis is not possible without sliding. The motion constraint that is derived looks identical to the rolling constraint for the fixed standard wheel in equation (3.12), except that the formula is modified by adding γ such that the effective direction along which the rolling constraint holds is along this zero component rather than along the wheel plane:

$$[\sin(\alpha + \beta + \gamma) - \cos(\alpha + \beta + \gamma) (-l) \cos(\beta + \gamma)] R(\theta) \dot{\xi}_I - r \dot{\varphi} \cos \gamma = 0. \quad (3.19)$$

Orthogonal to this direction the motion is not constrained because of the free rotation $\dot{\varphi}_{sw}$ of the small rollers.

$$[\cos(\alpha + \beta + \gamma) \sin(\alpha + \beta + \gamma) l \sin(\beta + \gamma)] R(\theta) \dot{\xi}_I - r \dot{\varphi} \sin \gamma - r_{sw} \dot{\varphi}_{sw} = 0. \quad (3.20)$$

**Figure 3.9**

A spherical wheel and its parameters.

The behavior of this constraint and thereby the Swedish wheel changes dramatically as the value γ varies. Consider $\gamma = 0$. This represents the Swedish 90-degree wheel. In this case, the zero component of velocity is in line with the wheel plane, and so equation (3.19) reduces exactly to equation (3.12), the fixed standard wheel rolling constraint. But because of the rollers, there is no sliding constraint orthogonal to the wheel plane (see equation [3.20]). By varying the value of φ , any desired motion vector can be made to satisfy equation (3.19), and therefore the wheel is omnidirectional. In fact, this special case of the Swedish design results in fully decoupled motion, in that the rollers and the main wheel provide orthogonal directions of motion.

At the other extreme, consider $\gamma = \pi/2$. In this case, the rollers have axes of rotation that are parallel to the main wheel axis of rotation. Interestingly, if this value is substituted for γ in equation (3.19) the result is the fixed standard wheel sliding constraint, equation (3.13). In other words, the rollers provide no benefit in terms of lateral freedom of motion since they are simply aligned with the main wheel. However, in this case the main wheel never needs to spin, and therefore the rolling constraint disappears. This is a degenerate form of the Swedish wheel, and therefore we assume in the remainder of this chapter that $\gamma \neq \pi/2$.

3.2.3.5 Spherical wheel

The final wheel type, a ball or spherical wheel, places no direct constraints on motion (figure 3.9). Such a mechanism has no principal axis of rotation, and therefore no appropriate rolling or sliding constraints exist. As with castor wheels and Swedish wheels, the spherical

wheel is clearly omnidirectional and places no constraints on the robot chassis kinematics. Therefore, equation (3.21) simply describes the roll rate of the ball in the direction of motion v_A of point A of the robot.

$$[\sin(\alpha + \beta) - \cos(\alpha + \beta) (-l) \cos \beta] R(0) \dot{\xi}_I - r \dot{\varphi} = 0. \quad (3.21)$$

By definition, the wheel rotation orthogonal to this direction is zero.

$$[\cos(\alpha + \beta) \sin(\alpha + \beta) l \sin \beta] R(0) \dot{\xi}_I = 0. \quad (3.22)$$

As can be seen, the equations for the spherical wheel are exactly the same as for the fixed standard wheel. However, the interpretation of equation (3.22) is different. The omnidirectional spherical wheel can have any arbitrary direction of movement, where the motion direction given by β is a free variable deduced from equation (3.22). Consider the case that the robot is in pure translation in the direction of Y_R . Then equation (3.22) reduces to $\sin(\alpha + \beta) = 0$, thus $\beta = -\alpha$, which makes sense for this special case.

3.2.4 Robot kinematic constraints

Given a mobile robot with M wheels we can now compute the kinematic constraints of the robot chassis. The key idea is that each wheel imposes zero or more constraints on robot motion, and so the process is simply one of appropriately combining all of the kinematic constraints arising from all of the wheels based on the placement of those wheels on the robot chassis.

We have categorized all wheels into five categories: (1) fixed and (2) steerable standard wheels, (3) castor wheels, (4) Swedish wheels, and (5) spherical wheels. But note from the wheel kinematic constraints in equations (3.17), (3.18), and (3.19) that the castor wheel, Swedish wheel, and spherical wheel impose *no* kinematic constraints on the robot chassis, since $\dot{\xi}_I$ can range freely in all of these cases owing to the internal wheel degrees of freedom.

Therefore, only fixed standard wheels and steerable standard wheels have impact on robot chassis kinematics and therefore require consideration when computing the robot's kinematic constraints. Suppose that the robot has a total of N standard wheels, comprising N_f fixed standard wheels and N_s steerable standard wheels. We use $\beta_s(t)$ to denote the variable steering angles of the N_s steerable standard wheels. In contrast, β_f refers to the orientation of the N_f fixed standard wheels as depicted in figure 3.4. In the case of wheel spin, both the fixed and steerable wheels have rotational positions around the horizontal axle that vary as a function of time. We denote the fixed and steerable cases separately as $\varphi_f(t)$ and $\varphi_s(t)$ and use $\varphi(t)$ as an aggregate matrix that combines both values:

$$\varphi(t) = \begin{bmatrix} \varphi_f(t) \\ \varphi_s(t) \end{bmatrix}. \quad (3.23)$$

The rolling constraints of all wheels can now be collected in a single expression:

$$J_1(\beta_s)R(\theta)\dot{\xi}_I - J_2\dot{\varphi} = 0. \quad (3.24)$$

This expression bears a strong resemblance to the rolling constraint of a single wheel, but substitutes matrices in lieu of single values, thus taking into account all wheels. J_2 is a constant diagonal $N \times N$ matrix whose entries are radii r of all standard wheels. $J_1(\beta_s)$ denotes a matrix with projections for all wheels to their motions along their individual wheel planes:

$$J_1(\beta_s) = \begin{bmatrix} J_{1f} \\ J_{1s}(\beta_s) \end{bmatrix}. \quad (3.25)$$

Note that $J_1(\beta_s)$ is only a function of β_s and not β_f . This is because the orientations of steerable standard wheels vary as a function of time, whereas the orientations of fixed standard wheels are constant. J_{1f} is therefore a constant matrix of projections for all fixed standard wheels. It has size $(N_f \times 3)$, with each row consisting of the three terms in the three-matrix from equation (3.12) for each fixed standard wheel. $J_{1s}(\beta_s)$ is a matrix of size $(N_s \times 3)$, with each row consisting of the three terms in the three-matrix from equation (3.15) for each steerable standard wheel.

In summary, equation (3.24) represents the constraint that all standard wheels must spin around their horizontal axis an appropriate amount based on their motions along the wheel plane so that rolling occurs at the ground contact point.

We use the same technique to collect the sliding constraints of all standard wheels into a single expression with the same structure as equations (3.13) and (3.16):

$$C_1(\beta_s)R(\theta)\dot{\xi}_I = 0. \quad (3.26)$$

$$C_1(\beta_s) = \begin{bmatrix} C_{1f} \\ C_{1s}(\beta_s) \end{bmatrix}. \quad (3.27)$$

C_{1f} and C_{1s} are $(N_f \times 3)$ and $(N_s \times 3)$ matrices whose rows are the three terms in the three-matrix of equations (3.13) and (3.16) for all fixed and steerable standard wheels. Thus

equation (3.26) is a constraint over all standard wheels that their components of motion orthogonal to their wheel planes must be zero. This sliding constraint over all standard wheels has the most significant impact on defining the overall maneuverability of the robot chassis, as explained in the next section.

3.2.5 Examples: Robot kinematic models and constraints

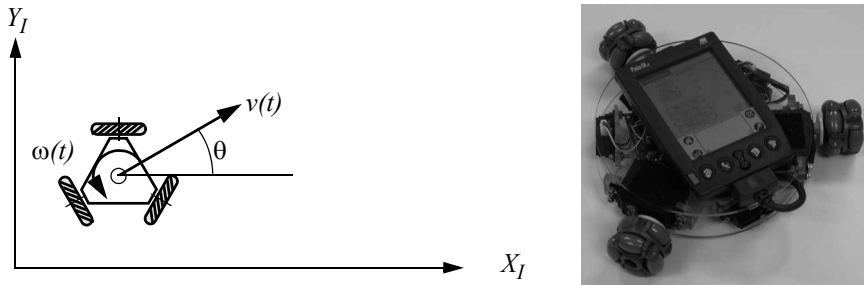
In section 3.2.2 we presented a forward kinematic solution for $\dot{\xi}_I$ in the case of a simple differential-drive robot by combining each wheel's contribution to robot motion. We can now use the tools presented above to construct the same kinematic expression by direct application of the rolling constraints for every wheel type. We proceed with this technique applied again to the differential drive robot, enabling verification of the method as compared to the results of section 3.2.2. Then we proceed to the case of the three-wheeled omnidirectional robot.

3.2.5.1 A differential-drive robot example

First, refer to equations (3.24) and (3.26). These equations relate robot motion to the rolling and sliding constraints $J_1(\beta_s)$ and $C_1(\beta_s)$, and the wheel spin speed of the robot's wheels, $\dot{\phi}$. Fusing these two equations yields the following expression:

$$\begin{bmatrix} J_1(\beta_s) \\ C_1(\beta_s) \end{bmatrix} R(\theta) \dot{\xi}_I = \begin{bmatrix} J_2 \dot{\phi} \\ 0 \end{bmatrix}. \quad (3.28)$$

Once again, consider the differential drive robot in figure 3.3. We will construct $J_1(\beta_s)$ and $C_1(\beta_s)$ directly from the rolling constraints of each wheel. The castor is unpowered and is free to move in any direction, so we ignore this third point of contact altogether. The two remaining drive wheels are not steerable, and therefore $J_1(\beta_s)$ and $C_1(\beta_s)$ simplify to J_{1f} and C_{1f} respectively. To employ the fixed standard wheel's rolling constraint formula, equation (3.12), we must first identify each wheel's values for α and β . Suppose that the robot's local reference frame is aligned such that the robot moves forward along $+X_R$, as shown in figure 3.1. In this case, for the right wheel $\alpha = -\pi/2$, $\beta = \pi$, and for the left wheel, $\alpha = \pi/2$, $\beta = 0$. Note the value of β for the right wheel is necessary to ensure that positive spin causes motion in the $+X_R$ direction (figure 3.4). Now we can compute the J_{1f} and C_{1f} matrix using the matrix terms from equations (3.12) and (3.13). Because the two fixed standard wheels are parallel, equation (3.13) results in only one independent equation, and equation (3.28) gives:

**Figure 3.10**

A three-wheel omnidrive robot developed by Carnegie Mellon University (www.cs.cmu.edu/~pprk).

$$\begin{bmatrix} 1 & 0 & l \\ 1 & 0 & -l \\ 0 & 1 & 0 \end{bmatrix} R(\theta) \dot{\xi}_I = \begin{bmatrix} J_2 \phi \\ 0 \end{bmatrix}. \quad (3.29)$$

Inverting equation (3.29) yields the kinematic equation specific to our differential drive robot:

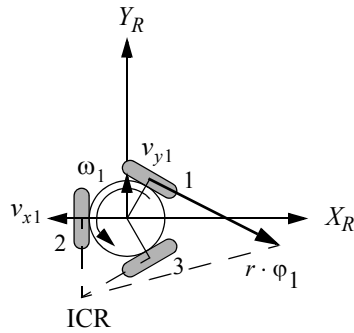
$$\dot{\xi}_I = R(\theta)^{-1} \begin{bmatrix} 1 & 0 & l \\ 1 & 0 & -l \\ 0 & 1 & 0 \end{bmatrix}^{-1} \begin{bmatrix} J_2 \phi \\ 0 \end{bmatrix} = R(\theta)^{-1} \begin{bmatrix} \frac{1}{2} & \frac{1}{2} & 0 \\ 0 & 0 & 1 \\ \frac{1}{2l} & -\frac{1}{2l} & 0 \end{bmatrix} \begin{bmatrix} J_2 \phi \\ 0 \end{bmatrix}. \quad (3.30)$$

This demonstrates that, for the simple differential-drive case, the combination of wheel rolling and sliding constraints describes the kinematic behavior, based on our manual calculation in section 3.2.2.

3.2.5.2 An omnidirectional robot example

Consider the omniwheel robot shown in figure 3.10. This robot has three Swedish 90-degree wheels, arranged radially symmetrically, with the rollers perpendicular to each main wheel.

First we must impose a specific local reference frame upon the robot. We do so by choosing point P at the center of the robot, then aligning the robot with the local reference

**Figure 3.11**

The local reference frame plus detailed parameters for wheel 1.

frame such that X_R is colinear with the axis of wheel 2. Figure 3.11 shows the robot and its local reference frame arranged in this manner.

We assume that the distance between each wheel and P is l , and that all three wheels have the same radius, r . Once again, the value of $\dot{\xi}_I$ can be computed as a combination of the rolling constraints of the robot's three omnidirectional wheels, as in equation (3.28). As with the differential-drive robot, since this robot has no steerable wheels, $J_1(\beta_s)$ simplifies to J_{1f} :

$$\dot{\xi}_I = R(\theta)^{-1} J_{1f}^{-1} J_2 \dot{\varphi}. \quad (3.31)$$

We calculate J_{1f} using the matrix elements of the rolling constraints for the Swedish wheel, given by equation (3.19). But to use these values, we must establish the values α, β, γ for each wheel. Referring to figure (3.8), we can see that $\gamma = 0$ for the Swedish 90-degree wheel. Note that this immediately simplifies equation (3.19) to equation (3.12), the rolling constraints of a fixed standard wheel. Given our particular placement of the local reference frame, the value of α for each wheel is easily computed: $(\alpha_1 = \pi/3)$, $(\alpha_2 = \pi)$, $(\alpha_3 = -\pi/3)$. Furthermore, $\beta = 0$ for all wheels because the wheels are tangent to the robot's circular body. Constructing and simplifying J_{1f} using equation (3.12) yields:

$$J_{1f} = \begin{bmatrix} \sin \frac{\pi}{3} & -\cos \frac{\pi}{3} & -l \\ 0 & -\cos \pi & -l \\ \sin -\frac{\pi}{3} & -\cos -\frac{\pi}{3} & -l \end{bmatrix} = \begin{bmatrix} \frac{\sqrt{3}}{2} & -\frac{1}{2} & -l \\ 0 & 1 & -l \\ -\frac{\sqrt{3}}{2} & -\frac{1}{2} & -l \end{bmatrix}. \quad (3.32)$$

Once again, computing the value of $\dot{\xi}_I$ requires calculating the inverse, J_{1f}^{-1} , as needed in equation (3.31). One approach would be to apply rote methods for calculating the inverse of a 3×3 square matrix. A second approach would be to compute the contribution of each Swedish wheel to chassis motion, as shown in section 3.2.2. We leave this process as an exercise for the enthusiast. Once the inverse is obtained, $\dot{\xi}_I$ can be isolated:

$$\dot{\xi}_I = R(\theta)^{-1} \begin{bmatrix} \frac{1}{\sqrt{3}} & 0 & -\frac{1}{\sqrt{3}} \\ -\frac{1}{3} & \frac{2}{3} & -\frac{1}{3} \\ -\frac{1}{3l} & -\frac{1}{3l} & -\frac{1}{3l} \end{bmatrix} J_2 \dot{\phi}. \quad (3.33)$$

Consider a specific omnidrive chassis with $l = 1$ and $r = 1$ for all wheels. The robot's local reference frame and global reference frame are aligned, so that $\theta = 0$. If wheels 1, 2, and 3 spin at speeds $(\varphi_1 = 4), (\varphi_2 = 1), (\varphi_3 = 2)$, what is the resulting motion of the whole robot? Using the equation above, the answer can be calculated readily:

$$\dot{\xi}_I = \begin{bmatrix} \dot{x} \\ \dot{y} \\ \dot{\theta} \end{bmatrix} = \begin{bmatrix} 1 & 0 & 0 \\ 0 & 1 & 0 \\ 0 & 0 & 1 \end{bmatrix} \begin{bmatrix} \frac{1}{\sqrt{3}} & 0 & -\frac{1}{\sqrt{3}} \\ -\frac{1}{3} & \frac{2}{3} & -\frac{1}{3} \\ -\frac{1}{3} & -\frac{1}{3} & -\frac{1}{3} \end{bmatrix} \begin{bmatrix} 1 & 0 & 0 \\ 0 & 1 & 0 \\ 0 & 0 & 1 \end{bmatrix} \begin{bmatrix} 4 \\ 1 \\ 2 \end{bmatrix} = \begin{bmatrix} \frac{2}{\sqrt{3}} \\ -\frac{4}{3} \\ -\frac{7}{3} \end{bmatrix}. \quad (3.34)$$

So this robot will move instantaneously along the x -axis with positive speed and along the y axis with negative speed while rotating clockwise. We can see from the preceding examples that robot motion can be predicted by combining the rolling constraints of individual wheels.

The sliding constraints comprising $C_1(\beta_s)$ can be used to go even further, enabling us to evaluate the maneuverability and workspace of the robot rather than just its predicted motion. Next, we examine methods for using the sliding constraints, sometimes in conjunction with rolling constraints, to generate powerful analyses of the maneuverability of a robot chassis.

3.3 Mobile Robot Maneuverability

The kinematic mobility of a robot chassis is its ability to directly move in the environment. The basic constraint limiting mobility is the rule that every wheel must satisfy its sliding constraint. Therefore, we can formally derive robot mobility by starting from equation (3.26).

In addition to instantaneous kinematic motion, a mobile robot is able to further manipulate its position, over time, by steering steerable wheels. As we will see in section 3.3.3, the overall maneuverability of a robot is thus a combination of the mobility available based on the kinematic sliding constraints of the standard wheels, plus the additional freedom contributed by steering and spinning the steerable standard wheels.

3.3.1 Degree of mobility

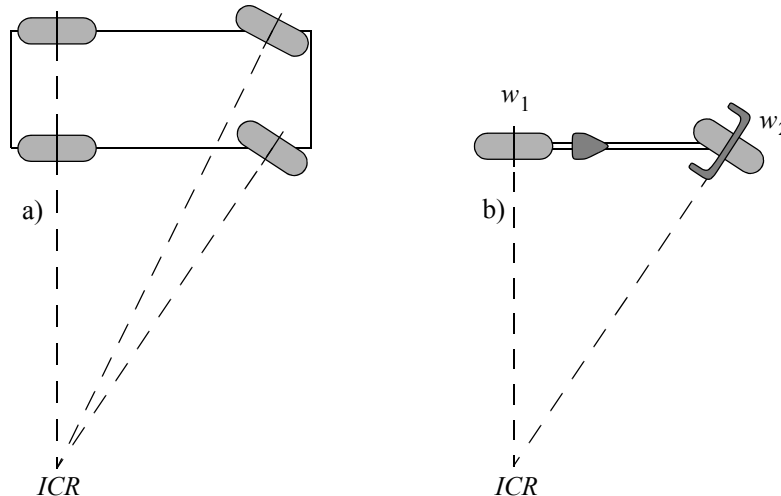
Equation (3.26) imposes the constraint that every wheel must avoid any lateral slip. Of course, this holds separately for each and every wheel, and so it is possible to specify this constraint separately for fixed and for steerable standard wheels:

$$C_{1f}R(\theta)\dot{\xi}_I = 0 . \quad (3.35)$$

$$C_{1s}(\beta_s)R(\theta)\dot{\xi}_I = 0 . \quad (3.36)$$

For both of these constraints to be satisfied, the motion vector $R(\theta)\dot{\xi}_I$ must belong to the *null space* of the projection matrix $C_1(\beta_s)$, which is simply a combination of C_{1f} and C_{1s} . Mathematically, the null space of $C_1(\beta_s)$ is the space N such that for any vector n in N , $C_1(\beta_s)n = 0$. If the kinematic constraints are to be honored, then the motion of the robot must always be within this space N . The kinematic constraints [equations (3.35) and (3.36)] can also be demonstrated geometrically using the concept of a robot's *instantaneous center of rotation (ICR)*.

Consider a single standard wheel. It is forced by the sliding constraint to have zero lateral motion. This can be shown geometrically by drawing a *zero motion line* through its horizontal axis, perpendicular to the wheel plane (figure 3.12). At any given instant, wheel motion along the zero motion line must be zero. In other words, the wheel must be moving

**Figure 3.12**

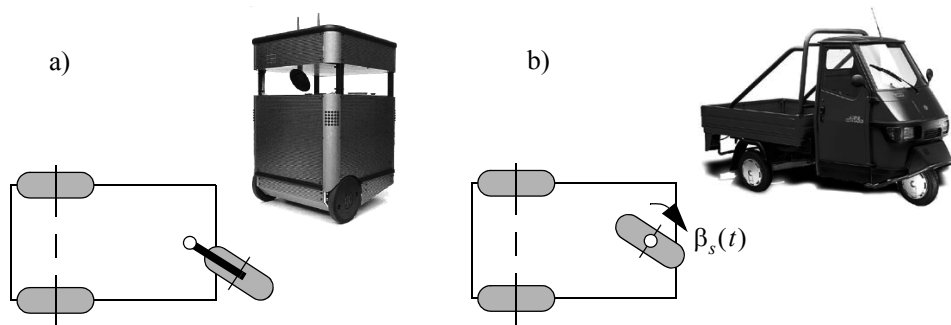
(a) Four-wheel with carlike Ackerman steering. (b) Bicycle.

instantaneously along some circle of radius R such that the center of that circle is located on the zero motion line. This center point, called the instantaneous center of rotation, may lie anywhere along the zero motion line. When R is at infinity, the wheel moves in a straight line.

A robot such as the Ackerman vehicle in figure 3.12a can have several wheels, but it must always have a single ICR . Because all of its zero motion lines meet at a single point, there is a single solution for robot motion, placing the ICR at this meet point.

This ICR geometric construction demonstrates how robot mobility is a function of the number of constraints on the robot's motion, not the number of wheels. In figure 3.12b, the bicycle shown has two wheels, w_1 and w_2 . Each wheel contributes a constraint, or a zero motion line. Taken together, the two constraints result in a single point as the only remaining solution for the ICR . This is because the two constraints are independent, and thus each further constrains overall robot motion.

But in the case of the differential drive robot in figure 3.13a, the two wheels are aligned along the same horizontal axis. Therefore, the ICR is constrained to lie along a line, not at a specific point. In fact, the second wheel imposes no additional kinematic constraints on robot motion since its zero motion line is identical to that of the first wheel. Thus, although the bicycle and differential-drive chassis have the same number of nonomnidirectional wheels, the former has two independent kinematic constraints while the latter has only one.

**Figure 3.13**

(a) Differential-drive robot with two individually motorized wheels and a castor wheel, e.g., the Pygmalion robot at EPFL. (b) Tricycle with two fixed standard wheels and one steered standard wheel, e.g., Piaggio minitransporter.

The Ackerman vehicle of figure 3.12a demonstrates another way in which a wheel may be unable to contribute an independent constraint to the robot kinematics. This vehicle has two steerable standard wheels. Given the instantaneous position of just one of these steerable wheels and the position of the fixed rear wheels, there is only a single solution for the *ICR*. The position of the second steerable wheel is absolutely constrained by the *ICR*. Therefore, it offers no independent constraints to robot motion.

Robot chassis kinematics is therefore a function of the set of *independent* constraints arising from all standard wheels. The mathematical interpretation of independence is related to the *rank* of a matrix. Recall that the rank of a matrix is the largest number of linearly independent rows or columns. Equation (3.26) represents all sliding constraints imposed by the wheels of the mobile robot. Therefore, $\text{rank}[C_1(\beta_s)]$ is the number of independent constraints.

The greater the number of independent constraints, and therefore the greater the rank of $C_1(\beta_s)$, the more constrained is the mobility of the robot. For example, consider a robot with a single fixed standard wheel. Remember that we consider only standard wheels. This robot may be a unicycle or it may have several Swedish wheels; however, it has exactly one fixed standard wheel. The wheel is at a position specified by parameters α, β, l relative to the robot's local reference frame. $C_1(\beta_s)$ comprises C_{1f} and C_{1s} . However, since there are no steerable standard wheels, C_{1s} is empty, and therefore $C_1(\beta_s)$ contains only C_{1f} . Because there is one fixed standard wheel, this matrix has a rank of one, and therefore this robot has a single independent constraint on mobility:

$$C_1(\beta_s) = C_{1f} = [\cos(\alpha + \beta) \ \sin(\alpha + \beta) \ l \sin \beta]. \quad (3.37)$$

Now let us add an additional fixed standard wheel to create a differential-drive robot by constraining the second wheel to be aligned with the same horizontal axis as the original wheel. Without loss of generality, we can place point P at the midpoint between the centers of the two wheels. Given α_1, β_1, l_1 for wheel w_1 and α_2, β_2, l_2 for wheel w_2 , it holds geometrically that $\{(l_1 = l_2), (\beta_1 = \beta_2 = 0), (\alpha_1 + \pi = \alpha_2)\}$. Therefore, in this case, the matrix $C_1(\beta_s)$ has two constraints but a rank of one:

$$C_1(\beta_s) = C_{1f} = \begin{bmatrix} \cos(\alpha_1) & \sin(\alpha_1) & 0 \\ \cos(\alpha_1 + \pi) & \sin(\alpha_1 + \pi) & 0 \end{bmatrix}. \quad (3.38)$$

Alternatively, consider the case when w_2 is placed in the wheel plane of w_1 but with the same orientation, as in a bicycle with the steering locked in the forward position. We again place point P between the two wheel centers and orient the wheels such that they lie on axis x_1 . This geometry implies that $\{(l_1 = l_2), (\beta_1 = \beta_2 = \pi/2), (\alpha_1 = 0), (\alpha_2 = \pi)\}$ and, therefore, the matrix $C_1(\beta_s)$ retains two independent constraints and has a rank of two:

$$C_1(\beta_s) = C_{1f} = \begin{bmatrix} \cos(\pi/2) & \sin(\pi/2) & l_1 \sin(\pi/2) \\ \cos(3\pi/2) & \sin(3\pi/2) & l_1 \sin(\pi/2) \end{bmatrix} = \begin{bmatrix} 0 & 1 & l_1 \\ 0 & -1 & l_1 \end{bmatrix}. \quad (3.39)$$

In general, if $\text{rank}[C_{1f}] > 1$ then the vehicle can, at best, only travel along a circle or along a straight line. This configuration means that the robot has two or more independent constraints due to fixed standard wheels that do not share the same horizontal axis of rotation. Because such configurations have only a degenerate form of mobility in the plane, we do not consider them in the remainder of this chapter. Note, however, that some degenerate configurations such as the four-wheeled slip/skid steering system are useful in certain environments, such as on loose soil and sand, even though they fail to satisfy sliding constraints. Not surprisingly, the price that must be paid for such violations of the sliding constraints is that dead reckoning based on odometry becomes less accurate and power efficiency is reduced dramatically.

In general, a robot will have zero or more fixed standard wheels and zero or more steerable standard wheels. We can therefore identify the possible range of rank values for any robot: $0 \leq \text{rank}[C_1(\beta_s)] \leq 3$. Consider the case $\text{rank}[C_1(\beta_s)] = 0$. This is possible only if there are zero independent kinematic constraints in $C_1(\beta_s)$. In this case there are neither fixed nor steerable standard wheels attached to the robot frame: $N_f = N_s = 0$.

Consider the other extreme, $\text{rank}[C_1(\beta_s)] = 3$. This is the maximum possible rank since the kinematic constraints are specified along three degrees of freedom (i.e., the constraint matrix is three columns wide). Therefore, there cannot be more than three indepen-

dent constraints. In fact, when $\text{rank}[C_1(\beta_s)] = 3$, then the robot is completely constrained in all directions and is therefore degenerate, since motion in the plane is totally impossible.

Now we are ready to formally define a robot's *degree of mobility* δ_m :

$$\delta_m = \dim N[C_1(\beta_s)] = 3 - \text{rank}[C_1(\beta_s)]. \quad (3.40)$$

The dimensionality of the null space ($\dim N$) of matrix $C_1(\beta_s)$ is a measure of the number of degrees of freedom of the robot chassis that can be immediately manipulated through changes in wheel velocity. It is logical, therefore, that δ_m must range between 0 and 3.

Consider an ordinary differential-drive chassis. On such a robot there are two fixed standard wheels sharing a common horizontal axis. As discussed earlier, the second wheel adds no independent kinematic constraints to the system. Therefore, $\text{rank}[C_1(\beta_s)] = 1$ and $\delta_m = 2$. This fits with intuition: a differential drive robot can control both the rate of its change in orientation and its forward/reverse speed, *simply by manipulating wheel velocities*. In other words, its *ICR* is constrained to lie on the infinite line extending from its wheels' horizontal axles.

In contrast, consider a bicycle chassis. This configuration consists of one fixed standard wheel and one steerable standard wheel. In this case, each wheel contributes an independent sliding constraint to $C_1(\beta_s)$. Therefore, $\delta_m = 1$. Note that the bicycle has the same total number of nonomnidirectional wheels as the differential-drive chassis, and indeed one of its wheels is steerable. Yet it has one less degree of mobility. Upon reflection, this is appropriate. A bicycle only has control over its forward/reverse speed by direct manipulation of wheel velocities. Only by steering can the bicycle change its *ICR*.

As expected, based on equation (3.40), any robot consisting only of omnidirectional wheels such as Swedish or spherical wheels will have the maximum mobility, $\delta_m = 3$. Such a robot can directly manipulate all three degrees of freedom.

3.3.2 Degree of steerability

The degree of mobility defined above quantifies the degrees of controllable freedom based on changes to wheel velocity. Steering can also have an eventual impact on a robot chassis pose ξ , although the impact is indirect because after changing the angle of a steerable standard wheel, the robot must move for the change in steering angle to have impact on pose.

As with mobility, we care about the number of independently controllable steering parameters when defining the *degree of steerability* δ_s :

$$\delta_s = \text{rank}[C_{1s}(\beta_s)]. \quad (3.41)$$

Recall that in the case of mobility, an increase in the rank of $C_1(\beta_s)$ implied more kinematic constraints and thus a less mobile system. In the case of steerability, an increase in the rank of $C_{1s}(\beta_s)$ implies more degrees of steering freedom and thus greater eventual maneuverability. Since $C_1(\beta_s)$ includes $C_{1s}(\beta_s)$, this means that a steered standard wheel can both decrease mobility and increase steerability: its particular orientation at any instant imposes a kinematic constraint, but its ability to change that orientation can lead to additional trajectories.

The range of δ_s can be specified: $0 \leq \delta_s \leq 2$. The case $\delta_s = 0$ implies that the robot has no steerable standard wheels, $N_s = 0$. The case $\delta_s = 1$ is most common when a robot configuration includes one or more steerable standard wheels.

For example, consider an ordinary automobile. In this case $N_f = 2$ and $N_s = 2$. But the fixed wheels share a common axle and so $\text{rank}[C_{1f}] = 1$. The fixed wheels and any one of the steerable wheels constrain the *ICR* to be a point along the line extending from the rear axle. Therefore, the second steerable wheel cannot impose any independent kinematic constraint and so $\text{rank}[C_{1s}(\beta_s)] = 1$. In this case $\delta_m = 1$ and $\delta_s = 1$.

The case $\delta_s = 2$ is possible only in robots with no fixed standard wheels: $N_f = 0$. Under these circumstances, it is possible to create a chassis with two separate steerable standard wheels, like a pseudobicycle (or the two-steer) in which both wheels are steerable. Then, orienting one wheel constrains the *ICR* to a line, while the second wheel can constrain the *ICR* to any point along that line. Interestingly, this means that the $\delta_s = 2$ implies that the robot can place its *ICR* anywhere on the ground plane.

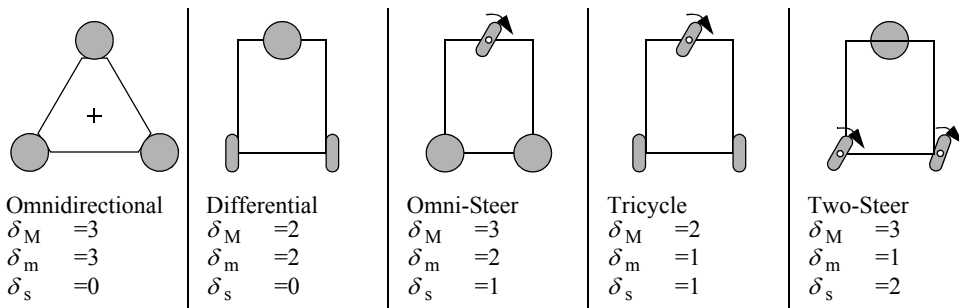
3.3.3 Robot maneuverability

The overall degrees of freedom that a robot can manipulate, called the *degree of maneuverability* δ_M , can be readily defined in terms of mobility and steerability:

$$\delta_M = \delta_m + \delta_s. \quad (3.42)$$

Therefore, maneuverability includes both the degrees of freedom that the robot manipulates directly through wheel velocity and the degrees of freedom that it indirectly manipulates by changing the steering configuration and moving. Based on the investigations of the previous sections, one can draw the basic types of wheel configurations. They are depicted in figure 3.14.

Note that two robots with the same δ_M are not necessarily equivalent. For example, differential drive and tricycle geometries (figure 3.13) have equal maneuverability $\delta_M = 2$. In differential drive all maneuverability is the result of direct mobility because $\delta_m = 2$ and $\delta_s = 0$. In the case of a tricycle the maneuverability results from steering also: $\delta_m = 1$ and $\delta_s = 1$. Neither of these configurations allows the *ICR* to range anywhere on the plane. In both cases, the *ICR* must lie on a predefined line with respect to the robot refer-

**Figure 3.14**

The five basic types of three-wheel configurations. The spherical wheels can be replaced by castor or Swedish wheels without influencing maneuverability. More configurations with various numbers of wheels are found in chapter 2.

ence frame. In the case of differential drive, this line extends from the common axle of the two fixed standard wheels, with the differential wheel velocities setting the *ICR* point on this line. In a tricycle, this line extends from the shared common axle of the fixed wheels, with the steerable wheel setting the *ICR* point along this line.

More generally, for any robot with $\delta_M = 2$ the *ICR* is always constrained to lie on a line and for any robot with $\delta_M = 3$ the *ICR* can be set to any point on the plane.

One final example will demonstrate the use of the tools we have developed here. One common robot configuration for indoor mobile robotics research is the *synchro drive* configuration (figure 2.28). Such a robot has two motors and three wheels that are locked together. One motor provides power for spinning all three wheels, while the second motor provides power for steering all three wheels. In a three-wheeled synchro drive robot $N_f = 0$ and $N_s = 3$. Therefore, $\text{rank}[C_{1s}(\beta_s)]$ can be used to determine both δ_m and δ_s . The three wheels do not share a common axle; therefore, two of the three contribute independent sliding constraints. The third must be dependent on these two constraints for motion to be possible. Therefore, $\text{rank}[C_{1s}(\beta_s)] = 2$ and $\delta_m = 1$. This is intuitively correct. A synchro drive robot with the steering frozen manipulates only one degree of freedom, consisting of traveling back and forth on a straight line.

However, an interesting complication occurs when considering δ_s . Based on equation (3.41) the robot should have $\delta_s = 2$. Indeed, for a three-wheel-steering robot with the geometric configuration of a synchro drive robot this would be correct. However, we have additional information: in a synchro drive configuration a single motor steers all three wheels using a belt drive. Therefore, although ideally, if the wheels were independently steerable, then the system would achieve $\delta_s = 2$; in the case of synchro drive the drive

system further constrains the kinematics such that in reality $\delta_s = 1$. Finally, we can compute maneuverability based on these values: $\delta_M = 2$ for a synchro drive robot.

This result implies that a synchro drive robot can only manipulate, in total, two degrees of freedom. In fact, if the reader reflects on the wheel configuration of a synchro drive robot, it will become apparent that there is no way for the chassis orientation to change. Only the $x-y$ position of the chassis can be manipulated, and so, indeed, a synchro drive robot has only two degrees of freedom, in agreement with our mathematical conclusion.

3.4 Mobile Robot Workspace

For a robot, maneuverability is equivalent to its control degrees of freedom. But the robot is situated in some environment, and the next question is to situate our analysis in the environment. We care about the ways in which the robot can use its control degrees of freedom to position itself in the environment. For instance, consider the Ackerman vehicle, or automobile. The total number of control degrees of freedom for such a vehicle is $\delta_M = 2$, one for steering and the second for actuation of the drive wheels. But what are the total degrees of freedom of the vehicle in its environment? In fact, it is three: the car can position itself on the plane at any x, y point and with any angle θ .

Thus, identifying a robot's space of possible configurations is important because, surprisingly, it can exceed δ_M . In addition to *workspace*, we care about how the robot is able to move between various configurations: What are the types of paths that it can follow and, furthermore, what are its possible trajectories through this configuration space? In the remainder of this discussion, we move away from inner kinematic details such as wheels and focus instead on the robot chassis pose and the chassis degrees of freedom. With this in mind, let us place the robot in the context of its workspace now.

3.4.1 Degrees of freedom

In defining the workspace of a robot, it is useful to first examine its *admissible velocity space*. Given the kinematic constraints of the robot, its velocity space describes the independent components of robot motion that the robot can control. For example, the velocity space of a unicycle can be represented with two axes, one representing the instantaneous forward speed of the unicycle and the second representing the instantaneous change in orientation, $\dot{\theta}$, of the unicycle.

The number of dimensions in the velocity space of a robot is the number of independently achievable velocities. This is also called the *differential degrees of freedom (DDOF)*. A robot's *DDOF* is *always* equal to its degree of mobility δ_m . For example, a bicycle has the following degree of maneuverability: $\delta_M = \delta_m + \delta_s = 1 + 1 = 2$. The *DDOF* of a bicycle is indeed 1.

In contrast to a bicycle, consider an *omnibot*, a robot with three Swedish wheels. We know that in this case there are zero standard wheels, and therefore $\delta_M = \delta_m + \delta_s = 3 + 0 = 3$. So, the omnibot has three differential degrees of freedom. This is appropriate, given that because such a robot has no kinematic motion constraints, it is able to independently set all three pose variables: $\dot{x}, \dot{y}, \dot{\theta}$.

Given the difference in *DDOF* between a bicycle and an omnibot, consider the overall degrees of freedom in the workspace of each configuration. The omnibot can achieve any pose (x, y, θ) in its environment and can do so by directly achieving the goal positions of all three axes simultaneously because $DDOF = 3$. Clearly, it has a workspace with $DOF = 3$.

Can a bicycle achieve any pose (x, y, θ) in its environment? It can do so, but achieving some goal points may require more time and energy than an equivalent omnibot. For example, if a bicycle configuration must move laterally 1 m, the simplest successful maneuver would involve either a spiral or a back-and-forth motion similar to *parallel parking* of automobiles. Nevertheless, a bicycle can achieve any (x, y, θ) , and therefore the workspace of a bicycle has $DOF = 3$ as well.

Clearly, there is an inequality relation at work: $DDOF \leq \delta_M \leq DOF$. Although the dimensionality of a robot's workspace is an important attribute, it is clear from the preceding example that the particular paths available to a robot matter as well. Just as workspace DOF governs the robot's ability to achieve various poses, so the robot's *DDOF* governs its ability to achieve various paths.

3.4.2 Holonomic robots

In the robotics community, when describing the path space of a mobile robot, often the concept of holonomy is used. The term *holonomic* has broad applicability to several mathematical areas, including differential equations, functions, and constraint expressions. In mobile robotics, the term refers specifically to the kinematic constraints of the robot chassis. A *holonomic robot* is a robot that has zero nonholonomic kinematic constraints. Conversely, a *nonholonomic robot* is a robot with one or more nonholonomic kinematic constraints.

A *holonomic kinematic constraint* can be expressed as an explicit function of position variables only. For example, in the case of a mobile robot with a single fixed standard wheel, a holonomic kinematic constraint would be expressible using $\alpha_1, \beta_1, l_1, r_1, \varphi_1, x, y, \theta$ only. Such a constraint may not use derivatives of these values, such as $\dot{\varphi}$ or $\ddot{\xi}$. A *nonholonomic kinematic constraint* requires a differential relationship, such as the derivative of a position variable. Furthermore, it cannot be integrated to provide a constraint in terms of the position variables only. Because of this latter point of view, nonholonomic systems are often called *nonintegrable* systems.

Consider the fixed standard wheel sliding constraint:

$$[\cos(\alpha + \beta) \sin(\alpha + \beta) l \sin \beta] R(\theta) \dot{\xi}_I = 0. \quad (3.43)$$

This constraint must use robot motion $\dot{\xi}$ rather than pose ξ because the point is to constrain robot motion perpendicular to the wheel plane to be zero. The constraint is nonintegrable, depending explicitly on robot motion. Therefore, the sliding constraint is a nonholonomic constraint. Consider a bicycle configuration, with one fixed standard wheel and one steerable standard wheel. Because the fixed wheel sliding constraint will be in force for such a robot, we can conclude that the bicycle is a nonholonomic robot.

But suppose that one locks the bicycle steering system, so that it becomes two fixed standard wheels with separate but parallel axes. We know that $\delta_M = 1$ for such a configuration. Is it nonholonomic? Although it may not appear so because of the sliding and rolling constraints, the locked bicycle is actually holonomic. Consider the workspace of this locked bicycle. It consists of a single infinite line along which the bicycle can move (assuming the steering was frozen straight ahead). For formulaic simplicity, assume that this infinite line is aligned with X_I in the global reference frame and that $\{\beta_{1,2} = \pi/2, \alpha_1 = 0, \alpha_2 = \pi\}$. In this case the sliding constraints of both wheels can be replaced with an equally complete set of constraints on the robot pose: $\{y = 0, \theta = 0\}$. This eliminates two nonholonomic constraints, corresponding to the sliding constraints of the two wheels.

The only remaining nonholonomic kinematic constraints are the rolling constraints for each wheel:

$$[-\sin(\alpha + \beta) \cos(\alpha + \beta) l \cos \beta] R(\theta) \dot{\xi}_I + r \dot{\varphi} = 0. \quad (3.44)$$

This constraint is required for each wheel to relate the speed of wheel spin to the speed of motion projected along the wheel plane. But in the case of our locked bicycle, given the initial rotational position of a wheel at the origin, φ_o , we can replace this constraint with one that directly relates position on the line, x , with wheel rotation angle, φ : $\varphi = (x/r) + \varphi_o$.

The locked bicycle is an example of the first type of holonomic robot—where constraints do exist but are all holonomic kinematic constraints. This is the case for all holonomic robots with $\delta_M < 3$. The second type of holonomic robot exists when there are no kinematic constraints, that is, $N_f = 0$ and $N_s = 0$. Since there are no kinematic constraints, there are also no nonholonomic kinematic constraints, and so such a robot is always holonomic. This is the case for all holonomic robots with $\delta_M = 3$.

An alternative way to describe a holonomic robot is based on the relationship between the differential degrees of freedom of a robot and the degrees of freedom of its workspace: *a robot is holonomic if and only if $DDOF = DOF$* . Intuitively, this is because it is only through nonholonomic constraints (imposed by steerable or fixed standard wheels) that a robot can achieve a workspace with degrees of freedom exceeding its differential degrees of freedom, $DOF > DDOF$. Examples include differential drive and bicycle/tricycle configurations.

In mobile robotics, useful chassis generally must achieve poses in a workspace with dimensionality 3, so in general we require $DOF = 3$ for the chassis. But the “holonomic” abilities to maneuver around obstacles without affecting orientation and to track at a target while following an arbitrary path are important additional considerations. For these reasons, the particular form of holonomy most relevant to mobile robotics is that of $DDOF = DOF = 3$. We define this class of robot configurations as omnidirectional: an *omnidirectional robot* is a holonomic robot with $DDOF = 3$.

3.4.3 Path and trajectory considerations

In mobile robotics, we care not only about the robot’s ability to reach the required final configurations but also about *how* it gets there. Consider the issue of a robot’s ability to follow paths: in the best case, a robot should be able to trace any path through its workspace of poses. Clearly, any omnidirectional robot can do this because it is holonomic in a three-dimensional workspace. Unfortunately, omnidirectional robots must use unconstrained wheels, limiting the choice of wheels to Swedish wheels, castor wheels, and spherical wheels. These wheels have not yet been incorporated into designs that allow far larger amounts of ground clearance and suspensions. Although powerful from a path space point of view, they are thus much less common than fixed and steerable standard wheels, mainly because their design and fabrication are somewhat complex and expensive.

Additionally, nonholonomic constraints might drastically improve stability of movements. Consider an omnidirectional vehicle driving at high speed on a curve with constant diameter. During such a movement the vehicle will be exposed to a non-negligible centripetal force. This lateral force pushing the vehicle out of the curve has to be counteracted by the motor torque of the omnidirectional wheels. In case of motor or control failure, the vehicle will be thrown out of the curve. However, for a carlike robot with kinematic constraints, the lateral forces are passively counteracted through the sliding constraints, mitigating the demands on motor torque.

But recall an earlier example of high maneuverability using standard wheels: the bicycle on which both wheels are steerable, often called the *two-steer*. This vehicle achieves a degree of steerability of 2, resulting in a high degree of maneuverability: $\delta_M = \delta_m + \delta_s = 1 + 2 = 3$. Interestingly, this configuration is not holonomic, yet it has a high degree of maneuverability in a workspace with $DOF = 3$.

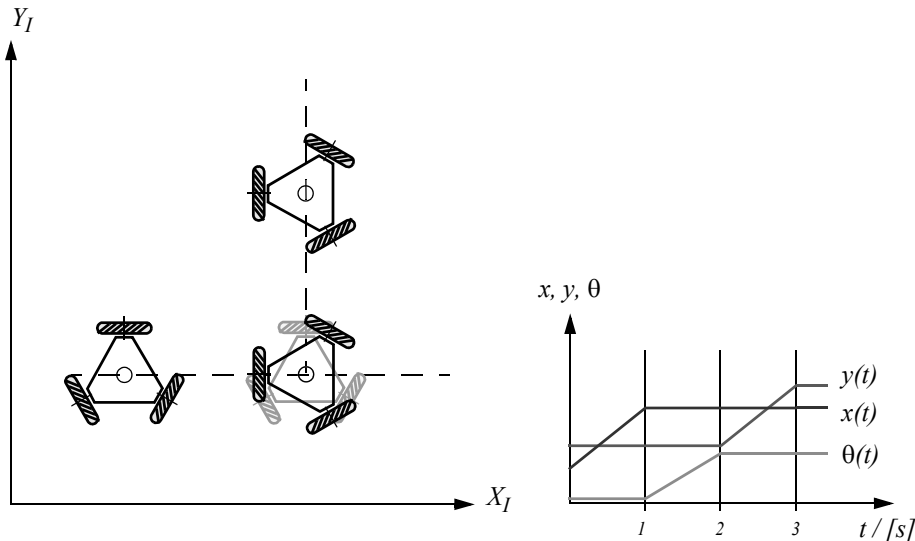


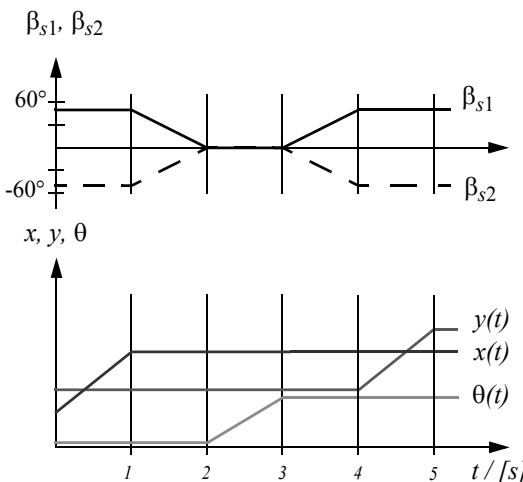
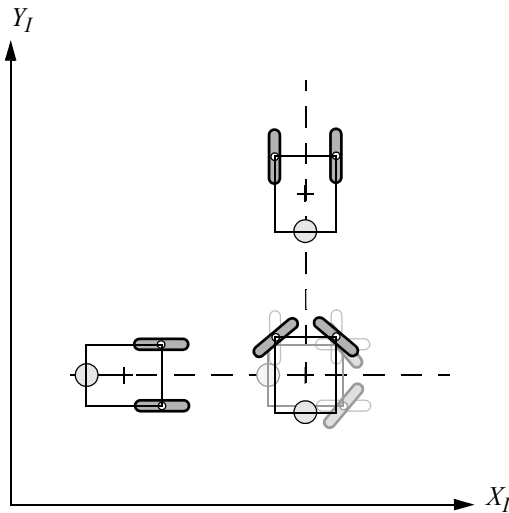
Figure 3.15

Example of robot trajectory with omnidirectional robot: move for 1 second with constant speed of 1 m/s along axis X_I ; change orientation counterclockwise 90 degree, in 1 second; move for 1 second with constant speed of 1 m/s along axis Y_I .

The maneuverability result, $\delta_M = 3$, means that the two-steer can select any *ICR* by appropriately steering its two wheels. So, how does this compare to an omnidirectional robot? The ability to manipulate its *ICR* in the plane means that the two-steer can follow *any* path in its workspace. More generally, any robot with $\delta_M = 3$ can follow any path in its workspace from its initial pose to its final pose. An omnidirectional robot can also follow any path in its workspace and, not surprisingly, since $\delta_m = 3$ in an omnidirectional robot, then it must follow that $\delta_M = 3$.

But there is still a difference between a degree of freedom granted by steering versus by direct control of wheel velocity. This difference is clear in the context of *trajectories* rather than paths. A trajectory is like a path, except that it occupies an additional dimension: time. Therefore, for an omnidirectional robot on the ground plane, a path generally denotes a trace through a 3D space of pose; for the same robot, a trajectory denotes a trace through the 4D space of pose plus time.

For example, consider a goal trajectory in which the robot moves along axis X_I at a constant speed of 1 m/s for 1 second, then changes orientation counterclockwise 90 degrees also in 1 second, then moves parallel to axis Y_I for 1 final second. The desired 3-second trajectory is shown in figure 3.15, using plots of x , y and θ in relation to time.

**Figure 3.16**

Example of robot trajectory similar to figure 3.15 with two steered wheels: move for 1 second with constant speed of 1 m/s along axis \$X_I\$; rotate steered wheels -50 / 50 degree respectively; change orientation counterclockwise 90 degree in 1 second; rotate steered wheels 50 / -50 degree respectively; move for 1 second with constant speed of 1 m/s along axis \$Y_I\$.

Can the omnidirectional robot accomplish this trajectory? We assume that the robot can achieve some arbitrary, finite velocity at each wheel. For simplicity, we further assume that acceleration is infinite; that is, it takes zero time to reach any desired velocity. Under these assumptions, the omnidirectional robot can indeed follow the trajectory of figure 3.15. The transition between the motion of second 1 and second 2, for example, involves only changes to the wheel velocities.

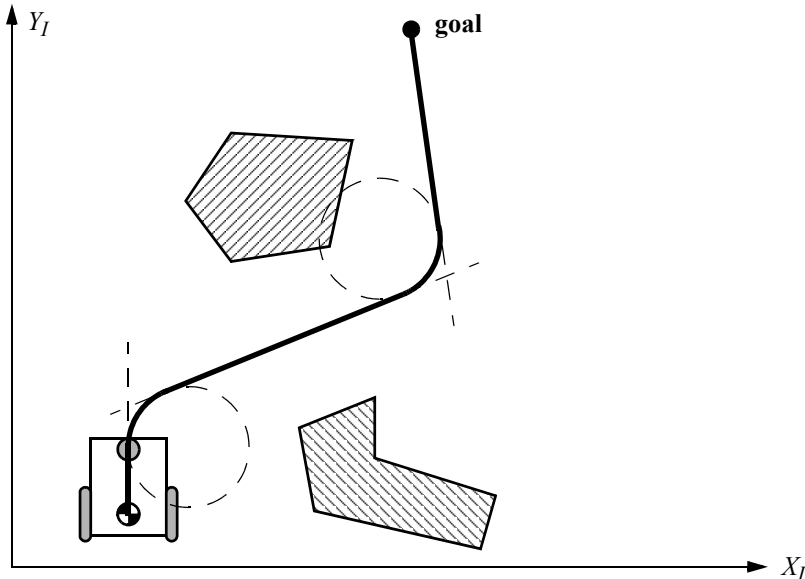
Because the two-steer has $\delta_M = 3$, it must be able to follow the path that would result from projecting this trajectory into timeless workspace. However, it cannot follow this 4D trajectory. Even if steering velocity is finite and arbitrary, although the two-steer would be able to change steering speed instantly, it would have to wait for the angle of the steerable wheels to change to the desired position before initiating a change in the robot chassis orientation. In short, the two-steer requires changes to internal degrees of freedom and because these changes take time, arbitrary trajectories are not attainable. Figure 3.16 depicts the most similar trajectory that a two-steer can achieve. In contrast to the desired three phases of motion, this trajectory has five phases.

3.5 Beyond Basic Kinematics

This discussion of mobile robot kinematics is only an introduction to a far richer topic. When speed and force are also considered, as is particularly necessary in the case of high-speed mobile robots, dynamic constraints must be expressed in addition to kinematic constraints. Furthermore, many mobile robots such as tank-type chassis and four-wheel slip/skid systems violate the preceding kinematic models. When analyzing such systems, it is often necessary to explicitly model the dynamics of viscous friction between the robot and the ground plane.

More significantly, the kinematic analysis of a mobile robot system provides results concerning the theoretical workspace of that mobile robot. However, to move effectively in this workspace a mobile robot must have appropriate actuation of its degrees of freedom. This problem, called motorization, requires further analysis of the forces that must be actively supplied to realize the kinematic range of motion available to the robot.

In addition to motorization, there is the question of controllability: under what conditions can a mobile robot travel from the initial pose to the goal pose in bounded time? Answering this question requires knowledge, both knowledge of the robot kinematics and knowledge of the control systems that can be used to actuate the mobile robot. Mobile robot control is therefore a return to the practical question of designing a real-world control algorithm that can drive the robot from pose to pose using the trajectories demanded for the application.

**Figure 3.17**

Open-loop control of a mobile robot based on straight lines and circular trajectory segments.

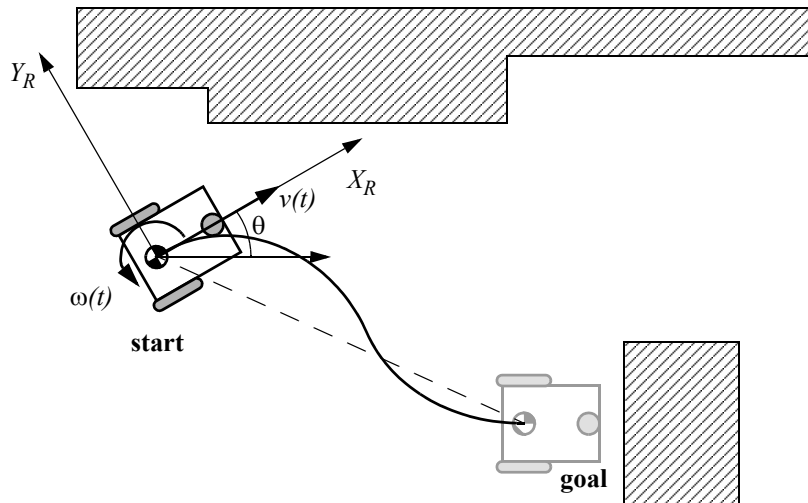
3.6 Motion Control (Kinematic Control)

As we have seen, motion control might not be an easy task for nonholonomic systems. However, it has been studied by various research groups, for example, [10, 61, 90, 92, 300], and some adequate solutions for motion control of a mobile robot system are available.

3.6.1 Open loop control (trajectory-following)

The objective of a kinematic controller is to follow a trajectory described by its position or velocity profile as a function of time. This is often done by dividing the trajectory (path) in motion segments of clearly defined shape, for example, straight *lines* and segments of a *circle*. The control problem is thus to precompute a smooth trajectory based on line and circle segments that drives the robot from the initial position to the final position (figure 3.17). This approach can be regarded as open-loop motion control, because the measured robot position is not fed back for velocity or position control. It has several disadvantages:

- It is not at all an easy task to precompute a feasible trajectory if all limitations and constraints of the robot's velocities and accelerations have to be considered.

**Figure 3.18**

Typical situation for feedback control of a mobile robot

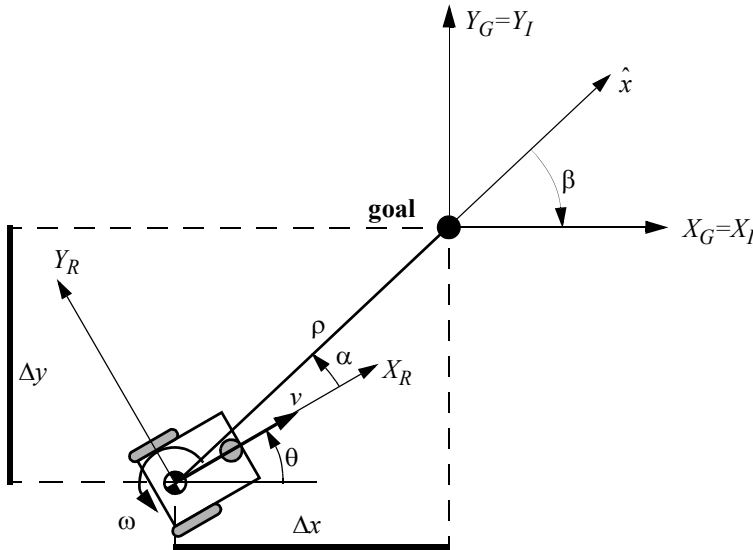
- The robot will not automatically adapt or correct the trajectory if dynamic changes of the environment occur.
- The resulting trajectories are usually not smooth, because the transitions from one trajectory segment to another are, for most of the commonly used segments (e.g., lines and part of circles), not smooth. This means there is a discontinuity in the robot's acceleration.

3.6.2 Feedback control

A more appropriate approach in motion control of a mobile robot is to use a real-state feedback controller. With such a controller the robot's path-planning task is reduced to setting intermediate positions (subgoals) lying on the requested path. One useful solution for a stabilizing feedback control of differential-drive mobile robots is presented in section 3.6.2.1. It is very similar to the controllers presented in [61, 189]. Others can be found in [10, 90, 92, 300].

3.6.2.1 Problem statement

Consider the situation shown in figure 3.18, with an arbitrary position and orientation of the robot and a predefined goal position and orientation. The actual pose error vector given in

**Figure 3.19**

Robot kinematics and its frames of interest.

the robot reference frame $\{X_R, Y_R, \theta\}$ is $e = {}^R[x, y, \theta]^T$ with x, y , and θ being the goal coordinates of the robot.

The task of the controller layout is to find a control matrix K , if it exists

$$K = \begin{bmatrix} k_{11} & k_{12} & k_{13} \\ k_{21} & k_{22} & k_{23} \end{bmatrix} \quad \text{with } k_{ij} = k(t, e), \quad (3.45)$$

such that the control of $v(t)$ and $\omega(t)$

$$\begin{bmatrix} v(t) \\ \omega(t) \end{bmatrix} = K \cdot e = K \begin{bmatrix} x \\ y \\ \theta \end{bmatrix} \quad (3.46)$$

drives the error e toward zero.²

2. Remember that $v(t)$ is always heading in the X_R direction of the robot's reference frame due to the nonholonomic constraint.

$$\lim_{t \rightarrow \infty} e(t) = 0. \quad (3.47)$$

3.6.2.2 Kinematic model

We assume, without loss of generality, that the goal is at the origin of the inertial frame (figure 3.19). In the following the position vector $[x, y, \theta]^T$ is always represented in the inertial frame.

The kinematics of a differential-drive mobile robot described in the inertial frame $\{X_I, Y_I, \theta\}$ is given by

$${}^I \begin{bmatrix} \dot{x} \\ \dot{y} \\ \dot{\theta} \end{bmatrix} = \begin{bmatrix} \cos \theta & 0 \\ \sin \theta & 0 \\ 0 & 1 \end{bmatrix} \begin{bmatrix} v \\ \omega \end{bmatrix}. \quad (3.48)$$

where \dot{x} and \dot{y} are the linear velocities in the direction of the X_I and Y_I of the inertial frame.

Let α denote the angle between the x_R axis of the robot's reference frame and the vector \hat{x} connecting the center of the axle of the wheels with the final position. If $\alpha \in I_1$, where

$$I_1 = \left(-\frac{\pi}{2}, \frac{\pi}{2} \right], \quad (3.49)$$

then consider the coordinate transformation into polar coordinates with its origin at the goal position.

$$\rho = \sqrt{\Delta x^2 + \Delta y^2}. \quad (3.50)$$

$$\alpha = -\theta + \text{atan}2(\Delta y, \Delta x). \quad (3.51)$$

$$\beta = -\theta - \alpha. \quad (3.52)$$

This yields a system description, in the new polar coordinates, using a matrix equation

$$\begin{bmatrix} \dot{\rho} \\ \dot{\alpha} \\ \dot{\beta} \end{bmatrix} = \begin{bmatrix} -\cos \alpha & 0 \\ \frac{\sin \alpha}{\rho} & -1 \\ -\frac{\sin \alpha}{\rho} & 0 \end{bmatrix} \begin{bmatrix} v \\ \omega \end{bmatrix}, \quad (3.53)$$

where ρ is the distance between the center of the robot's wheel axle and the goal position, θ denotes the angle between the X_R axis of the robot reference frame and the X_f axis associated with the final position, and v and ω are the tangent and the angular velocity respectively.

On the other hand, if $\alpha \in I_2$, where

$$I_2 = (-\pi, -\pi/2] \cup (\pi/2, \pi], \quad (3.54)$$

redefining the forward direction of the robot by setting $v = -v$, we obtain a system described by a matrix equation of the form

$$\begin{bmatrix} \dot{\rho} \\ \dot{\alpha} \\ \dot{\beta} \end{bmatrix} = \begin{bmatrix} \cos \alpha & 0 \\ -\frac{\sin \alpha}{\rho} & 1 \\ \frac{\sin \alpha}{\rho} & 0 \end{bmatrix} \begin{bmatrix} v \\ \omega \end{bmatrix}. \quad (3.55)$$

3.6.2.3 Remarks on the kinematic model in polar coordinates [eq. (3.53) and (3.55)]

- The coordinate transformation is not defined at $x = y = 0$; in such a point the determinant of the Jacobian matrix of the transformation is not defined, that is unbounded.
- For $\alpha \in I_1$ the forward direction of the robot points toward the goal; for $\alpha \in I_2$ it is the reverse direction.
- By properly defining the forward direction of the robot at its initial configuration, it is always possible to have $\alpha \in I_1$ at $t = 0$. However, this does not mean that α remains in I_1 for all time t . Hence, to avoid that the robot changes direction during approaching the goal, it is necessary to determine, if possible, the controller in such a way that $\alpha \in I_1$ for all t , whenever $\alpha(0) \in I_1$. The same applies for the reverse direction (see the following stability issues).

3.6.2.4 The control law

The control signals v and ω must now be designed to drive the robot from its actual configuration, say $(\rho_0, \alpha_0, \beta_0)$, to the goal position. It is obvious that equation (3.53) presents a discontinuity at $\rho = 0$; thus, the theorem of Brockett does not obstruct smooth stabilizability.

If we consider now the linear control law

$$v = k_\rho \rho, \quad (3.56)$$

$$\omega = k_\alpha \alpha + k_\beta \beta, \quad (3.57)$$

we get with equation (3.53) a closed-loop system described by

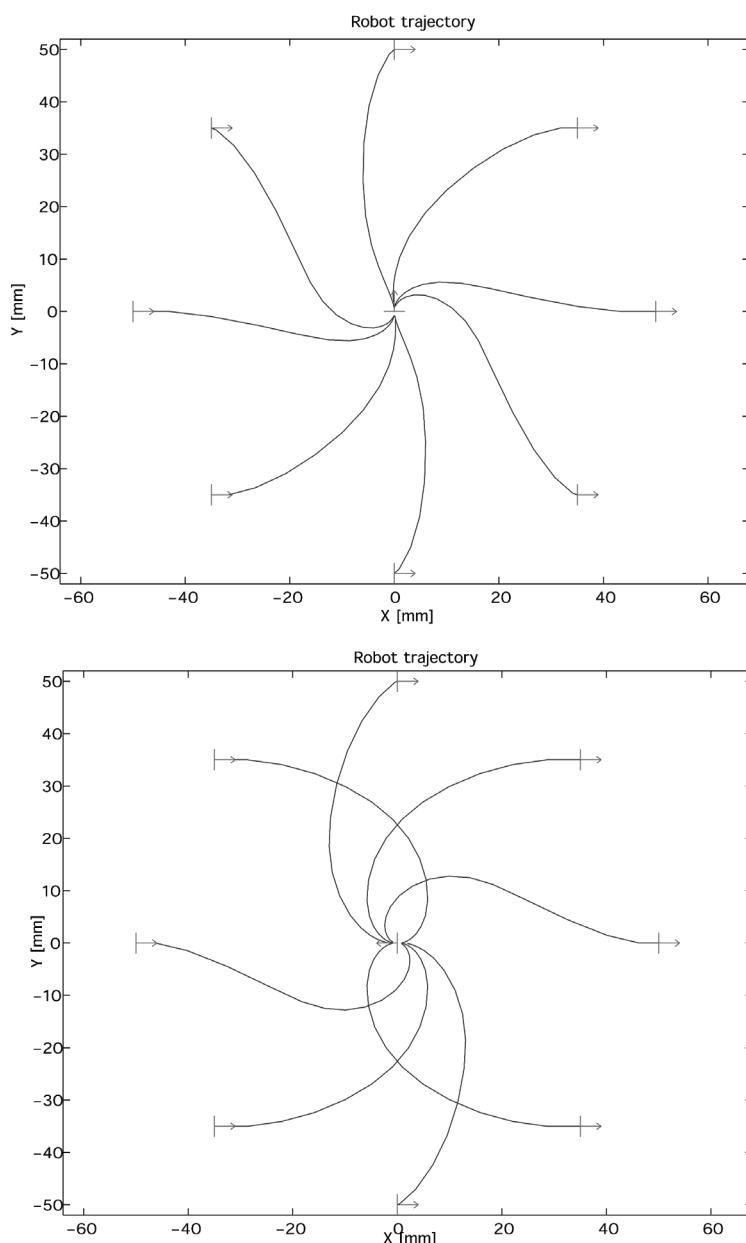
$$\begin{bmatrix} \dot{\rho} \\ \dot{\alpha} \\ \dot{\beta} \end{bmatrix} = \begin{bmatrix} -k_\rho \rho \cos \alpha \\ k_\rho \sin \alpha - k_\alpha \alpha - k_\beta \beta \\ -k_\rho \sin \alpha \end{bmatrix}. \quad (3.58)$$

The system does not have any singularity at $\rho = 0$ and has a unique equilibrium point at $(\rho, \alpha, \beta) = (0, 0, 0)$. Thus, it will drive the robot to this point, which is the goal position.

- In the Cartesian coordinate system the control law (equation [3.57]) leads to equations that are not defined at $x = y = 0$.
- Be aware of the fact that the angles α and β have always to be expressed in the range $(-\pi, \pi)$.
- Observe that the control signal v always has a constant sign—that is, it is positive whenever $\alpha(0) \in I_1$ and it is always negative otherwise. This implies that the robot performs its parking maneuver always in a single direction and without reversing its motion.

In figure 3.20 you find the resulting paths when the robot is initially on a circle in the xy plane. All movements have smooth trajectories toward the goal in the center. The control parameters for this simulation were set to

$$k = (k_\rho, k_\alpha, k_\beta) = (3, 8, -1.5). \quad (3.59)$$

**Figure 3.20**

Resulting paths when the robot is initially on the unit circle in the x,y plane.

3.6.2.5 Local stability issue

It can further be shown that the closed-loop control system (equation [3.58]) is locally exponentially stable if

$$k_\rho > 0 ; \quad k_\beta < 0 ; \quad k_\alpha - k_\rho > 0 . \quad (3.60)$$

Proof:

Linearized around the equilibrium ($\cos x = 1$, $\sin x = x$) position, equation (3.58) can be written as

$$\begin{bmatrix} \dot{\rho} \\ \dot{\alpha} \\ \dot{\beta} \end{bmatrix} = \begin{bmatrix} -k_\rho & 0 & 0 \\ 0 & -(k_\alpha - k_\rho) & -k_\beta \\ 0 & -k_\rho & 0 \end{bmatrix} \begin{bmatrix} \rho \\ \alpha \\ \beta \end{bmatrix}, \quad (3.61)$$

hence it is locally exponentially stable if the eigenvalues of the matrix

$$A = \begin{bmatrix} -k_\rho & 0 & 0 \\ 0 & -(k_\alpha - k_\rho) & -k_\beta \\ 0 & -k_\rho & 0 \end{bmatrix} \quad (3.62)$$

all have a negative real part. The characteristic polynomial of the matrix A is

$$(\lambda + k_\rho)(\lambda^2 + \lambda(k_\alpha - k_\rho) - k_\rho k_\beta) \quad (3.63)$$

and all roots have negative real part if

$$k_\rho > 0 ; \quad -k_\beta > 0 ; \quad k_\alpha - k_\rho > 0 , \quad (3.64)$$

which proves the claim.

For robust position control, it might be advisable to apply the strong stability condition, which ensures that the robot does not change direction during its approach to the goal:

$$k_\rho > 0 ; \quad k_\beta < 0 ; \quad k_\alpha + \frac{5}{3}k_\beta - \frac{2}{\pi}k_\rho > 0 . \quad (3.65)$$

This implies that $\alpha \in I_1$ for all t , whenever $\alpha(0) \in I_1$ and $\alpha \in I_2$ for all t , whenever $\alpha(0) \in I_2$ respectively. This strong stability condition has also been verified in applications.

3.7 Problems

- Suppose a differential drive robot has wheels of differing diameters. The left wheel has diameter 2 and the right wheel has diameter 3. $l = 5$ for both wheels. The robot is positioned at $\theta = \pi/4$. The robot spins both wheels at a speed of 6. Compute the robot's instantaneous velocity in the global reference frame. Specify \dot{x} , \dot{y} , and $\dot{\theta}$.
- Consider a robot with two powered spherical wheels and a passive castor wheel (no power). Derive the kinematics equations of the form of 3.30 and 3.33 for this robot.
- Determine the degrees of mobility, steerability, and maneuverability for each of the following: (a) bicycle; (b) dynamically balanced robot with a single spherical wheel; (c) automobile.

4. Challenge Question

Consider the robot of figure 3.10 with dimensions $l = 10$ and $r = 1$. Suppose you wish to command this robot in its local reference frame with speed \dot{x} , \dot{y} , and $\dot{\theta}$. Write a formula translating the desired \dot{x} , \dot{y} , $\dot{\theta}$ into speeds for all three wheels. Specifically, identify f_1 , f_2 , and f_3 such that:

$$\varphi_1 = f_1(\dot{x}, \dot{y}, \dot{\theta})$$

$$\varphi_2 = f_2(\dot{x}, \dot{y}, \dot{\theta})$$

$$\varphi_3 = f_3(\dot{x}, \dot{y}, \dot{\theta})$$

